Stony Brook University

Genetic analysis of the GABA synthetic enzymes: from synapse development to activity dependent transcription

A Dissertation Presented

by

Xiaoyun Wu

to

The Graduate School

in Partial Fulfillment of the

Requirements

for the Degree of

Doctor of Philosophy

in

Genetics

Stony Brook University

August 2010

Stony Brook University

The Graduate School

Xiaoyun Wu

We, the dissertation committee for the above candidate for the degree of Doctor of Philosophy In Genetics, hereby recommend acceptance of this dissertation.

Z. Josh Huang – Thesis Advisor
Professor, Neurobiology, Cold Spring Harbor Laboratory

Shaoyu Ge – Chairperson of Defense
Assistant Professor, Department of Neurobiology and Behavior

Hollis T. Cline
Professor, Department of Cell Biology, The Scripps Research Institute

Mirjana Maletic-Savatic
Assistant Professor, Department of Pediatrics, Baylor College of Medicine

Gary G. Matthews
Professor, Department of Neurobiology and Behavior, Stony Brook University

Karel Svoboda
Group Leader, Janelia Farm Research Campus

This dissertation is accepted by the Graduate School

Lawrence Martin
Dean of the Graduate School

Abstract of the Dissertation

Genetic analysis of the GABA synthetic enzymes: from synapse development to activity dependent transcription

by

Xiaoyun Wu

Doctor of Philosophy

in

Genetics

Stony Brook University

2010

GABA mediates inhibitory synaptic transmission in the mammalian brain. GABA is synthesized through two glutamate decarboxylases, GAD67 and GAD65. My thesis addresses two questions of GABA signaling through the genetic manipulation of the GABA synthetic enzymes.

First, I examined the role of GABA transmission in inhibitory synapse development in the mouse neocortex. I used a genetic strategy to specifically block GABA synthesis or release in single neurons and examined the impact on axon and synapse development. Such cell autonomous manipulation of GABA signaling without disturbing circuit activity level is critical to reveal its precise function in synapse formation. Chronic blockade of transmission caused a profound increase in axon and bouton density with apparently normal synapse structures, suggesting the involvement of GABA in synapse elimination and axon pruning. Live imaging showed that developing GABA axons form

many transient boutons and only a subset of them are stabilized. Acute blockade of GABA transmission led to significantly increased bouton stability and density, increased axon extension and decreased axon retraction. Together, these results suggest that developing GABAergic axons are capable of highly exuberant axon growth and form a large number of transient contacts throughout their length while searching for potential synaptic partners; GABA transmission is crucial to eliminate inappropriate contacts and validate appropriate contacts, thereby sculpting the pattern of synaptic connections guided by activity.

Second, I developed a method to monitor the physiological state of GABAergic neurons through visualizing activity dependent transcription of the *Gad67* gene. *Gad67*, the best characterized activity regulated gene in GABAergic neurons, is dynamically regulate during development and by sensory experience. I generated two versions of knock-in reporter mice; Gad67-d2EGFP and Gad67- t2a-nls-d4EGFP, both express a short half-life EGFP under the control of the endogenous Gad67 promoter. I showed that GFP fluorescence reliably reports Gad67 transcription bi-directionally in response to pathological, pharmacological and physiological stimuli. Furthermore, in a chronic restraint stress paradigm, the reporter revealed cell-type specific change in the hippocampus. Therefore, these reporters allow visualization of the transcriptional state of the *Gad67* gene with cellular and cell type resolution and will facilitate our understanding of plasticity in GABAergic neuronal circuits.

Table of Contents

List of Figures

List of Abbreviations

μg	microgram
μl	microliter
μm	micron
nm	nanometer
μM	micromolar
mM	millimolar
NMJ	neuromuscular Junction
ACh	acetylcholine
CNS	central nervous system
GABA	gamma amino butyric acid
GAD 67/65	Glutamic Acid Decarboxylase 67/65
$GABA_A$ /$GABA_B$ R	gamma amino butyric acid-A/B receptor
GAT	Glutamic acid transporter
VGAT	vesicular glutamic acid transporter
GFP	green fluorescent protein
Syn	synaptophysin
PV	parvalbumin
SOM	somatostatin
CR	calretinin
NOS	nitric oxide synthase
BDNF	Brain Derived Neurotrophic Factor

Ca^{2+}	calcium
WT	wild type
KO	knock out
EP	equivalent of postnatal
AAV	adeno-associated virus
BAC	Bacterial Artificial Chromosome
IEG	Immediate Early Gene
bp	base pair
Kb	kilo base
mRNA	messenger ribonucleic acid
RT	room temperature
pA	poly adenylation signal
PCR	Polymerase chain reaction

Acknowledgements

First and foremost, I would like to thank Dr. Z. Josh Huang, my thesis supervisor, for his support, guidance and encouragement. The extent of his broad knowledge, his expertise in research and his vision about the future has been an inspiration for me.

I gratefully acknowledge the help of Dr. Hollis Cline, who provided thoughtful and wise counsel throughout these projects. Also, special thanks to Dr. Gary Matthews, Dr. Shaoyu Ge, Dr. Mirjana Maletic-Savtic, Dr. Karel Svoboda for being on my thesis committee, for their critical comments to make me a better scientist, and for their thorough review of my thesis.

To my colleagues, Yu Fu, Miao He, Matthew Lazarus, Priscilla Wu, Rae Hum Paik, Dr Jiangteng Lu, Dr. Ying Lin, Dr. Keerthi Krishnan, Dr. Anirban Paul, Dr. Hiroki Taniguchi, many thanks for your technical assistances, wonderful discussions and much laughter. To my collaborators, Dr. Graham Knott in Ecole Polytechnique Federale de Lausanne and Dr. Deqiang Jing in Dr. Francis Lee's lab in Weill Cornell Medical College, my sincere thanks for their generous help in enabling key components of my research projects.

Graduate school is a long and enduring journey. I am lucky to have so many friends surrounding me to share the experience and support me whenever I am feeling weak. Especially I would like to thank Rui, Maria, Yang Yang, and Qiaojie. I will always

remember the fun we had together! My thanks also go to Lei Zhu, who assisted me in so many ways when I first came to this foreign country. I thank Stony Brook Genetics Program for selecting me into the PhD program.

Lastly, my great thanks go to Lucas Carey, my husband. The magic happened at the welcoming barbeque on my first day of graduate school. Though we both experienced tough water in the sailing of our thesis projects, I am so glad we both went through the difficulties and got our doctorates. Most heartfelt thankfulness goes to my parents and grandma for bringing me up. Their unconditioned love enables me to do my best and aspire to a higher place.

Chapter 1. Introduction

In the past two decades, neuroscience has made great strides in understanding the structures and function of synapses at the level of molecules. At a higher level, the emerging challenge is to understand how information is represented, processed, and transmitted in neural networks. GABAergic neurons, although numerically a minority, play key functions in controlling spatial and temporal aspects of brain activity. Ramon y Cajal believed that the functional superiority of the human brain is intimately related to the prodigious abundance of inhibitory neurons (Ramon y Cajal, Recuerdos de mi vida, 1917). Inhibitory neurons provide the functional balance, complexity and computational architecture of neuronal circuits (Buzsáki 2006). Misregulated inhibitory neurons are implicated in the majority of neurological diseases such as epilepsy, schizophrenia, autism, Alzheimer's and Parkinson's Diseases (de Lanerolle et al 1989; Levitt et al 2004; Lewis et al 2005; Li et al 2009; Pisani et al 2007). Deciphering the precise organization and function of neural network computations therefore will require a deep understanding of inhibitory neurons.

1.1 GABAergic circuits in the neocortex

GABAergic neurons in the mammalian neocortex are primarily interneurons that act locally to fine tune excitatory transmission. γ-Aminobutyric acid, then known as Factor-1, was first isolated in the 1950s (Bazemore et al 1956). Soon after it was revealed that interneurons release GABA, and form inhibitory synapses (Kravitz et al 1963; Kuffler & Edwards 1958; Obata 1972; Purpura et al 1957). The initial systematic study on interneu-

rons came from the hippocampus where a homogenous distribution of spatially aligned principal pyramidal cells allows easy analysis of their organization along with the array of local GABAergic interneurons that innervate them (Freund & Buzsaki 1996; Somogyi et al 1983b; Somogyi et al 1998). These rigorous studies laid the framework of the study of different interneuron subtypes and connectivity pattern. However, all these experiments were done acutely and required laborious cycles of randomly patching onto an interneuron, searching nearby connected pyramidal cell, recording from the pair, filling them with a dye to reconstruct the connected cells and examining the synapses under electron microscopy. The low-throughput approach fails to capture the wealth of interneuron diversity and the static approach does not chacterize the dynamic image of circuit development.

Cortical interneurons exhibit stunning diversity. Different classes of interneurons possess different molecular, morphological, subcellular targeting, biophysical and synaptic properties (Markram et al 2004; Somogyi et al 1998). Importantly, during network oscillation contingent to behavior, interneurons of different classes show distinct firing pattern, suggesting that specific interneuron types regulate Pyramidal cells in a precise, dynamic, spatio-temporal manner. Therefore, GABAergic interneurons are well suited to orchestrate cell assemblies and representations in the neocortex (Somogyi & Klausberger 2005).

To understand the development of specific GABAergic circuits and synapses, it is crucial to distinguish among different classes of interneurons, which may have distinct developmental timelines and involve different cellular and molecular mechanisms. There

have been many attempts to classify GABAergic interneurons, using criteria such as physiological properties, morphology, molecular markers and secreted neuropepties and postsynaptic subcellular targeting (DeFelipe 2002; Kawaguchi & Kubota 1997) For example, based on their axonal morphology, cortical interneurons can be classified into bitufted cells, basket cells, neurogliaform cells, martinotti cells, double bouquet cells etc. Most criteria have a good correlation to the respective classes. For instance, basket cells, as identified by the basket-like axon innervation they form around pyramidal cell soma, are fast spiking, express calcium binding protein parvalbumin (PV), target the soma and proximal dendrites of the postsynaptic pyramidal cells and functionally maybe important in synchronizing a pyramidal cell ensemble (Freund & Katona 2007). Bitufted cells, as identified by bi-polar axons, are low threshold spiking, express somatostatin (SOM), target the distal dendrites of postsynaptic pyramidal cells and functionally maybe important for the efficacy and plasticity of excitatory synaptic inputs by inhibiting dendritic Ca^{++} spikes (Miles et al 1996).

The diversity of GABAergic neurons lies in the heart of cortical architecture. The structural framework of the GABAergic connections can bring disparate populations of pyramidal cells together to support functional interactions between networks (Cobb et al 1995; Foldy et al 2005). Since many of the inhibitory cell types have specific sub-cortical inputs, the inhibitory network can encode information on emotional states (Bacci et al 2005; Freund 2003). Recent studies have identified distinct interneuron populations in different cortical states and behavior *in vivo* (Klausberger et al 2003).

In the first part of my thesis, I choose to concentrate on basket cells, which comprise almost 50% of the total interneuron population (Gonchar et al 2007). Basket cells target the soma and proximal dendrites of hundreds of local pyramidal cells and are functionally critical for synchrony and output among large numbers of pyramidal cells (Galarreta & Hestrin 1999). They are fast spiking, generate feedback inhibition and frequently form reciprocal connections with the innervated pyramidal cells (Kapfer et al 2007). Fast Spiking (FS) cells were shown to enforce precise coincidence detection in the soma (Pouille & Scanziani 2001). A recent study combining computational modeling and physiological recordings suggested that maturation of inhibition in visual cortex ensures that the temporally coherent inputs control Spike Timing Dependent Plasiticity of post-synaptic pyramidal cells and therefore could contribute towards engaging plasticity mechanisms during postnatal development in the cortex (Kuhlman et al 2010).

1.2 GABA signaling system

All neurons that use GABA as neurotransmitter contain the GABA signaling system, which can be divided into five components: synthesis (GAD67, GAD65); packaging (VGAT); binding ($GABA_A$ and $GABA_B$ receptors); re-uptake (GAT) and degradation (GABA transminase).

GABA is synthesized from glutamate by two isoforms of GAD (Glutamic Acid De-carboxylase) enzymes (Erlander et al 1991); the names GAD67 and 65 refer to their respective molecular weight in Kilo-Daltons. Although both enzymes synthesize GABA, they are different in several ways. GAD67 is the main GABA producing enzyme, making

95% of the GABA in soma, dendrites, and axon terminals whereas GAD65 is largely localized to presynaptic terminals (Pinal & Tobin 1998). While GAD65 activity is mainly regulated at the post-translational level such as palmitoylation (Kanaani et al 2002), and proteolytic cleavage, GAD67 regulation is mostly transcriptional (Battaglioli et al 2003; Buddhala et al 2009). A genetic deletion of either, or both GAD genes would reduce, or eliminate, GABA synthesis. Knockout mice for both GAD genes have been generated. The GAD65-/- mice do not have measurably altered brain GABA contents or behavior, except for a slight increase in susceptibility to epilepsy(Asada et al 1996; Kash et al 1997). On the other hand, GAD67-/- mice die at P0 and manifest a severely defective cleft palate (Asada et al 1997). Fortunately, Richard Palmiter lab developed a conditional knock out mouse strain of GAD67 ($Gad67^{flx/flx}$). By combining $Gad67^{flx/flx}$ and $Gad65^{-/-}$, I was able to knockout both GAD genes in single basket cells using an organotypic slice culture system.

Vesicular GABA transporter (VGAT), also known as vesicular inhibitory amino acid transporter (VIAAT), is responsible for loading GABA into the vesicles. Unlike glutamatergic synapses, which rely on three vesicular glutamate transporters (Shigeri et al 2004), GABAergic synapses all require vesicular transporter VGAT (Wojcik et al 2006). VGAT knock out animals also die at birth because of CNS dysfunction and manifest severely defective cleft palate (Oh et al 2010). Conditional knock out animals ($VGAT^{flx/flx}$) have been generated to specifically knock out VGAT in Cre recombinase expressing cell populations (Tong et al 2008). I used $VGAT^{flx/flx}$ with a single cell knockout as another approach to knockout inhibitory neurotransmission.

There are two types of GABA receptors in the CNS, $GABA_A$ and $GABA_B$. $GABA_A$ receptor is an ionotropic ligand-gated chloride channel and is expressed on the postsynaptic and extrasynaptic membrane of neurons and on astrocytes (Fritschy & Brunig 2003; Moss & Smart 2001). Sixteen different subunits (a1-6, b1-3, g1-3, d, e, g, q) can be components of the pentameric $GABA_A$ receptor. The classical $GABA_A$ receptor is composed of two a, two b and one g subunits. $GABA_B$ receptors on the other hand are metabotropic receptors formed by a heterodimer of $GABA_BR1$ with $GABA_BR2$. $GABA_B$ receptors are located both on the presynaptic and postsynaptic membrane and act through G-protein induced signaling of second messengers, different enzymes cascades, and other receptor signaling pathways (Bettler & Tiao 2006).

Three GABA transporters have been identified in the CNS, GABA transporter subtype 1, 2, 3 (GAT1, 2, 3) (Radian et al 1990). GAT is responsible for GABA reuptake after it is released from the presynaptic terminal. GAT1 is highly expressed in inhibitory terminals in the neocortex and cerebellum. GAT2 is weakly expressed throughout the brain, primarily in arachnoid and ependymal cells. GAT3 is predominantly expressed on glia cells and in the olfactory bulb, midbrain regions and deep cerebellar nuclei (Itouji et al 1996). GAT1 knock out mice are largely normal and fertile but display reduced body weight and motor disorders (Chiu et al 2005).

GABA transaminase (GABA-T) is a mitochondrial enzyme involved in the breakdown of GABA into succinic semialdehyde. In turn, succinic semialdehyde is converted either to succinic acid by succinic semialdehyde dehydrogenase or into g-hydroxybutyric acid (GHB) by succinic semialdehyde reductase (Tillakaratne et al 1995; Wong et al

2003). International Knockout Mice Consortium generated GABA transaminase knock-out mice but the phenotype has not been reported.

The therapeutic scope targeting the GABA signaling system covers a large number of neurological and psychiatric disorders. For example, gene therapy with an adeno-associated virus (AAV) borne *Gad67* gene was demonstrated to improve motor deficit in Parkinson's patients (Kaplitt et al 2007). $GABA_A$ modulator Valium and Clonazepam are used to treat anxiety, migraine and epilepsy. Similarly, Tiagabin and Vigabatrin, which target GAT and GABA-T respectively, are two commonly prescribed anti-epileptic drugs (Foster & Kemp 2006). GABA serves as a neurotransmitter or neuromodulator in the peripheral nervous system and as a hormone or trophic factor in non-neuronal peripheral tissue (Ong & Kerr 1990). Interestingly, GAD is considered to be one of the strongest candidate auto-antigens involved in triggering b cell-specific autoimmunity. Stiff-man syndrome and type 1 diabetes patients have anti-GAD in their serum, which could contribute to the disease progression as well as causing seizure (Jun et al 2002; Pearce et al 2004).

In summary, all five of components of GABA signaling are considered as good drug targets, with both the GADs and the GABA receptors being particularly attractive, due to the potential for increased synthesis or signal transduction with protein modifications or through interaction with antibodies.

1.3 Inhibitory axon and synapse development

The maturation of inhibitory transmission proceeds well into adolescence in the visual cortex (Morales et al 2002). The maturation of inhibition is directly linked to visual cortex plasticity (Fagiolini & Hensch 2000; Huang et al 1999).

In mature visual cortex, a basket cell innervates hundreds of pyramidal neurons (Holmgren et al 2003). At each pyramidal cell, basket cell axons extend multiple terminals with large boutons clustered around pyramidal cell soma and proximal dendrites, forming the characteristic perisomatic synapses (Tamas et al 1997; Wang et al 2002).

Our lab first characterized the development of the perisomatic innervation in the visual cortex (Chattopadhyaya et al 2004). Characteristic perisomatic synapses formed through a stereotyped process, involving the extension of distinct terminal branches, proliferation of perisomatic boutons and enlargement of perisomatic boutons from P14 to P28. The formation of perisomatic synapses is intrinsic to the cortex (Di Cristo et al 2004) and proceeds in a similar time course in organotypic slice culture. Neural activity or visual experience can influence the maturation and pattern of perisomatic innervation, especially during the third week when the axon arbor growth and bouton additions are the fastest.

Synaptogenesis involves a complex series of events, spanning neuronal differentiation, cell–cell contact and localized induction of presynaptic and postsynaptic differentiation (Craig et al 2006). For the presynaptic axons, although they come into contact with a multitude of neurons during their journeys, they refrain from synapsing onto inappropri-

ate target cells. Synaptic specificity is probably primarily determined by cell adhesion molecules on both partner cells, with some influence by glial cues (Shapiro et al 2007; Ullian et al 2004). Axons extend processes and turn on genes encoding synaptic proteins, resulting in the formation, accumulation, and directional trafficking of vesicles carrying synaptic protein complexes (Cline 2001; Waites et al 2005). Transient contacts are made and various secreted factors, receptors, and signaling molecules are at work to make neurons receptive to form synapses (Cline 2001). Synaptogenic molecules such as Neurexin and Neuroligin induce synapse formation (Huang & Scheiffele 2008; Missler & Sudhof 1998). Presynaptic and postsynaptic components are subsequently recruited and the synapse maturation phase begins. During maturation, synapses expand in size and the number of synaptic vesicles per terminal increases (Vaughn 1989). For glutamatergic synapse, pre and postsynaptic elements develop in a coordinated fashion and maintain correlation across different components: bouton volume, number of total synaptic vesicles, docked vesicles, active zone area and postsynaptic density area (Schikorski & Stevens 1997).

Several experimental methodologies have been established to study synaptogenesis, among which are immunohistochemical, fluorescent imaging, electron microscopy and electrophysiology (Ahmari & Smith 2002).

The immunohistochemistry method identifies protein localized at the putative synaptic site. From the 1990s and onward, proteins that are preferentially localized to synapse have been steadily reported. One of the first examples is the punctuated distribution of synapsin I and synaptophysin (Fletcher et al 1991). However, several reports on presyn-

aptic clusters or postsynaptic clusters identified by marker staining have revealed the absence of corresponding postsynaptic or presynaptic partner (Kannenberg et al 1999; Kraszewski et al 1995), calling into doubt the ability of these data to predict function. Therefore, cautions should be taken when interpreting synaptic marker staining data.

Fluorescent imaging takes advantage of GFP variants (Shaner et al 2004; Tsien 1998) to report protein localization, expression, and to label neurons. Observing short-term and long-term dynamics of GFP or RFP labeled neurons has greatly advanced our understanding of the structural plasticity of neuronal circuits (De Paola et al 2006; O'Rourke et al 1994; Ruthazer et al 2003; Trachtenberg et al 2002). Another widely used approach is using fluorescent fusion proteins as synaptic markers in living cells. Markers such as GFP fusions of VAMP/synaptobrevin and synaptophysin have been used to label synaptic vesicles. Live imaging allows powerful direct observation of the order and time course of synaptic assembly by tracking GFP fusion proteins of synaptic components (Niell & Smith 2004). However, much like the problem with marker staining, these puncta do not all represent synapses and likely correspond to delivery units of building blocks for the presynaptic apparatus. Yet another technique is the use of styryl dyes, such as FM 4–64, to pulse label vesicle and observe vesicle turnover (Cochilla et al 1999). This technique has been useful to track the progression of synaptogenesis; the onset of FM dye loading can be considered as the new synapse formation time point (Friedman et al 2000).

Using electron microscopy to gain insights into synapse ultrastructure has long been regarded as the gold standard of defining what a synapse is. Inhibitory synapses in the

neocortex are characterized by their symmetric appearance. Symmetric synapses involve axons containing clusters of predominantly flattened or elongated vesicles and do not contain a prominent postsynaptic density. Without the prominent postsynaptic density, it can be problematic to identify inhibitory synapse. But there is one area that has inhibitory synapse exclusively – the perisomatic area that contains mostly parvalbumin positive, basket cell terminals (Alonso-Nanclares et al 2004). Even more difficult to identify are the nascent inhibitory synapses. Inferring from the study done on excitatory synapse, filopodia contacts typically have close membrane apposition, presence of irregular structure, including clear vesicles, tubulovesicular structures and dense core vesicles (Ahmari & Smith 2002).

Electrophysiology can be used to measure change in synaptic transmission, a process fundamental to synaptic function. The intracellular recording techniques are sensitive enough to detect a single synaptic transmission event. However, it is very difficult to localize the effect to a specific synaptic site. Moreover, silent synapses (Malenka & Nicoll 1997) complicate the interpretation of synapse formation.

To summarize, all these different methodologies provide unique information in regards to synapse formation, but none of them provides a complete picture on its own. A reliable description of synapse formation likely requires a multi-layer approach including dynamic data obtained from fluorescence imaging, analysis at the ultrastructural level using EM, complimentary marker staining and functional studies.

1.4 GABA function in postnatal development

GABA has been studied mainly in the context of synaptic inhibition in the CNS. In recent years, increasing evidence suggest that, in addition to its function as inhibitory neurotransmitter, GABA also plays crucial roles in neuronal migration, differentiation and synaptogenesis (Owens & Kriegstein 2002; Represa & Ben-Ari 2005).

The trophic role of GABA in early postnatal periods could be ascribed to the depolarizing effects of $GABA_A$ receptor activation and high intracellular chloride concentration. Upon reversal of intracellular chloride gradient by expression of KCC2, GABA is thought to act its classic role as fast inhibitory neurotransmitter (Ben-Ari 2002).

Recently, our lab provided evidence that during adolescent development, when GABA's action is hyperpolarizing, GABA can also function as effector in activity dependent regulation of GABAergic innervation. Conditional knockdown of the rate-limiting synthetic enzyme GAD67 in basket cells in adolescent visual cortex resulted in less axon branching, fewer perisomatic synapses and reduced complexity of the innervation fields. Interestingly, this manipulation is sensitive to developmental period; there is a profound effect if the knock down occurs before 3 weeks, but almost none if the knock-down occurs after 4 weeks. Since intracellular GABA levels are modulated by neuronal activity, the results implicate GAD67-mediated GABA synthesis in activity-dependent regulation of inhibitory innervation patterns (Chattopadhyaya et al 2007).

However, the role of GABA transmission in circuit development is still somewhat controversial (Wang & Kriegstein 2009). In GAD $67^{-/-}$: $GAD65^{-/-}$ mice (double knock-

out for glutamic acid decarboxylase 67 and 65), GABA levels in the brain were reduced to less than 5%, but the size and shape of the brains at E14 and P0 were indistinguishable from heterozygous littermates. While these GAD $67^{-/-}$: $GAD65^{-/-}$ mice die at birth due to cleft palate, no gross neural developmental defects were detected in the neocortex, cerebellum, or hippocampus (Ji et al 1999).

1.5 Activity dependent transcriptional regulation of Gad67 gene

Activity-dependent regulation of GAD67 transcription and GABA levels have been well documented in numerous brain regions by *in vivo* physiological manipulations. For example, GABA is down regulated in sensory cortical areas following sensory deprivation. In the rodent visual cortex, visual deprivation reduces GAD67 mRNA and protein levels (Bartoletti et al 2004; Hendry et al 1986). In the rodent somatosensory cortex, whisker deprivation decreases GAD67 while whisker stimulation increases GAD67 in the corresponding barrel (Welker et al 1989). GAD67 is regulated during development according to neuronal activity level (Kiser et al 1998). Paradigms of short intracortical stimulations can also increase GAD67 mRNA levels (Liang et al 1998). Modulatory influences from cholinergic systems and hormones can also regulate GAD67 levels (Nakamura et al 2004).

The activity regulation of GAD67 is intrinsic to neocortex. Manipulation of activity in cortical slice culture rapidly induces change in GAD67 transcription (Patz et al 2003). Blocking neural activity by TTX in the organotypic culture system decreases GABA levels and GAD67 protein level (Chattopadhyaya et al 2007). GABA metabolism readily

influences inhibitory synaptic strength and presynaptic GABA content is a regulated parameter for synaptic plasticity (Engel et al 2001). Therefore GAD67 transcriptional level is a good correlate of inhibitory synaptic strength and plasticity.

Altered Gad67 mRNA expression level is a hallmark of multiple neurological disorders such as schizophrenia, autism, epilepsy, bipolar disorders, drug and alcohol addiction (Wong et al 2003). It is not surprising since neurological disorders are characterized by abnormal neuronal activity level, learning disability and attention deficits due to impaired inhibition (Clancy et al 2010). Particularly, reduced *Gad67* mRNA expression in the dorsal lateral prefrontal cortex is one of the most consistent molecular pathology in individuals with schizophrenia (Lewis et al 2005). More recently, genetic studies revealed that SNPs in the 5' regulatory region (UTR) of the *Gad67* gene are associated with the childhood onset schizophrenia, a particularly severe form of the disease(Addington et al 2005). The reduced GAD67 expression in cortical GABAergic interneurons of schizophrenia brains may be the consequence of an epigenetic hypermethylation in the GAD67 promoters by DNA-methyltransferase 1 (Veldic et al 2005). Treating mice with l-Methionine can induce hypermethylation of Gad67 promoter CpG islands and the down-regulation of GAD67 expression, whereas treating the same mice again with valproic acid (VPA), a histone deacetylase inhibitor can reverse the epigenetic regulation and increase Gad67 transcription. The methlyation state of Gad67 also affects MeCP2 binding (Dong et al 2005). MeCP2 is a methyl CpG binding protein and MeCP2 gene is the casual gene in Rett's syndrome, a severe form of Autism Spectrum Disorders (Van den Veyver & Zoghbi 2000). Altogether, these evidences suggest that the *Gad67* gene regulation may reflect the development and function of the GABAergic inhibitory

system underlying neurological pathogenesis. The challenge is to directly link alternations of *Gad67* expression in specific cell types, brain regions, and developmental processes, and to discover their impacts on synaptic connectivity, transmission, network functions, and behavior.

1.6 Experimental outline

My thesis addresses two questions of GABA signaling through the genetic manipulation of the GABA synthetic enzymes GADs. First, what is the role of GABA transmission in axon and synapse development; second, how is Gad67 regulated in GABAergic neuronal circuit in response to sensory experience.

In the first project, I focused on the role of neurotransmission in axon growth and synapse development. I utilized mouse genetics and the unique simplicity of GABAergic signaling to examine the effect on synapse formation following complete and single-cell mannered removal of GABA transmission. I mainly used a cortical organotypic slice culture system where I could image and manipulate few basket cells in intact neuronal circuit and study the process of their axon and synapse development. I used a construct containing 10kb of the GAD67 promoter region driving GFP expression to enrich labeling of basket cell and simultaneously used the same promoter driving a Cre recombinase to manipulate the labeled cell. I used slice cultures prepared from $Gad67^{flx/flx}$: $Gad65^{-/-}$ or $VGAT^{flx/flx}$ mice so that upon Cre expression, sparsely labeled basket cells are depleted of neurotransmission because of no GABA synthesize or GABA loading into the vesicles. This genetic method on GABAergic cortical interneurons should be considered as

providing one of the best contexts to address such fundamental question in neurobiology. First, it completely abolish neurotransmission; second, it block both action potential dependent and spontaneous neurotransmitter release; third, it leave the vesicular delivery pathway of synaptic molecules untouched; fourth, it can be restricted to different developmental stages so effect on synapse pattern formation or synapse maintenance can be separated.

To verify my finding in slice culture, I injected adeno-associated virus (AAV) bearing a plasmid encoding GFP-ires-Cre to label and deplete GABA transmission in a small volume of primary visual cortex *in vivo*. The measurements are comparable and the results are consistent with the finding in slice culture, excluding the possible complication of using a reduced preparation such as organotypic slice culture.

To analyze the effect of synaptic inactivity on axon growth and synapse patterning, I used fluorescent live imaging to characterize the differential short-term dynamics of presynaptic puncta and filopodia as well as long term dynamics of axon growth pattern in the absence of neurotransmission. Several imaging protocols were used with the intention of capturing different layers of synapse development regulation. For example, the nascent synapse is estimated to emerge within several minutes (McAllister 2007; Sabo et al 2006). To capture these very short-term dynamics I used 2-photon microscopy to take an image stack every minute over the course of an hour. Several hours is not long enough to observe significant axon growth, so I adapted a long term protocol of using environment-controlled, inverted confocol microscope to carry out day-to-day time lapse imaging. In conjunction, I used immunohistochemistry on presynaptic and postsynaptic markers to

identify the molecular entities of both the static mutant boutons and retrospectively, the presynaptic moving puncta that I have collected dynamics information from. However, because of the complexity of antibody staining in slice culture, the results from the immunohistochemistry are rather suggestive than definitive. Since electrophysiology is primarily based on assaying synaptic transmission, it is problematic to come up with testable hypothesis in inhibitory synapses that are devoid of transmission. I used electron microscopy to study the ultrastructures of these mutant boutons, with the hope to firstly examine the presence of all synaptic components and secondly extract some information from analysis of active zone and vesicle numbers on how inactivity impacts the synaptic strength. In summary, I have used an array of methods to generate a full picture of the dynamic properties of basket cell axon and synapse development, and the examined the role of neurotransmission in regulating this process.

Several control experiments were done to validate the experimental manipulations and avoid complication of other interpretations. All the images were analyzed blind, although the differences between control and the mutant are striking and obvious to the analyzer so the human bias could not be totally excluded. The genetic knock out with 10kb-Cre construct was completed by 48 hours or possibly sooner. The knock out with AAV-GFP-ires-Cre happened within 6 days or possibly sooner. Importantly, intracellular recording of knock out cells demonstrated that they do not have different intrinsic properties than control cells. Therefore, the effects I examined were most likely to be mediated by synaptic inactivity but not from a gross change in the biophysical properties of the cell.

In my second project, I generated tools for studying interneuron activity in live animal with cellular resolution. Gad67 is arguably the best-characterized activity regulated gene identified in GABAergic neurons. Although there is a large diversity of GABAergic neurons that release GABA and a similarly large diversity of GABAA receptors that signal GABA, there is only a single mechanism to synthesize GABA – by conversion from glutamate through a single decarboxylation step. Between the two GABA synthetic enzymes, GAD67 is the rate-limiting enzyme, and alterations in GAD67 levels readily influence the cellular and vesicular GABA contents. The major step at which GAD67 activity is controlled physiologically is gene transcription, which is dynamically regulated during development, and by neural activity and experience. Alterations of *Gad67* transcription likely influence not only inhibitory transmission but also inhibitory synapse development and plasticity. Importantly, there is evidence that Gad67 is differentially regulated in different interneuron cell types in various physiological and pathological states (e.g. significant reduction in parvalbumin- and somatostatin-interneurons in the prefrontal cortex of schizophrenic patients). Therefore, it is important to develop tools to visualize Gad67 transcriptional level as a correlate of GABAergic neuron activity, which can be analyzed online after sensory input or behavior paradigm.

To meet the challenge, I have generated two knock-in mouse lines, Gad67-d2EGFP and Gad67-nls-t2a-d4EGFP. For the first line, a destabilized (2h half life) form of EGFP was targeted to the translational initiation site of Gad67 so that the transcripts of d2EGFP are directly under the control of the endogenous Gad67 promoter. Because d2EGFP has a short life span, the level of GFP fluorescent reflects the endogenous Gad67 transcription level. For the second line, another version of destabilized (4h half life) form of EGFP

was targeted to and substituted the translational stop codon so that GFP is coproduced with GAD67 and then the connecting self-cleaving t2a peptide will separate them apart. In this way, the targeted allele of Gad67 gene still express and generate indicative GFP simultaneously. A nuclear localization signal (NLS) was used at the N-terminal to preferentially localize GFP into the nucleus so as to improve the chance of resolving cell bodies by imaging.

After obtaining the two reporter lines, I went on to test if they faithfully report Gad67 transcriptional regulation and the time course is comparable with other methodologies such as mRNA in situ. I found that in both strains, GFP fluorescence reliably reported transcriptional regulation of *Gad67* bi-directionally in response to pathological (limbic system seizure), pharmacological (HDAC inhibitor) and physiological (whisker stimulation) stimulus. The up and down regulations of GFP were rapid, similar to the existing in situ data.

For one application using these reporters, I chose to map GABAergic neuronal circuit change in response to a chronic restraint stress paradigm. Chronic restraint stress has been shown to cause dramatic neurite retraction in pyramidal cells in medial prefrontal cortex and hippocampus (Galea et al 1997; Radley et al 2006). But the impact of chronic stress on GABAergic neurons is almost entirely unknown. The fluorescent reporter strains revealed cell-type specific change in Hippocampus. One type of interneurons (nNOS+) cells in stratum lacunosum moleculare (slm) of the hippocampus showed a different directional response than the other types of interneurons. These reporters are likely to reveal pathway specific plasticity in response to stress.

My experiments were done in collaboration with several colleagues. Fellow graduate student Yu Fu made the P_{G67}-Nrx 1b SEP construct and kindly provided his MatLab image analysis applications as reference for me to develop my own applications. All electrophysiology mentioned in the thesis was done by Dr. Jiangteng Lu. Dr. Graham Knott at Ecole Polytechnique Federale de Lausanne prepared all the brain samples for electron microscopy analysis. Dr. Deqiang Jing at Weill Cornell Medical College is responsible for the processing, immunohistochemistry and neurostereology analysis of GAD67-d2EGFP and GAD67-nls-t2a-d4EGFP brain tissues after chronic stress.

Chapter 2. Role of GABA transmission in inhibitory axon and synapse development

2.1 Introduction

Synapse formation is a crucial component of neural circuit assembly. In the developing vertebrate central nervous system, synapse formation involves multiple steps (Niell et al 2004). The initial contact of an axon with a potential postsynaptic target often leads to rapid initiation of transient synapse formation (Chao et al 2009), which triggers the accumulation of adhesion molecules and recruitment of pre- and post-synaptic signaling machinery (Waites et al 2005). These "nascent synapses" undergo an extensive process of validation (e.g. the matching of synapse types, transmitter and receptor types) and competition (for limited pre- and post-synaptic resources); only a subset of nascent contacts mature into more stable and functional synapses. The development of synaptic connections is influenced by synaptic activity (Cline 2001). Synaptic transmission could be at the ideal place to mediate synapse validation and competition, but how transmission directly regulates synapse development remains poorly understood. In particular, whether and how GABAergic transmission regulates inhibitory synapse and axon development is largely unknown.

Synapse formation is a dynamic process, requiring bi-directional coordination between pre-and post-synaptic partners (Cohen-Cory 2002). In order to understand how synapse connections are established from the basket interneuron to their postsynaptic partners, I first characterize the dynamic process of synapse formation and axon growth in the basket cell. Although the basic feature of basket cell axon development was characterized in fixed tissue (Chattopadhyaya et al 2004), no dynamic information has been obtained regarding basket cell axon growth pattern and synaptogenesis. I would like to ask 1) Does

the basket cell axon use filopodia to find postsynaptic target? 2) Does the basket cell axon grow in an iterative fashion? 3) Do most nascent synapses form and then are eliminated or do almost all the nascent synapses get stabilized? 4) Is the density of presynaptic boutons regulated on the axon? Answers to these questions are not only relevant to elucidate the mechanism of interneuron synapse patterning, but also provide insights into the general principles of establishment and maintence of synapse patterning in the central nervous system.

Synapse elimination has been observed in many parts of the nervous system, including the visual system, cerebellum, autonomic ganglia, and neuromuscular junction (Katz & Shatz 1996; Sanes & Lichtman 1999), suggesting the existence of a conserved process of synaptic disassembly. In axon development, branch elimination is another prominent feature, arguably just as important as branch addition and extension. In Drosophila, axons of mushroom body neurons are eliminated during metamorphosis by axonal degeneration, which requires ubiquitin-proteasome system (Watts et al 2003). In the mouse hippocampus, pruning is primarily manifested as axon tip retraction (Bagri et al 2003). Whether synapse elimination and axon pruning is a component of inhibitory synapse and axon development has not been explored. The following questions remain unresolved: 1) When does synapse elimination happen in basket cell synaptogenesis? Do basket cell axons and synapses undergo separate period of synapse formation and elimination or are synapse addition and elimination concurrent? 2) Does it regulate at the time when nascent synapse is transitioning to stabilized synapse, or does it refine stabilized and mature

synapse? 3) What is the primary action of axon elimination, is it axon degeneration alike or just axon tip retraction?

I am interested in determining the function of synaptic activity in axon and synapse formation and how does synaptic activity regulate dynamics of synaptic connection development. The intimate link between appropriate synaptic transmission and synapse morphogenesis seems well suited to sculpt neuronal connections with appropriate spatial and temporal precision. One way to study the role of synaptic activity is to completely remove neurotransmission and see how correspondingly, axon and synapse development is affected.

In C. elegans, the development of synaptic connection does not seem to be at all dependent on neurotransmission. C. elegans has a single GAD gene *unc-25*. The null mutation in *unc-25* does not disrupt either synaptic development or synaptic maintenance at neuromuscular junctions in C. elegans (Jin et al 1999). None of the aspects, including density of synaptic varicosities, axonal trajectories, connectivity with the muscles and synapse ultrastructures are altered in *unc-25* mutants. These mutant synapses are fully functional upon bath application of GABA.

At the mammalian neuromuscular junction (NMJ), on the other hand, depletion of transmission by the disruption of ChAT (choline acteyltransferase – the enzyme producing acetylcholine) profoundly affects multiple aspects of synapse development. Motor axon terminals differentiate extensively in the absence of neurotransmitter. Changes include the numbers of pre- and postsynaptic partners, the distribution of synapses in the

target field, the number of synaptic sites per target cell, and the number of axons per synaptic site. Neurotransmission also regulates the formation or stability of transient acetylcholine receptor-rich processes (myopodia) that may initiate nerve-muscle contact (Misgeld et al 2002).

In contrast, other studies in the mammalian CNS have concluded that neuronal activity is not required for synapse formation during development (Varoqueaux et al 2002; Verhage et al 2000). Munc18 or Munc13 1, 2 are vesicle-priming proteins, which upon genetic knockout, leads to a complete loss of all type of neurotransmitter secretion. However, since these knockout mice die at P0, the results are only on synapse morphology at P0, before activity may play a role in sculpting neural connections. Particularly, GABA inhibitory synapses are not yet developed at P0. Also, these germline knockouts grossly affect activity level in the brain, which cause general circuit abnormality and thus complicate the interpretations.

In the mammalian CNS, The difficulty of completely and specifically blocking synaptic transmission at defined stages of synapse development has long hindered detailed analysis of how neurotransmission affects synaptogenesis. Here, we used two strategies that take advantage of the unique feature of GABA signaling to eliminate transmission specifically and completely in GABAergic cells and ask how it alters axon and synapse development. The first strategy is through GABA synthesis. Unlike glutamate, which is generated by many metabolic processes (Fonnum 1984), GABA can only be synthesized from glutamate with two Glutamate Decarboxylases: GAD67 and GAD65. Second

method is through vesicular loading of GABA. Unlike glutamatergic system, which has several vesicular glutamate transporter VGlut 1,2,3 (Moriyama & Yamamoto 2004), GABAergic system has only one vesicular GABA transporter (Wojcik et al 2006). Using conditional knock out alleles - LoxP flanked GAD genes or VGAT gene, I have developed two independent strategies to eliminate neurotransmission in a single cell manner in an intact neuronal circuit.

This genetic manipulation provides a great context for elucidating the role of neurotransmission in the development of the mammalian CNS, as it avoids many caveats and side effects associated with many previous manipulations. First, some manipulations that block synaptic transmission deprive the postsynaptic cell of more than transmitter release. For example, blocking exocytosis from axon terminals (Sweeney et al 1995; Verhage et al 2000) may also prevent release of trophic factors or synaptic organizing molecules that use vesicular pathway. Second, studies that disrupt synaptogenesis-dependent signaling components such as Agrin-MuSK signaling in NMJ may elicit outcomes due to the secondary effects of the signaling pathways (DeChiara et al 1996; Gautam et al 1996; Gautam et al 1995). Third, germline KO of GABA in the CNS alters the global activity and therefore the results may reflect circuit level homeostasis regulation, but not the specific effect of activity on synaptogenesis (Ji et al 1999). Fourth, most pharmacological interventions cannot completely inhibit neurotransmitter release, blocking evoked but not spontaneous release (Deitcher et al 1998; Houenou et al 1990). Even low, spontaneous levels of neurotransmitter release affect postsynaptic receptor number and distribution (Akaaboune et al 1999; Saitoe et al 2001) and therefore enough for synapse formation. Particularly for GABAergic system, chronic GABA-A receptor blockade

results in overexcitation and epilepsy, and neuronal damage, which preclude the study of synapse development. Furthermore, pharmacological methods block GABA receptors at all types of interneurons and synapses, which may be differentially sensitive to GABAergic regulation.

To avoid these issues, I analyzed basket cell axon and synapses using conditional knock out system in which GABA synthesis or GABA vesicular loading can be specifically and completely removed in single cells with the Cre-LoxP system (Schwenk et al 1995). GABA is required for both evoked and spontaneous synaptic activity at all inhibitory synapses. After GABA's action becomes hyperpolarizing at P14, neurotransmission is the only established function for GABA. There is no GABA in the vesicles without GADs or VGAT, but the vesicles can still undergo exocytosis and other synaptic protein's delivery is not affected.

Experimental Outline

To understand the role of transmission in the formation, maturation and maintenance of basket cell axons and perisomatic synapses, I used genetic method to specifically abolish neurotransmission and study the impact on axon growth and synaptogenesis by a combinatorial approach of time-lapse fluorescence imaging, immunocytochemistry and electron microscopy.

The manipulation was achieved by sparsely expressing Cre recombinase in organotypic cortical slice culture prepared from conditional knock out animal of $GAD67^{flx/flx}$:

GAD65$^{-/-}$ or VGAT$^{flx/flx}$. The GFP and/or Cre construct is controlled by a P_{G67} promoter, which contains 10kb promoter region of *Gad67* and preferentially targets expression in basket interneurons. Then I quantified the morphological changes in parameters such as axon density, axon branch density and bouton density. To verify my finding in organotypic slice culture, I injected AAV-GFP-ires-Cre to label and deplete GABA transmission in a small volume of primary visual cortex *in vivo*.

To analyze the effect of synaptic inactivity on axon growth and synapse patterning, I used live imaging to characterize the short-term dynamics of presynaptic punctas and filopodia like transient structure as well as long-term dynamics of axon growth pattern in the absence of neurotransmission. Several imaging protocols were used with the intention of capturing different stages of synapse development. For example, the nascent synapse is estimated to emerge within several minutes (McAllister 2007; Sabo et al 2006), so I adapted a protocol that in every minute, a 2-photon image was taken for a total of 60 minutes. With axon growth pattern, it proved to be difficult to track a local axon arbor over several hours to observe enough events to reveal the difference, so I adapted a long term protocol of using environment-controlled, inverted confocal microscope to carry out day-to-day time lapse imaging. In conjunction, I used immunohistochemistry on presynaptic and postsynaptic markers to identify the molecular entities of both the static mutant boutons and retrospectively, the presynaptic moving punctas that I have collected dynamics information from. I used electron microscopy to study the ultrastructure of these mutant boutons, to firstly examine the presence of all synaptic components and secondly extract information from analysis of active zone and vesicle numbers on how inactivity impact the synaptic strength.

Major results and conclusion

In this study, I established a method to block GABA transmission from a single defined type of GABAergic neurons in neocortex and to examine the acute and long term impact on synapse and axon development using live imaging. This method allowed me to address, for the first time, the precise role of synaptic transmission on inhibitory synapse formation and patterning in GABAergic neurons. I found that blockade of transmission for a few days caused a profound increase in axon and bouton density with apparently normal synapse structures, suggesting the involvement of GABA transmission in synapse elimination and axon pruning. Live imaging showed that developing GABA axons form many transient boutons and filopodia while searching for potential synaptic targets, only a subset of these are stabilized. Acute blockade of GABA release results in 1) decreased elimination of transient boutons, 2) increased bouton stability and density, 3) increased axon extension and 4) decreased axon retraction. Together, these results suggest that developing GABAergic axons are capable of highly exuberant axon growth and form a large number of transient contacts throughout their length while searching for potential synaptic partners; GABA transmission is crucial to eliminate inappropriate contacts and validate appropriate contacts, thereby sculpting the pattern of synaptic connections guided by activity.

2.2 Blockade of GABA transmission in developing basket interneurons results in axon and bouton overgrowth

The basic features of basket cell innervation of pyramidal cells mature in cortical organotypic cultures (Chattopadhyaya et al 2004; Di Cristo et al 2004; Klostermann & Wahle 1999). Basket interneurons started out with sparse axons and small boutons at EP14 (EP, equivalent of postnatal), which developed into highly elaborate arbors and prominent perisomatic bouons at EP28. To examine the effect of blockade of transmission on axon growth and synapse development, I focused study between EP18 and EP24, when there was most significant and stereotyped maturation of perisomatic innervations.

I used a 10kb region of the GAD67 promoter P_{G67}-GFP (Chattopadhyaya et al 2007) to express GFP in basket interneuron in cortical slice cultures. Wild type cells are in slice cultures prepared from $Gad67^{flx/flx}$: $Gad65^{+/+}$ mice and transfected with P_{G67}-GFP; mutant cells are in slice cultures prepared from $Gad67^{flx/flx}$: $Gad65^{-/-}$ and transfected with P_{G67}-GFP/Cre. The biolistic transfection typically labeled less than ten isolated basket cells in the entire slice and therefore allowed me to visualize axons and synapses at high resolution. Also, since GABA synthesis was perturbed in only a few cells the global activity level of the slice is likely unaltered. Similar manipulation was done on $VGAT^{flx/flx}$ animals to generate single cell knock-outs of GABA release. Cortical slices were prepared from P3 mouse pups and transfected at EP18 (equivalent postnatal day 18 = P3 pups + 15 days in vitro), then imaged by confocol microscopy. Most of GFP-labeled boutons most likely represented presynaptic terminals as they contained synaptic marker GAD65 and they were confirmed by electron microscopy (Chattopadhyaya et al 2007).

In basket cells from Gad67$^{flx/flx}$: Gad65$^{-/-}$ cultures transfected with P_{G67}-GFP/Cre (referred as Gad-/- cells) from EP18 to EP24, the size and the projection pattern of axon arbors appeared similar to that of control cells. However, Gad-/- cells appeared to have a much denser axon arbor and many more boutons. In basket cell from VGAT$^{flx/flx}$ cultures transfected with P_{G67}-GFP/Cre (referred as VGAT-/- cells), the phenotype is largely similar to Gad-/- cells, indicating the effect is due to the blockade of GABA transmission (Fig. 2.1). Two sets of control basket cells are used – those from Gad67$^{flx/flx}$: Gad65$^{+/+}$ slice cultures transfected with P_{G67}-GFP and those from VGAT$^{flx/flx}$ slice cultures transfected with P_{G67}-GFP. These two groups were similar in all parameters (axon density, bouton density, bouton size) and were pooled as control cells. For another control, I used slice culture prepared from FVB mice and transfected with P_{G67}-GFP or P_{G67}-GFP/Cre, essentially I observed no discernable difference between the two groups (data not shown), indicating the usage of Cre construct does not introduce additional effects.

I then quantified axon density and interbouton distance. Axon density is defined as the percentage of the pixels containing GFP in the outline of the Z-projection of the axon arbor. Axon density is increased from 16.0 $\pm$ 1.3 in the control cells to 29.6 $\pm$ 2.1 in the GAD-/- cells and 26.7 $\pm$ 3.2 in the VGAT-/- cells. The interbouton distance is reduced from 3.1 $\pm$ 0.3 mm in the control cells to 2.3 $\pm$ 0.4 mm in the GAD-/- cells and 2.4 $\pm$ 0.2 mm in the VGAT-/- cells. These results suggest that GABA transmission has a role in refining axon arbor and bouton formation.

2.3 Blockade of GABA transmission in developing basket interneurons results in smaller and homogenous boutons

To investigate the effect of blockade of transmission on synapse maturation, I measured the bouton diameter. In slice culture, the average bouton size is significantly decreased from 0.8mm in controls to 0.6mm in mutants. Interestingly, although all the boutons demonstrated a normal distribution, mutant boutons have a much narrower distribution, with a significantly smaller variance (0.53 in control boutons versus 0.36 in GAD-/- boutons and 0.42 in VGAT-/- boutons), indicating the mutant basket interneurons have more, smaller boutons. (Figure 2.2 A1).

To examine whether transmission regulates the maturation of perisomatic synapses in adolescent visual cortex *in vivo*, I used a strain of adeno-associate virus expressing Cre and GFP (AAV-GFP-ires-Cre) to inactivate Gad67 in $Gad67^{flx/flx}$: $Gad65^{-/-}$ or inactivate VGAT in $VGAT^{flx/flx}$ mice. To make sure the manipulation sufficiently knocked out GABA synthesis from P18-P26, GABA level in AAV-infected basket cells was quantified. In the nearby uninfected visual cortex area, all the basket cells, identified by parvalbumin immunoreactivity, expressed GABA; whereas in the infected visual cortex area, all the basket cells, no longer express GABA (Figure 2.3).

Because AAV infected both interneurons and pyramidal cells in the cortex, I focused my analysis on perisomatic boutons as these boutons are exclusively from basket cells. In control mice, GFP labeled basket axon terminals surrounded NeuN-positive pyramidal cell somata with distinct perisomatic boutons at rather regular interbouton intervals. In $Gad67^{flx/flx}$: $Gad65^{-/-}$ mice infected with AAV-GFP-ires-Cre, boutons around pyramidal

cell somata were smaller and crowded. The most consistent and quantifiable effect was the significantly smaller size of perisomatic boutons (about 30% average reduction in bouton diamater; Mann-Whitney test, $p < 0.001$), a result consistent with those obtained in organotypic cultures (Figure 2.2).

These results suggest that neurotransmission has a role in regulating bouton size and possibly synapse maturation. Without out transmission, there were many more small boutons and possibly all weak boutons.

2.4 GABA depletion and GABA reduction result in opposite effects on axon development

Our lab has previously reported that reduction of GABA synthesis and transmission results in reduced bouton density and axon branches (Chattopadhyaya et al 2007). These phenotypes are opposite to the effect of GABA depletion that I observed. Thus I set out to determine how different level of GABA signaling influence basket cell axon and synapse development.

I carried out a series of characterization involving different combination of Gad67 and Gad65 alleles to vary GABA level and examine basket cells of each genotype (Figure 2.4). First, I confirmed the results described in (Chattopadhyaya et al 2007) that Gad65-/- basket cells do not have a distinguishable morphology in terms of axon branching and perisomatic synapses formation when compared to wildtypes. Second, I also confirmed that Gad67-/-: Gad65+/+ basket cells, which have reduced GABA level, have simpler axon morphology. Third, Gad67-/-: Gad65+/- basket cells have a simpler axon morphol-

ogy and they are not significantly different from Gad67-/-: Gad65+/+ basket cells, indicating even a low level of GABA is sufficient in regulating axon and synapse refinement.

These results confirm the previous finding in the lab and more importantly, elucidate how depletion and reduction of GABA signaling result in opposite effects. GABA signaling is involved in the competition among nascent synapses, so a reduction in GABA signaling results in overall smaller boutons. Complete blockade of GABA signaling inactivates this competition process and therefore no synapse validation, maturation and elimination can occur. As a result, basket interneurons have more boutons and grow a much denser axon arbor.

2.5 Transmission deficient boutons contain presynaptic markers and co-localize with postsynaptic markers

To have more insights into the molecular identities of these excessive mutant boutons, I used immunohistochemistry method to examine whether some known pre/post inhibitory synaptic markers still colocalize with them.

For pre-synaptic markers, I chose to examine VGAT in Gad-/- cells and Gad65 in VGAT-/- cells. In controls, 90% of GFP labeled boutons colocalize with VGAT/Gad65; in the knock outs, 82% Of GFP labeled boutons colocalize with VGAT in Gad-/- and 75% Of GFP labeled boutons colocalize with Gad65 in VGAT-/- (Figure 2.5). This suggests that the localization of VGAT/Gad65 may be an early event preceding activity dependent regulating stage of synaptogenesis. For post-synaptic markers, I chose to examine Gephyrin and $GABA_A$ receptors b2. They appear to be still opposing GFP

labeled mutant boutons and even in a greater number. The possible increase in postsynaptic markers could be explained by homeostasis as demonstrated in cultured rodent neurons (Turrigiano & Nelson 2004). In these systems, decreased postsynaptic activity leads to an increase in synaptic size or efficacy. Therefore, inactivity at the presynaptic site might lead the postsynaptic site to increase receptor expression.

These results suggest that first, inhibitory synaptic markers such as VGAT/Gad65 and Gephyrin and $GABA_A$ cluster independent of neurotransmission; second, intrinsically basket cell axon can generate many more boutons and these excessive boutons are capable of attracting some synaptic components.

2.6 Transmission depleted basket cell axons express less and homogenous level of activity-dependent cell adhesion molecule neurexin 1b

Neurexins and neuroligins are important organizing molecules of synapses in mammalian brain. They function as activity dependent cell adhesion molecules, transducing information across synaptic cleft. Neurexin can trigger formation of postsynaptic differentiation (Graf et al 2004). Curiously, KO animals of neurexins or neuroligins demonstrate a more obvious defect in inhibitory synapses than in excitatory synapses (Etherton et al 2009; Varoqueaux et al 2006), indicating the neurexin/neuroligin signaling may be more essential in inhibitory synapse formation.

To examine how transmission affects cell adhesion molecule in inhibitory axon terminals, we expressed a pH-sensitive GFP fused neurexin-1b in mutant and control basket cells. Because the GFP is pH sensitive, the construct not fluoresce when it is

inside vesicle but only fluoresce when the construct is inserted into the membrane and exposed to extracellular environment (Li et al 2005). Therefore with the GFP signal, we are examining membrane inserted neurexin molecules, which are potentially interacting with post-synaptic neuroligin.

In the controls, neurexin is concentrated in axonal boutons, occupying a large area of bouton. In mutants without GABA transmission, neurexin still is specifically expressed in axonal boutons, but occupying a much reduced area of bouton. As quantified, in mutants the neurexin punctas are of significant smaller size and more homogenous sized (Figure 2.6). This phenotype is remarkably similar to the phenotype of smaller size in bouton morphology.

These results suggest that the transmission-depleted boutons do contain low level of synaptic adhesion molecules, indicative of low level of postsynaptic interaction. The mutant boutons are probably all immature boutons.

2.7 Mutant bouton is still a bona-fide inhibitory synapse

With ultrastructual study by electron microscopy, we observed that mutant bouton forms symmetric synapse, which contains active zone, vesicles and mitochondria, typical of perisomatic inhibitory synapse (Figure 2.7). The plan is to compare the parameters such as vesicle numbers and active zone size. If active zone size reflects synaptic strength and maturation, the prediction is that mutant boutons have overall smaller active zone

size and more homogenous distribution, indicating these mutant synapses are weak, nascent synapses.

2.8 Synaptophysin-GFP labels presynaptic terminal in basket cell axons

First, I examined whether I can use Synaptophysin-GFP to label pre-synaptic terminals. I used a plasmid, which has the P_{G67} promoter driving a fusion of enhanced GFP to the C terminus of synaptophysin, a major synaptic vesicle membrane protein. Various groups have used Syn-GFP to label presynaptic terminal in different kinds of neurons in different species (Kelsch et al 2008; Meyer & Smith 2006; Nakata et al 1998; Ruthazer et al 2006). In basket cell axon, Syn-GFP appears to have a discrete, punctate pattern, colocalize with varicosity (Figure 2.8 A). Also, inhibitory synapse postsynaptic marker Gephyrin is juxtaposed to Syn-GFP puncta (Figure 2.5 C).

Then I examined the expression pattern of Syn-GFP in mutant basket cells of which the GABA transmission is depleted. Syn-GFP labeling still appeared to be punctuated. Moreover, consistent with the result of increased linear density of varicosities, linear density of Syn-GFP puncta was also significantly increased (Figure 2.8 C, D). As synaptophysin represents the accumulation of synaptic vesicles at presynaptic terminal, these results suggest that 1) vesicle clustering is not affected by the depletion of synaptic activity; 2) synaptic transmission plays a function in refining vesicle-clustering sites.

2.9 GABAergic synapses develop in a dynamic fashion with simultaneous puncta formation and elimination

To characterize the dynamic process of synapse development in basket cell, I chose to transfect cultured slices at EP16 and image at EP19, the peak stage of bouton number addition. Because synapses can develop in the time frame of minutes, I used a rapid imaging protocol to image the Syn-GFP puncta every minute for a total of 60 minutes.

I observed some puncta shuffling events at this stage (Figure 2.9 A1). The puncta were quite dynamic and frequently move, appear and disappear. Profile plot showed that along a stretch of axon, the intensity profile fluctuated significantly overtime (Figure 2.9 A2). Although there was only 1.1 $\pm$ 0.5% puncta net gain at the end of the imaging session, many more transient puncta appeared at some point. To quantify, I traced the axons and counted the puncta to calculate average puncta distance (mm). Indeed, the average puncta distance is not significantly changed from t0 (3.5 $\pm$ 0.2 mm) to t60 (3.4 $\pm$ 0.2 mm).

This result shows that similar to other developing axons (Ruthazer et al 2006), basket cell axons also have Syn-GFP form and disappear simultaneously. In our system, at this developmental stage, the Syn-GFP is likely to represent presynaptic side of synapse formation.

2.10 Absence of synaptic transmission results in increased puncta stabilization at transient contact sites

To investigate the role of synaptic transmission in regulating Syn-GFP puncta dynamics, I imaged Gad-/- or VGAT-/- cells at EP19 (transfected with Cre recombinase at EP16) and used the rapid imaging protocol aforementioned to image the Syn-GFP puncta every minute for a total of 60 minutes.

In these mutant cells, I observed that puncta are overall more stable with less puncta shuffling events (Figure 2.9 B1). The existing puncta mostly stay with some new puncta appear in between the existing puncta. Profile plot showed that along a stretch of axon, the intensity profile preserve the peaks representing puncta overtime (Figure 2.9 B2). There is about 5.2 $\pm$ 1.7% puncta net gain at the end of the imaging session. The average puncta distance is not significantly changed either, from t0 (2.5 $\pm$ 0.2) to t60 (2.4 $\pm$ 0.2).

Since Syn-GFP puncta exhibit an exploring behavior, I hypothesized that the exploration sites for the axon is intrinsic and could be the same in the control and mutant axons. To quantify the exploration behavior, I defined a parameter called the minimum average interpuncta distance. It is calculated by taking a stretch of axon, dividing the axon length (mm) to the maximum number of Syn-puncta appeared on the axon in the 60 minute imaging period, then another stretch of axon is analyzed until all the imaged axon arbor is finished. Interestingly, the minimum average inter puncta distances in the control (2.7 $\pm$ 0.2), GAD-/- (2.5 $\pm$0.2) and VGAT -/- (2.5 $\pm$ 0.2) cells are not significantly different (Figure 2.9 C), suggesting that axon can form transient synapses at similar density with or without neurotransmission. Also the minimum average inter puncta distances in the

GAD-/- and VGAT -/- cells are not significantly different from the t60 inter puncta distances, suggest that the reason that GAD-/- and VGAT -/- cells have higher syn-GFP puncta density is because in this mutant axons, syn-GFP is form at the majority of the potential synaptic sites.

Taken together, these results indicate that during synapse formation, synaptic vesicle clusters could form at many more sites throughout the axon length but they are determined by transmission to be stabilized only at certain sites.

2.11 Blockade of GABA transmission results in less elimination of Syn-GFP puncta

To find out whether basket cell axon have a period demonstrating synapse refinement, I used live imaging to observe Syn-GFP puncta at EP24 (transfect at EP21). Around EP24 boutons numbers are approaching stable and mostly the growth is manifested in bouton size increase. Therefore at EP24 I may observe some phenomenon of refinement. Every 15 minutes a 2-photon z-stack was taken for a total of 2 hours. Images were sampled at 1mm Z interval to make sure the majority of puncta were imaged. Images were projected, threshold according to custom algorism and binerated to generate a mask which outline the contour of puncta. Puncta were tracked individually overtime. Then the outline mask was retrofitted to the original grayscale image to determine puncta average intensity.

Our time-lapse analysis revealed that the majority of the synaptic clusters remained stable over 2 hours (Figure 2.10 A1). On average, 93.0 ± 4.8 % of synaptic clusters were stable (n = 5 cells). Synaptic clusters were also added and lost between two-hour observa-

tion intervals. On average, 3.0 ± 0.9% new clusters were added, whereas 8.8 ± 4.9% clusters were eliminated. Thus, axons experienced a net 5.8% decrease in synaptic clusters every 2 hours. However, in VGAT-/- cells, 97.6 ± 1.0 % of synaptic clusters were stable (Figure 2.10 B1). On average, 8.5 ± 2.0 % new clusters were added from one observation interval to the next, whereas 2.4 ± 1.0% clusters were eliminated. Thus, axons experienced a net 5.7% increase in synaptic clusters every 2 hours (Figure 2.10 C). Analysis on puncta intensity revealed that the loss puncta or the newly formed puncta all have lower fluoresecent intensity. Since Syn-GFP puncta intensity reflects vesicle numbers (Ruthazer et al 2006), I interpret as that this indicate when puncta disappear or appear, vesicles disperse or accumulate.

These results suggest that lack of neurotransmission reduces the elimination of transient contact and results in increased Syn-GFP puncta stability and density.

2.12 The absence of neurotransmission induces more filopodia in developing basket cell axons

Filopodia are considered as the active searching "fingers" of axon to sample local environment and form transient synaptic contacts. A subset of filopodia will become future branches (Hua et al 2005). Because of the axon overgrowth phenotype at the end point (Figure 2.1), I hypothesized that in mutants, there are more filopodia.

It is highly likely that the mechanisms underlying activity-dependent axon elaboration and synapse development are shared. Ca^{2+} entry at presynaptic sites may promote depolymerization of actin and microtubules and reorganization of the cytoskeleton necessary for the emergence of new branches (Lautermilch & Spitzer 2000; Tang et al

2003). Indeed, local Ca2+ transients in growing retinal ganglion cell axons in Xenopus precede branch initiation (Edwards & Cline 1999). Moreover, the accumulation of vesicles may provide membrane components required for extension of new branches. Synaptic proteins were shown to localize at branch points (Alsina et al 2001; Niell et al 2004). The postsynaptic sites may also provide retrograde signaling cues, which trigger axon branch formation, and adhesion molecules, which stabilize axon filopodia.

I observed that most filopodia (82.2 ± 6.3%) appeared at structurally identified boutons and Syn-GFP presynaptic puncta. Also some filopodia do become branch (data not shown). These results suggest that the stability of Syn-GFP puncta may be related to filopodia formation, and subsequently, branch formation.

I used GFP to label axon processes at EP16 and examined filopodia dynamics at EP19. Time-lapse Z-stack images were taken every 10min for 3 hours. Here, I defined filopodia as processes of 0.3-1.5mm length that grow from the axon. In mutants, the filopodia densities are significantly increased when compared to control (0.09 $\pm$ 0.02 / mm, 0.08 $\pm$ 0.01 / mm versus 0.05 $\pm$ 0.01 / mm, Figure 2.11).

The result suggests that without transmission, basket cell axon extend more filopodia to search for postsynaptic target, which may be a homeostasis response from inactivity at the presynaptic side. Unfortunately, we could not infer the branching information from this experiment. Filopodia did not contribute much to axon arbor growth (<1% gain in axon total length) either in control or mutant. Therefore it is necessary to conduct longer term imaging to observe branch dynamics.

2.13 Basket cell axons grow recurrently over days and axon extension dominates basket cell axon arbor growth dynamics in the absence of transmission

I would like to determine in basket cells if synapse connection is established in a dynamic manner with trial and error. Basket cell could grow axons in a sequential manner, with two distinctive phases of axon formation and axon elimination; or in a recurrent manner, with axon formation and elimination happening simultaneously. As chronic blockade of activity profoundly increased axon density, I want to explore how this phenotype is achieved, whether by increasing axon growth or decrease axon retraction or both. The findings are likely to provides insights on how basket axon control its growth to achieve a complex, highly ordered arbor that innervate hundreds of pyramidal cells and how synaptic activity act to guide axon growth.

In order to determine the growth pattern of basket cell axon arbor, I collected two-photon time-lapse images of GFP-labeled axons over a period of three days in organotypic slice cultures. I tracked the axon arbor structure and followed the fate of each dynamic branch. In total I characterize the dynamics of 88 branches from 9 cells. Figures 2.12 A shows an example of a cell imaged for 3 consecutive days. Branch behaviors were categorized according to the changes in length of individual branches between day 1 and day 2 as well as day 2 and day 3. I classified different branch dynamic behaviors into four categories (Figure 2.13). Branches that were present on all three days but became longer were termed “extended.” Branches that did not exist on day 1 but were newly added were termed “added.” Branches that were seen on all three days but became shorter were

termed “retracted.” Branches that were detected on day 1 and disappeared were termed “lost.” I distinguished the different dynamic branch behaviors based on data suggesting that the cellular mechanisms underlying de novo branch addition are different from extension of existing branches (Sin et al 2002).

The proportions of branch behavior are balanced for dynamic branches: 14.5% added, 40% extended, 11% lost, and 34.5% retracted (Figure 2.14). The average change in lengths of branch extensions and retractions favors extension (+12 mm and –6 mm), and average change in lengths of added and lost branches are comparable (+2 mm and –2 mm). These data indicate that, basket cell axon branches are highly dynamic, during development both addition/extension and lost/retraction happens simultaneously with equilibrium. Overall the axon growth favors positive growth.

Base on the observation that absence of GABA transmission results in excessive axons, I set out to determine how axon grows differently without GABA transmission. The increase in axon arbor density could be due to increased proportions of branches that are either added or extended, or decreased proportions of branches that are either retracted or lost or both.

I tested whether the difference in arbor growth rates is due to a change in the proportion of branches exhibiting each behavior. Neurons in which GABA transmission is ablated exhibit significantly different branching behaviors compared to wild-type controls (Figure 2.14 C; $\chi 2$ test; $p < 0.001$). I observed a doubling of the frequency of the branch extension and 50% reduction in retraction and lost events, however, the frequency

of branch addition is not significantly changed. This increase in growth rate could also result from an increase in average change in branch length. I found both branch addition and extension groups increased their contribution to axon growth about one fold, from +8 mm/day to +17 mm/day and from +13 mm/day to +28 mm/day, respectively; while neither branch lost or retraction group was significantly different, from -12mm to -14mm and from -13mm to -15mm. Overall, the average branch length change greatly favors positive axon growth in knockouts. In the absence of GABA transmission, branch extension is at an accelerated rate while branch retraction becomes less frequent.

These results suggest that in normal development, axon grow in a balanced, recurrent fashion and prior to extension, branches are verified in a mechanism that involves transmission. GABA transmission promotes the elimination of inappropriate transient synapses and pruning of branches bearing inappropriate contacts.

2.14 GABA transmission is also important for the maintenance of perisomatic synapses

To examine whether GABA transmission is required to maintain basket cell axon arbors and perisomatic innervation, I inactivated both Gad67 and Gad65 alleles in basket interneurons from EP26–32, after the mature innervation pattern had been established (Chattopadhyaya et al 2004). Comparison between cells in $Gad67^{lox/lox}$: $Gad65^{+/+}$ cultures and $Gad67^{lox/lox}$: $Gad65^{-/-}$ cultures transfected with P_{G67}-GFP and P_{G67}-GFP/Cre showed a significant reduction in axon density and bouton size (Figure 2.15). This result is in contrast to the effect of just deleting Gad67 at the same period (Chattopadhyaya et al 2007), which does not yield a different morphology compared to control. This result

suggests that GABA transmission is necessary for the maintenance of perisomatic innervations.

2.15 Absence of GABA transmission does not alter the intrinsic biophysical properties of basket cell.

To make sure that depletion of GABA synthesis does not grossly change basket cell's physiological properties and the phenotype observed is not due to a cell wide response, I collaborated with Dr. Jiangteng Lu to use electrophysiology to compare the intrinsic properties of control and Gad-/- basket cell. We identified basket cell by GFP labeling of the axon morphology and patched on the cell with the guidance of the highly fluorescent cell body. Standard resistance test was conducted to extract parameters such as Ri (input resistance) and Ra (access resistance) to calculate Rm (membrane resistance). The action potential test is a sensitive test of intrinsic ion channel compositions. We mainly tested action potential half width. Because basket cell demonstrate unique physiological property of fast spiking; we also tested the fast spiking ability by calculating an adaption index. All the results are shown in Figure 2.16. These results showed that Gad-/- cells are not significantly different from control cells with regards to various intrinsic biophysical properties and therefore exclude the possibility that non-specific cell wide effect is elicited in the Gad-/- cells.

2.16 Pharmacology rescue demonstrated that $GABA_A$ signaling is possibly involved in the synapse elimination process

Chronic blockade of GABA transmission caused a profound increase in axon and bouton density. To examine whether the overgrowth phenotype involves GABA signaling at the postsynaptic side, I investigated whether an activation of $GABA_A$ receptor was

able to rescue the overgrowth phenotype of GAD -/- or VGAT -/- basket cells. $GABA_A$ receptor is mostly located at the postsynaptic side of inhibitory synapse (Kullmann et al 2005). Usually one pyramidal cell in the neocortex receives multiple inputs from basket cells (Somogyi et al 1983a). By increasing receptor sensitivity, the postsynaptic $GABA_A$ receptor opposing the transmission depleted presynaptic boutons could be activated by nearby tonic/spillover level of GABA.

To achieve this, I added the $GABA_A$ receptor agonist diazepam (10 μM) in the culture medium when $Gad67^{lox/lox}$: $Gad65^{-/-}$ slice cultures were transfected with P_{G67}-GFP/Cre between EP18 and EP24. Diazepam is an allosteric modulator of $GABA_A$ receptors that is able to discriminate between activated and nonactivated receptor states and enhances the GABA signaling. While diazepam treatment of control basket cells did not significantly affect the basic characteristics of perisomatic synapses, diazepam-treated VGAT–/– basket cells showed axon density much closer to a control basket cell. The interbouton distance was also rescued to levels comparable to control. The size and shape of diazepam treated boutons in VGAT-/- cells are larger and not significantly different from controls (Figure 2.17).

These results suggest that first, GABA transmission probably act partially through post-synaptic $GABA_A$ receptor, possibly through retrograde signaling to instruct axon/bouton growth on presynaptic basket cell axons; second, the overgrowth phenotype is probably indeed caused by no GABA transmission, as manipulation on the downstream $GABA_A$ receptor could reverse the phenotype.

2.17 Discussion

Summary

In this study, I studied basket cell axon and synapse development in the absence of GABA transmission to learn what aspect of synapse and axon development is dependent on neurotransmission. The array of phenotypes I observed included (1) increased axon density, (2) increased bouton density, (3) smaller and more homogenous bouton size, (4) boutons express less and more homogenous level of activity dependent cell adhesion molecule Neurexin (5) bouton is bona fide synapse examined by electron microscopy (6) bouton still process basic synaptic markers, and possibly there is an increase in postsynaptic components.

To elucidate the mechanism of how the absence of GABA transmission induces such phenotypes, I used live time-lapse imaging to follow axon growth and synaptophysin-GFP labeled puncta dynamics. I observed (1) Synapse patterning develops in a concurrent manner, with Syn-GFP puncta formation and elimination happening simultaneously, (2) Without transmission, puncta are more stable and puncta appear in all intrinsic sites, (3) Without transmission, more filopodia are observed, (4) axon grow in a balance manner, with incidence of addition/extension events more or less equal with lost/retraction event, (5) without transmission, axon greatly favors axon extension events and cuts back half of lost/retraction events.

These results demonstrated that neurotransmission is not necessary for basic synapse formation such as vesicle clustering, localization of some pre and postsynaptic components. However, neurotransmission is necessary for activity-dependent synapse

validation, maturation and elimination. Such activity dependent synapse formation and patterning in turn regulate branch extension, pruning and thus the development of axon arbor. My model on the role of GABA transmission in inhibitory synapse and axon development is illustrated in Figure 2.18.

Comparison with other related studies

Comparing to the previous studies, my conclusion agrees well with the outcome of genetically depleting neurotransmitter release in mammalian neuromuscular junction (Brandon et al 2003; Misgeld et al 2002). My conclusions are somewhat at odds with the findings that inhibitory synaptogenesis was normal in knock out mice lacking the vesicular GABA transporter VGAT or vesicular priming protein Munc 13, 18 (Varoqueaux et al 2002; Verhage et al 2000; Wojcik et al 2006). However, all these germ line knockout animals die around birth, thus precluding the analysis of brain regions in which synaptogenesis occurs postnatally. Plus these germ line knockouts change global activity in the CNS. Later careful follow up studies revealed similar nerve overgrowth phenotype in Munc13 KO mouse neuromuscular junction (Varoqueaux et al 2005). More filopodia per growth cone were observed in Munc18 null cell prepared from Munc18 KO (Broeke et al 2010).

My conclusion is also different from the findings in other organism. In C.elegans, there is only one gene *unc-25*, which encodes glutamic acid decarboxylase (GAD), the GABA biosynthetic enzyme. In *unc-25* mutants the GABAergic neurons have normal axonal trajectories and synaptic connectivity, and the size and shape of synaptic vesicles are normal. Therefore GAD activity and GABA are not necessary for the development or

maintenance of synaptic connections in C. elegans (Jin et al 1999). The difference between these two studies could be due to the organism examined. Mammalian CNS matures in a prolonged period and is activity regulated not only during development but also in adulthood (Goodman & Shatz 1993; Holtmaat & Svoboda 2009). It is likely that synaptic connections are hard wired by genetic factors in C. elegans, but are determined by a combination of genetic and activity dependent factors in the mammalian brain.

There are also studies manipulating postsynaptic $GABA_A$ receptors and examined presynaptic innervation. One study depleted $GABA_A$ receptor g unit in Punkinje cell and examined synapse formation on Punkinje cell dendrites (Patrizi et al 2008). Loss of $GABA_A$ receptors causes a slowdown in the formation of inhibitory synapses. However, activity dependent adhesion molecule NeuroLigand2 (NL2) still colocalize with the formed synapses. Another study use RNA interference to knock down the delivery of $GABA_A$ receptor on the pyramidal cell and examined presynaptic markers (Fang et al 2006). They showed that knock down of postsynaptic $GABA_A$ receptor clusters leads to a nearly complete loss of GABAergic innervation. The difference between their study and my study is that (1) whether GABA transmission is completely removed. Since postsynaptic $GABA_A$ receptor has many subunits and many combinations could constitute a functional receptor, it is difficult to make sure all the $GABA_A$ receptor are depleted. (2) Whether GABA transmission is depleted in a single cell manner in an intact circuit. The purkinje cell study essentially knock out all $GABA_A$ receptor g unit in cerebellum and thus cause a global activity change. The RNA interference study used dissociates cell culture system where the synaptic connections are artificially sparse. In the slice culture system, one basket cell is connected to hundreds of pyramidal cells and multiple basket

cells innervate one pyramidal cell. These key differences in manipulation and experimental preparation could explain the discrepancy in our findings.

Dynamic properties of basket cell axon and synapse development

Unlike mammalian neuromuscular junction, basket cell axon does not undergo formation and elimination in a sequential manner. As shown in my live imaging results, Syn-GFP puncta, some of which represent nascent synapses, are tested and then either stabilized or eliminated within minutes. This testing process possibly involves synaptic transmission. Without transmission, Syn-GFP puncta form at all intrinsic testing sites and results in an excessive amount of boutons. Basket cell axon also extends filopodia from presynaptic terminals and some filopodia do become future branches. In mutant cells, there are more filopodia, indicating a presynaptic homeostasis effect to reach out for postsynaptic contacts. Also correlated is the increased stability of presynaptic puncta in mutant cells, which suggest that maybe synaptic transmission could regulate filopodia or branch extension by increasing stability of presynaptic puncta. Similarly, basket cell axon also grows in a equilibrium, with branch addition and extension portioned equal to branch lost and retraction. Without transmission, axon grows much faster and reduces branch lost and retraction. These results suggest that synaptic transmission could destabilize a subset of synapses and therefore curb some intrinsic axon growth.

Limitation

Finally, I note some limitations of my study. First, although I used two genetic methods to manipulate neurotransmission, the end result are both that there is no GABA on

either the presynaptic site or postsynaptic site. There might still be some other function of GABA that could contribute to the phenotype. However, the overgrowth phenotype observed in neuromuscular junction study in ChAT-/- mice without transmitter acetylcholine is very similar to the phenotype observed here, argue against other specific function of GABA in regulating synaptic connections. Second, the genetic manipulation depletes GABA transmission in a whole cell, which is less ideal than manipulating just a segment of axon. There was report on dendritic release of GABA (Isaacson 2001), which is disrupted by the genetic manipulation as well. Third, it is difficult to track the exact time course of genetic manipulation. For example, it is not clear after the transfection, when axon stops releasing GABA. The answer has to do with the half life of Gad67 or VGAT protein as well as how long exactly it takes for the Cre recombinase to delete floxed alleles, which is hard to assay in the slice culture.

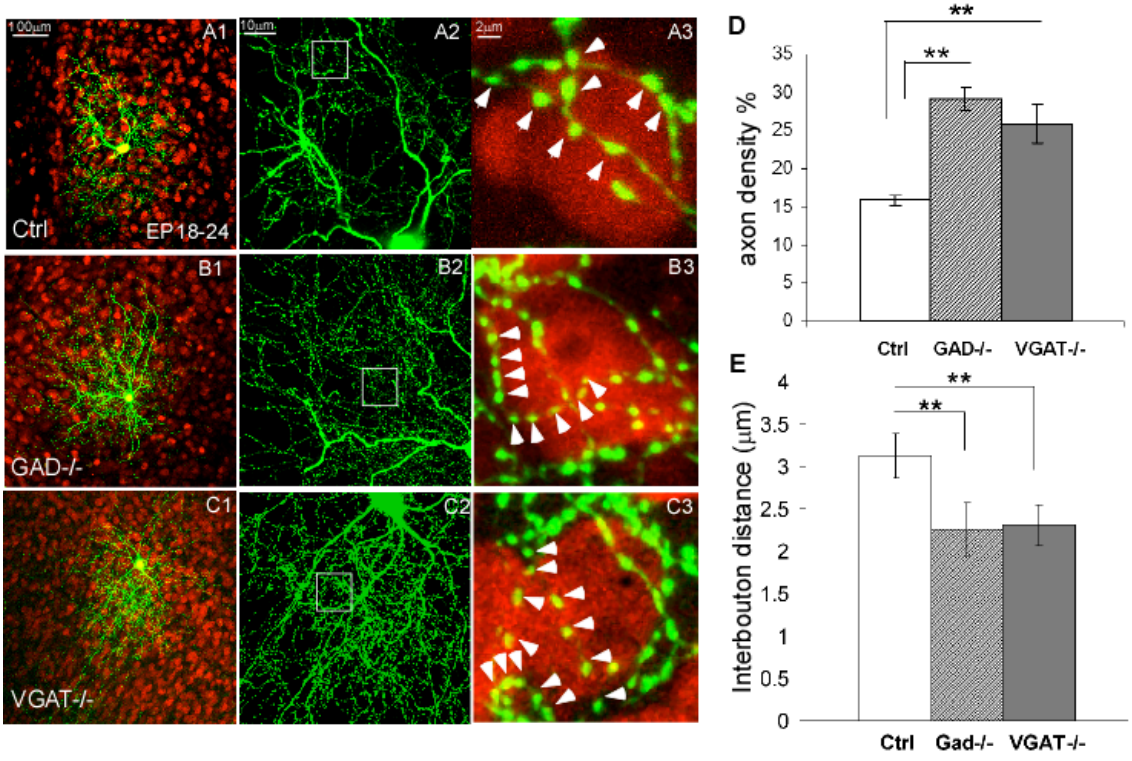

Figure 2.1 Blockade of GABA transmission in developing basket interneurons results in axon and bouton overgrowth

(**A1**) A control basket cell (green) at EP24 with extensive axon branching and innervate hundreds of nearby pyramidal cells, with boutons along axons (A2), terminal branches, and clustered boutons (arrowheads) around pyramidal cell soma (A3; NeuN immunostaining, red).
(**B1**) A GAD-/- basket cell shows overall similar arbor size but clear increase in axon density (B2), increase in boutons density (B3; arrowheads) and decrease in bouton size (B3).
(**C**) Inactivation of the VGAT gene in basket cells yields a phenotype comparable to GAD-/- cells.
(**D**) Axon density percentage are significantly increased in GAD-/- and VGAT-/- cells when compared to controls (n=10 basket cells for each group, one-way ANOVA, post-hoc Dunn's test, $P < 0.001$).
(**E**) Interbouton distances are significantly reduced in GAD-/- and VGAT-/- cells compared to controls (n=10 basket cells for each group, one-way ANOVA, post-hoc Dunn's test, $P < 0.001$)

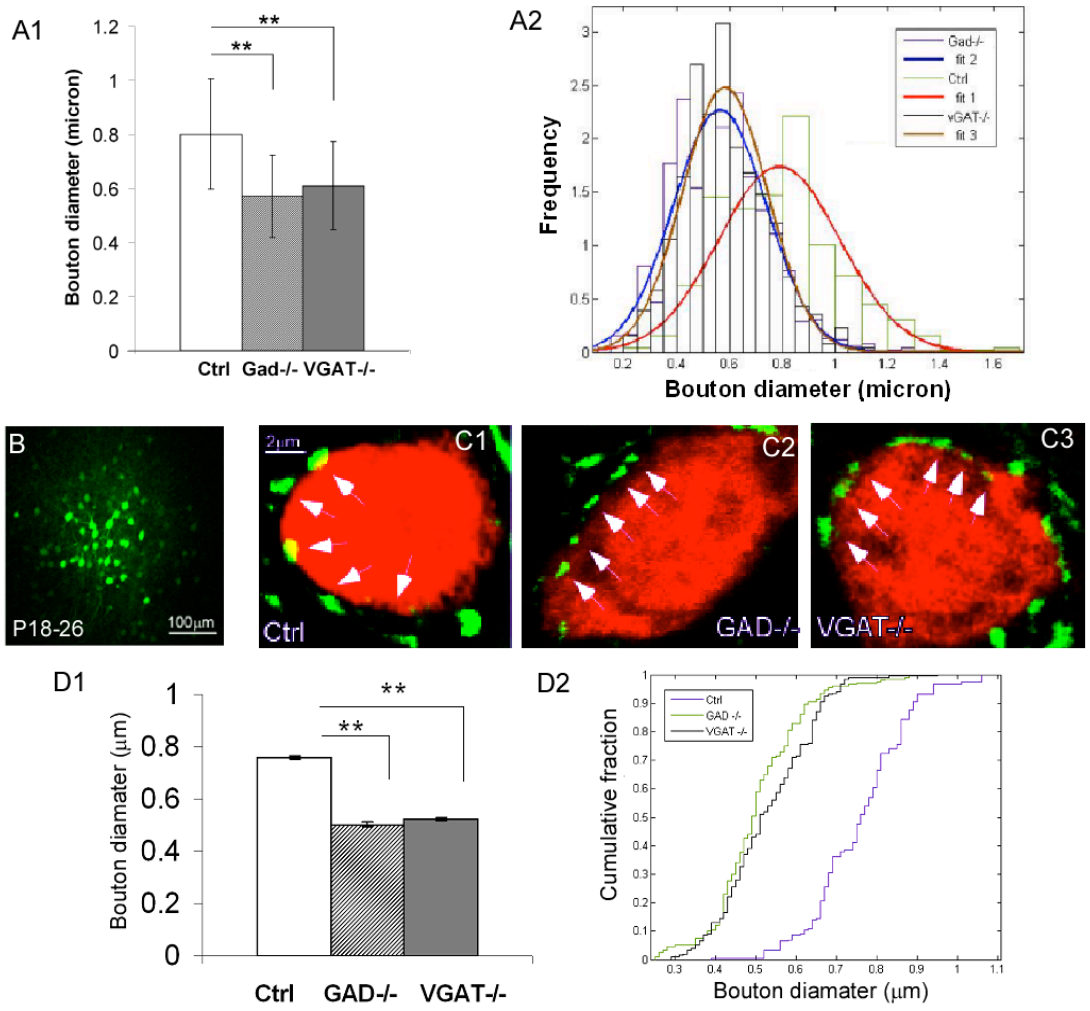

Figure 2.2 Blockade of GABA transmission in developing basket interneurons reduces bouton size

(A1) Perisomatic bouton sizes are significantly reduced in GAD-/- and VGAT-/- compared to controls (10 cells for each group and 200 perisomatic boutons from each cell; one-way ANOVA, post hoc Dunn's test, $P<0.001$). Error bar represents standard deviation (SD).

(A2) Bouton distributions in all three groups are normal distributions. Note that the spread (half width) of the distribution in GAD-/- and VGAT-/- groups are narrower than the control group.

(B) A representative infected area of AAV-GFPiresCre after 8 days, note that the virus only infected a small local area in the visual cortex.

(C) Infected GAD-/- (C2) and VGAT-/- cells (C3) in the visual cortex have smaller perisomatic boutons (arrows) around pyramidal cell soma (NeuN, red) as compared to control cells (C1). Note that the interval between boutons appears reduced in these mutant cells.

(D1) Perisomatic boutons sizes are significantly reduced in infected GAD-/- and VGAT-/- cells when compared to controls (3 animals for each group, 200 boutons from each animal; one-way ANOVA, post hoc Dunn's test, $P<0.001$). Error bar represents standard error mean (SEM). (D2) The cumulative distribution of bouton size in mutant cells in vivo is shifted towards the smaller size.

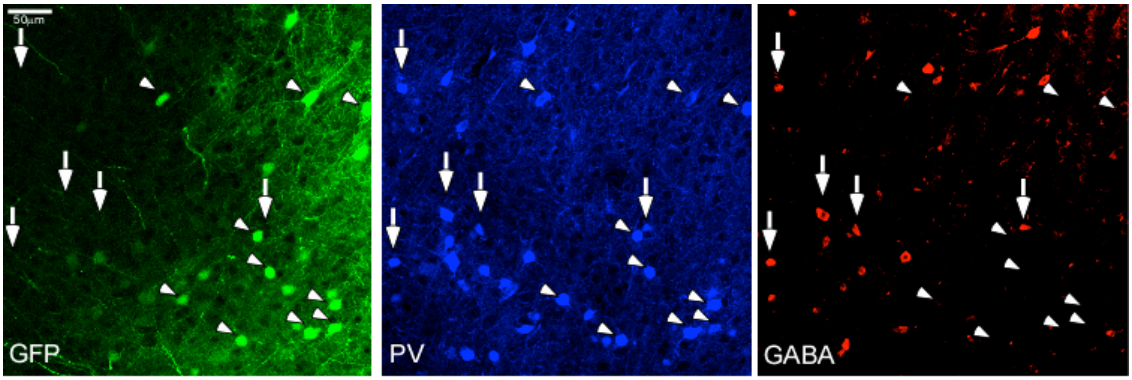

Figure 2.3 AAV-GFP-ires-Cre knock out GABA synthesis from P18-P26

Infected basket interneurons in GAD67flx/flx: GAD65-/- mice (arrowheads; blue, parvalbumin (Pv) immunostaining), show no GABA immunostaining (red) 7 days after injection compared to neighboring untransfected basket cells (arrows).

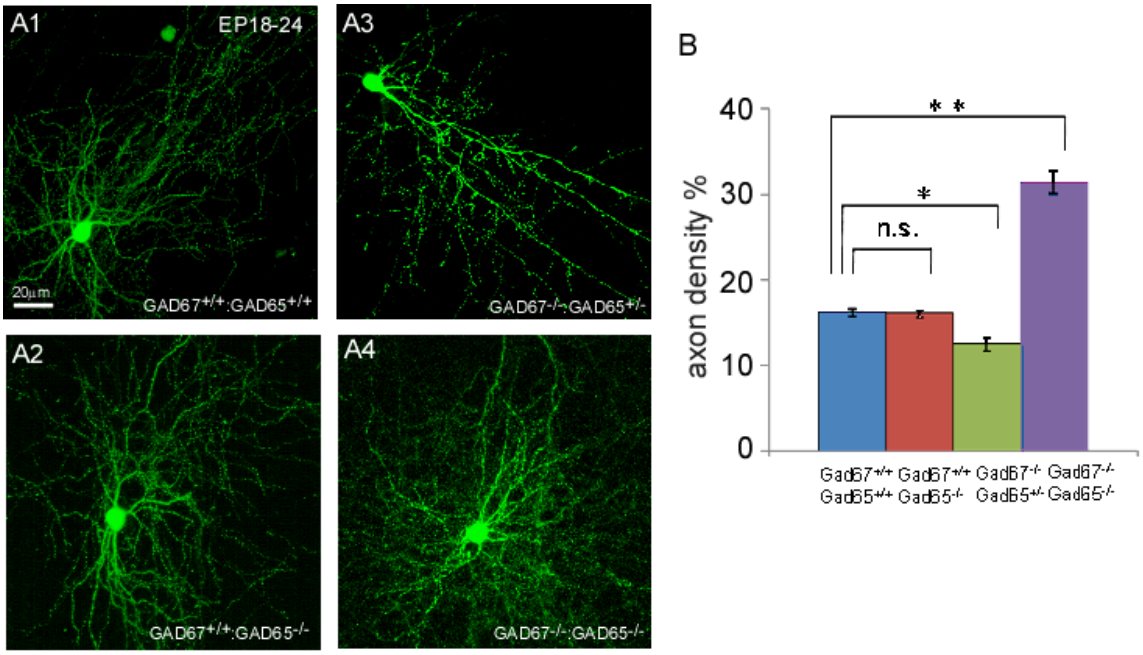

Figure 2.4 GABA reduction and GABA depletion result in opposite effects on axon and bouton development

(A1) An example of GAD67+/+: GAD65+/+ basket cell with a complex axon arbor at EP24;
(A2) An example of GAD67+/+: GAD65-/- basket cell with a comparable axon arbor to cell in (A1); GAD65 deletion showed little effects on axon and synapse development.
(A3) An example of GAD67-/-: GAD65+/- basket cell, which shows a much simpler axon arbor than cell in (A1);
(A4) An example of GAD67-/-: GAD65-/- basket cell with a much more complex axon arbor than the control cell in (A1).
(B) The comparison of axon density percentages in basket cells that have different GABA levels (n=5 cells for each group). The axon densities of GAD67+/+: GAD65+/+ and GAD67+/+: GAD65-/- are not significantly different ($P>0.1$, Mann-Whitney test). There is a significant decrease of axon density in GAD67-/-: GAD65+/- cells than GAD67+/+: GAD65+/+ cells ($P<0.05$, Mann-Whitney test). There is a highly significant increase of axon density in GAD67-/-: GAD65-/- compared to GAD67+/+: GAD65+/+ cells ($P<0.001$, Mann-Whitney test).

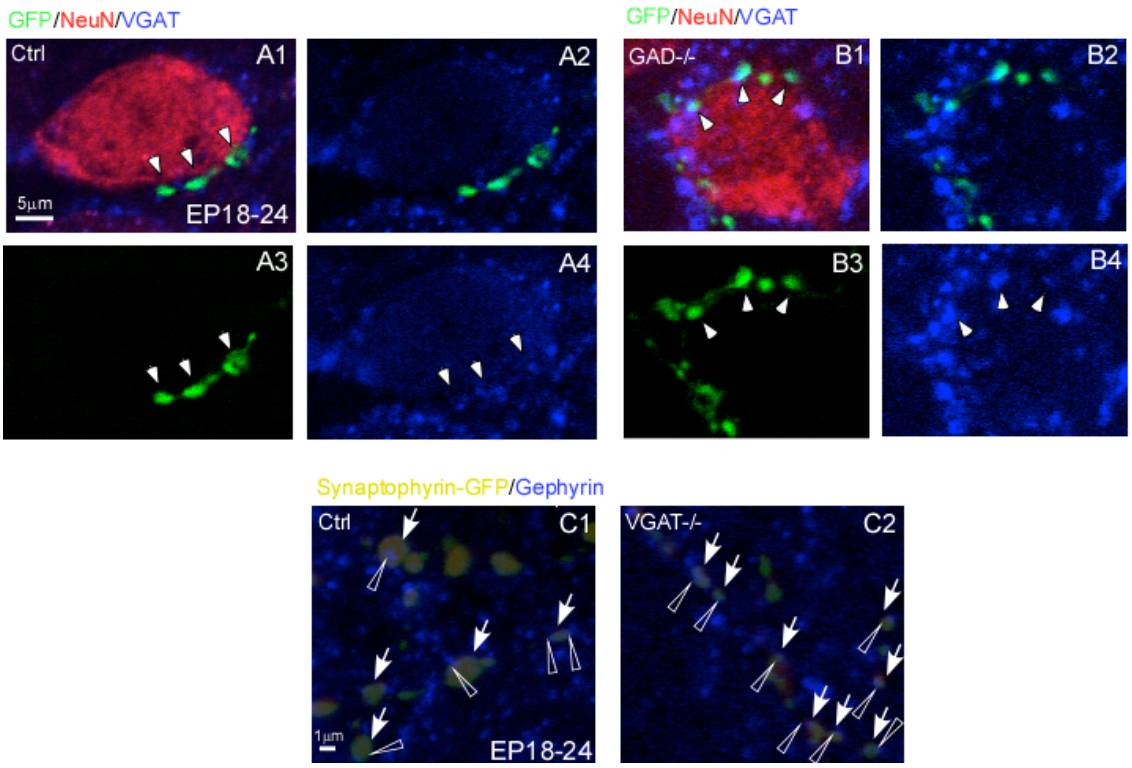

Figure 2.5 Transmission deficient boutons contain presynaptic markers and co-localize with postsynaptic markers

(A) Perisomatic boutons (arrowhead, in green) from control basket cell colocalize with presynaptic marker VGAT. GFP signal (A3) and VGAT immunostaining (A4) overlap (A2).

(B) Perisomatic boutons (arrowhead, in green) from GAD-/- basket cell colocalize with presynaptic marker VGAT. GFP signal (B3) and VGAT immunostaining (B4) overlap (B2).

(C1) Presynaptic punctas (arrow, in yellow) from control basket cell have opposed postsynaptic marker Gephyrin (empty arrowhead, in blue).

(C2) Presynaptic punctas (arrow, in yellow) from VGAT-/- basket cell, although much smaller in size, still have opposed postsynaptic marker Gephyrin (empty arrowhead, in blue).

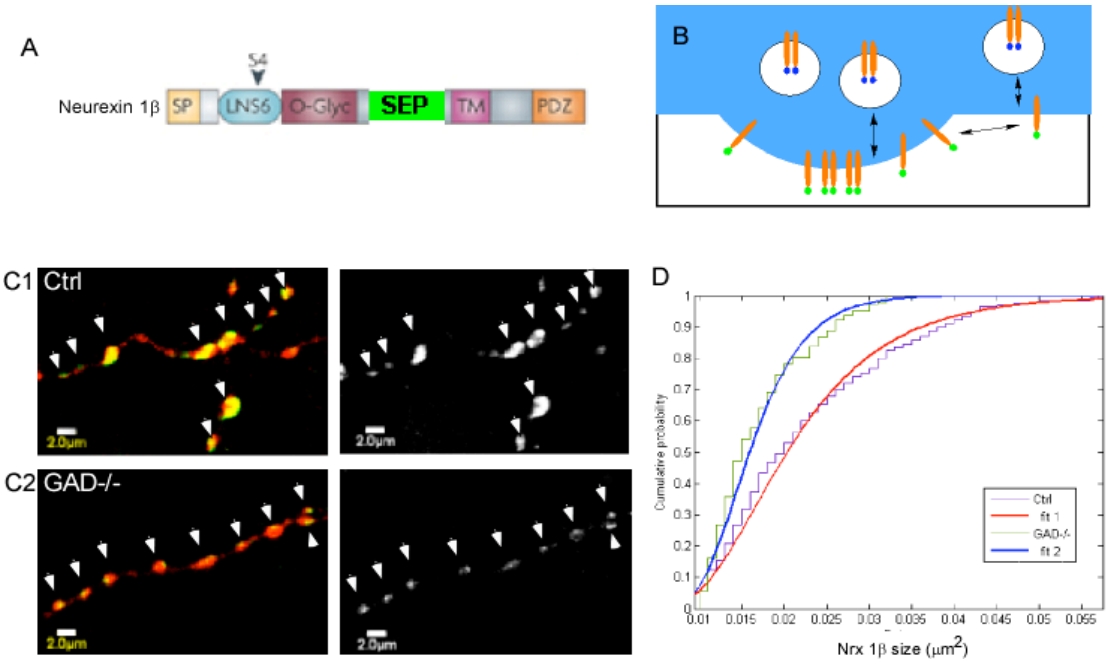

Figure 2.6 Transmission depleted basket cell axons express low and homogenous level of the synaptic adhesion molecule neurexin-1b.

(A) The schematic of the construct of neurexin1 b SEP (Super Ecliptic pHluorin), SEP was inserted in the extracellular portion right next to TM (transmembrane) domain.
(B) When neurexin-1 b SEP is in the vesicles, it does not emit fluorescence. Only after neurexin-1 b SEP is inserted into the membrane the SEP is fluorescent.
(C1) Expression pattern of neurexin 1 b SEP in control basket cell axon together with TdTomato. Neurexin 1b SEP exhibited a punctate pattern, localized to structually identified boutons (arrowheads). Note that the expression areas in some boutons are large, almost covering the boutons. (C2) Expression pattern of neurexin 1 b SEP in GAD-/- basket cell axon together with TdTomato. Neurexin 1b SEP still exhibited a punctate pattern, localized to structually identified boutons (arrowheads). Notice that expression areas in all the boutons are small and homogenous.
(D) Distribution of neurexin 1b SEP size in control and GAD-/- basket cells, red color line represents the sigmoid fit for controls and blue color line represents the shifted sigmoid fit for GAD-/-.

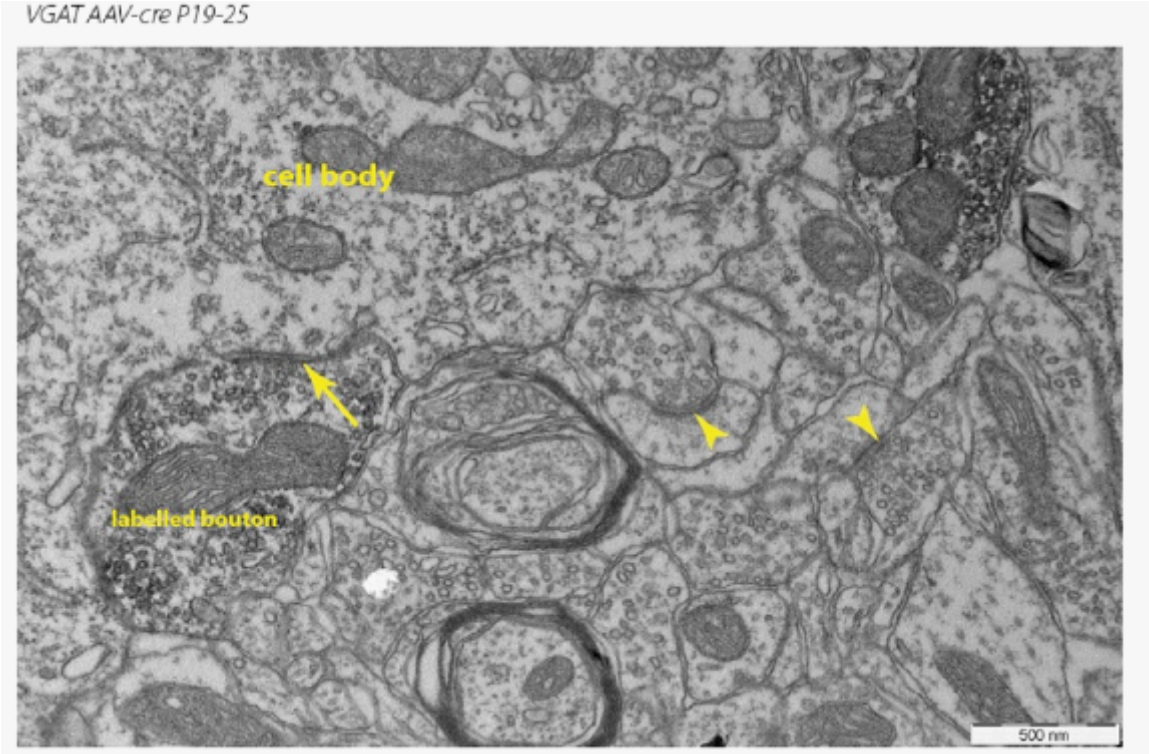

Figure 2.7 Transmission depleted boutons form symmetric synapses *in vivo*.

GFP labeled axonal bouton with synapse on the cell body. Note that the vesicles cluster around the active zone (arrow) and are misshaped, which is typical for symmetrical synapse. The synaptic cleft also looks typical, as it appears narrower than those of excitatory synapse (arrowheads) found on the heads of spines.

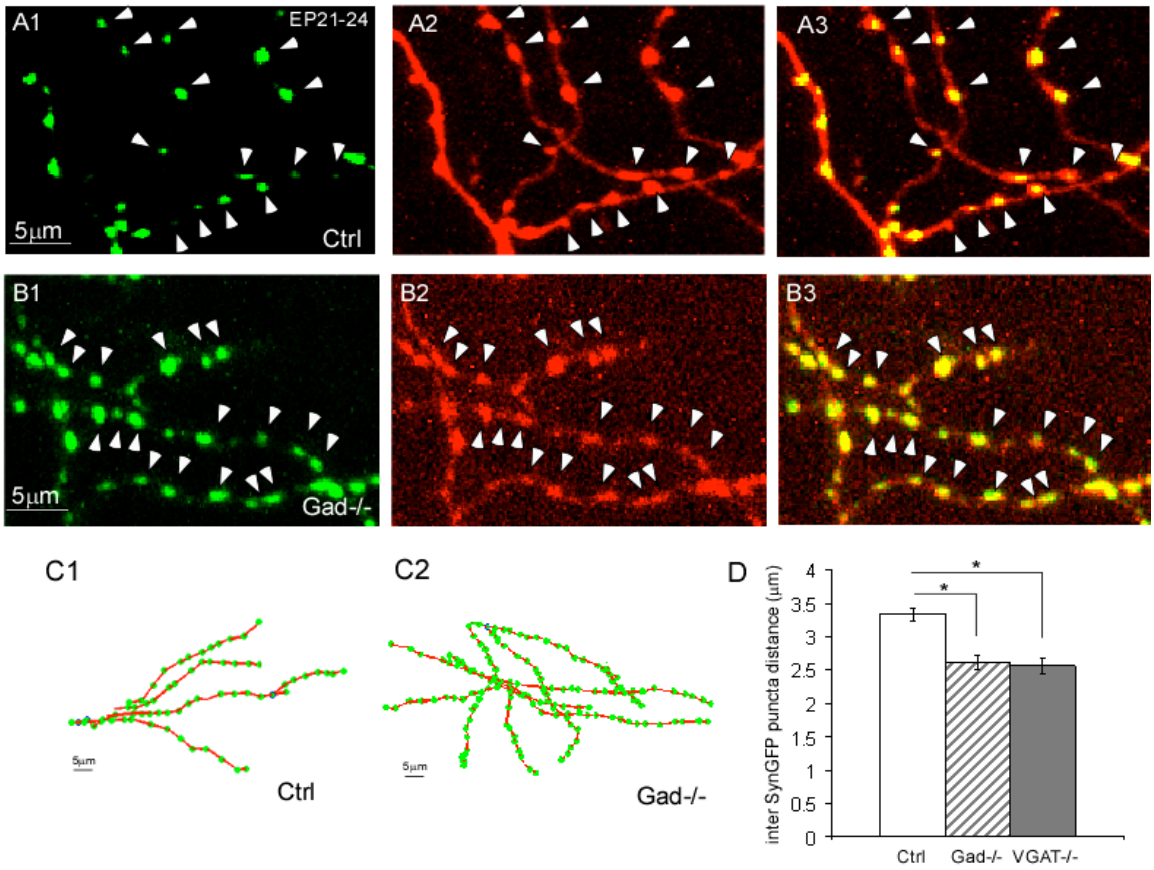

Figure 2.8 Increased Synaptophysin-GFP puncta density in GABA depleted basket cell axons

(A1-A3) Synaptophysin-GFP has a discrete, punctate pattern and colocalize with varicosities in the control basket cell axon. Syn-GFP labeling (A1), cytosolic tdTomato labeling (A2) and the merged image (A3). Note that GFP signal is largely concentrated to the varicosities.

(B1-B3) Synaptophysin-GFP also has a discrete, punctate pattern in Gad-/- basket cell axon. Syn-GFP labeling (B1), cytosolic tdTomato labeling (B2) and the merged image (B3). Note that GFP signal is largely concentrated to the varicosities and Syn-GFP puncta look much closer together.

(C1 and C2) Examples of local reconstruction of control and Gad-/- basket cell axons. The red line represents axon and green circle represents Syn-GFP puncta.

(D) Comparision of inter SynGFP puncta distance between controls cells and Gad-/- or VGAT-/- cells (n=5 cells for each group, $p<0.05$, Mann-Whitney test). Syn-GFP puncta density is significantly increased in mutant cells, similar to the increase in bouton density (Fig2.1).

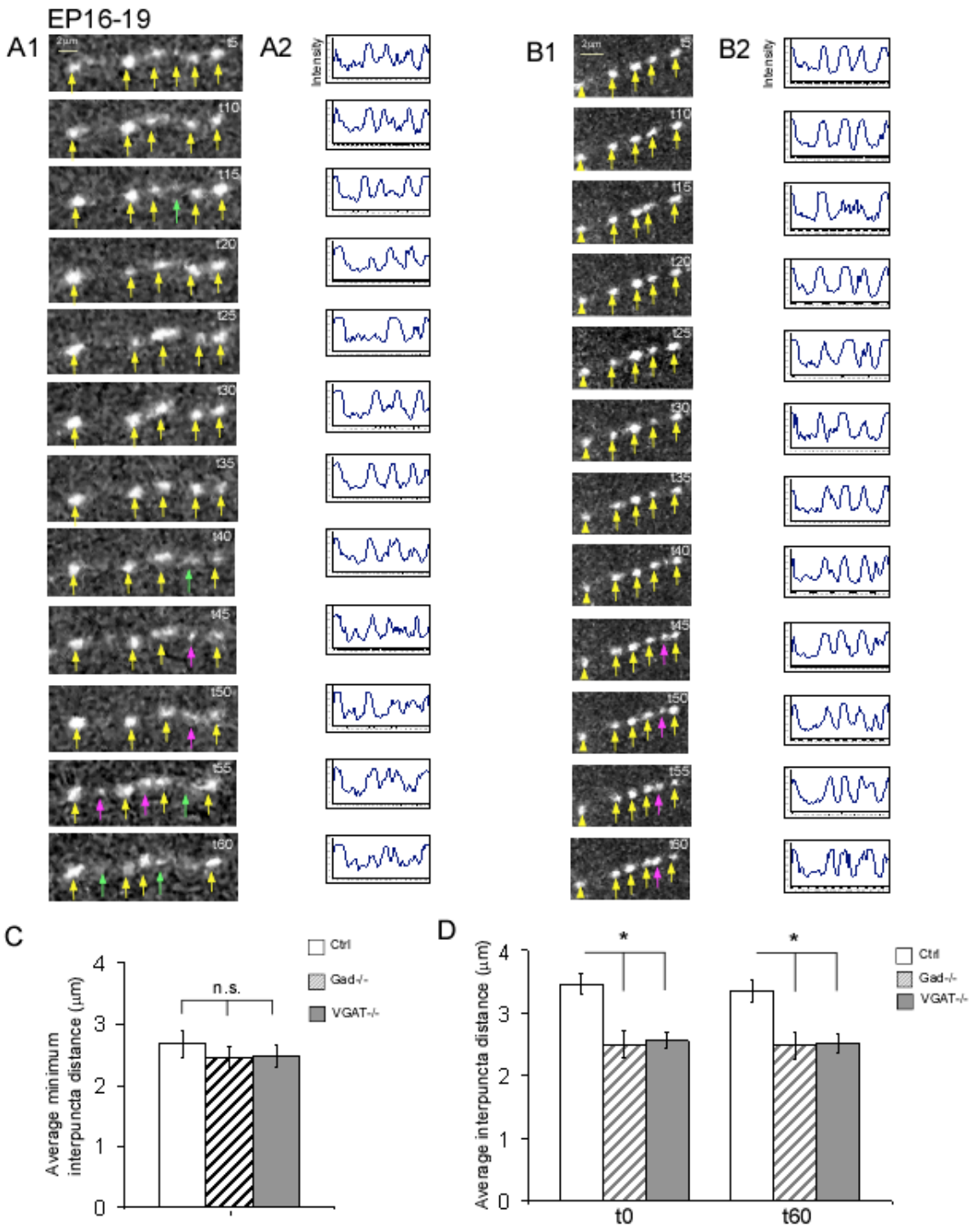

Figure 2.9 Blockade of GABA release results in more stable Syn-GFP puncta and formation of Syn-GFP puncta in the majority of potential nascent contact sites

(A1) A representative example of Syn-GFP puncta dynamics over 60 minutes along a stretch of axon in a control basket cell. Note that puncta actively form and then disappear. (A2) Profile plot along the axon bearing these puncta. Note that puncta intensities fluctuate, reflecting the dynamics of puncta.

(B1) A representative example of Syn-GFP puncta dynamics over 60 minutes in a stretch of axon in VGAT-/- cell. Note that puncta are more stable and a new puncta form in between two existing puncta. (B2) Profile plot along the axon bearing these puncta. Note that the intensities are relatively stable, reflecting the more static nature of VGAT-/- puncta.

(C) Comparison of minimum inter-puncta distance (see definition in page 38), which reflect all potential bouton formation sites, among 3 groups of cells: Ctrl, Gad-/- and VGAT-/-. Note that the distances are not significantly different (Mann-Whitney test, $p>0.05$)

(D) Comparison of average puncta distance among 3 groups of cells: Ctrl, Gad-/- and VGAT-/-. Note that at both t0 and t60, control cells have large inter-puncta distance than those of mutant cells (Mann-Whitney test, $p<0.05$)

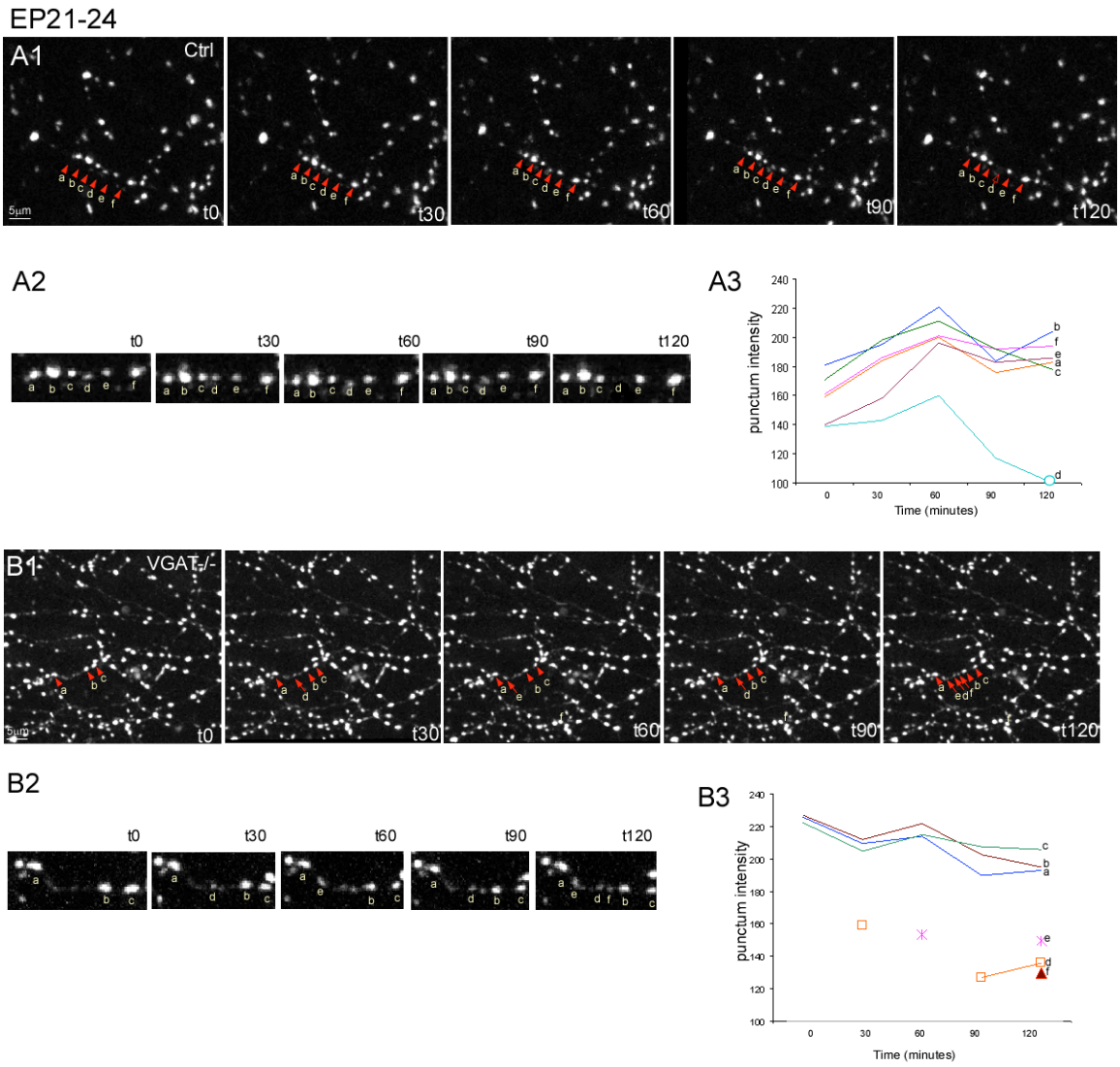

C

VGAT-/- cells	Punctum number (t0)	Added puncta (t120)	Lost puncta (t120)	Net change puncta (t120)	VGAT-/- cells	Punctum number (t0)	Added puncta (t120)	Lost puncta (t120)	Net change puncta (t120)
1	65	+2(3%)	-7 (-11%)	-5 (-8%)	1	206	+13 (6%)	-4 (-2%)	+9 (4%)
2	183	+3 (2%)	-8 (-4%)	-5 (-3%)	2	139	+9 (7%)	-1 (-1%)	+8 (6%)
3	37	+1 (3%)	-6 (-16%)	-5 (-13%)	3	140	+16 (11%)	-5 (-4%)	+11 (8%)
4	224	+9 (4%)	-15 (-7%)	-14 (-6%)	4	251	+25 (17%)	-8 (-3%)	+17 (7%)
5	167	+5 (4%)	-9 (-5%)	-3 (-2%)	5	40	+4 (9%)	-1 (-2%)	+3 (6%)

Figure 2.10 Blockade of GABA release results in less elimination of Syn-GFP puncta in developing basket cell axons

(A1) An example of Syn-GFP puncta in control cells at EP24. Note that the majority of puncta are stable over time. (A2) 6 puncta indicated by arrowheads in A1 over 120 minutes. Note that punctum d is lost at t120. Overall punctum number was decreased from 37 to 32 over 120 minutes.
(A3) Plot of puncta intensity fluctuation over time for puncta annotated in A1.

(B1) An example of Syn-GFP puncta in a VGAT-/- cell at EP24.
(B2) Arrows pointed to puncta from B1 over 120 minutes. Note that 3 new puncta formed. Puncta d and e formed and disappeared (the puncta d intensity dropped below threshold) and then appeared again. Overall there is a net increase in punctum number (from 139 to 147).
(B3) Plot of puncta intensity fluctuation over time for the puncta annotated in B1. Note that newly formed puncta have much lower intensity.
(C) Summary table for puncta behavior over a 2 hour imaging period (n=5 cells for each group). Note that control cells have a net loss of puncta and while in VGAT-/- cells have a net gain of puncta.

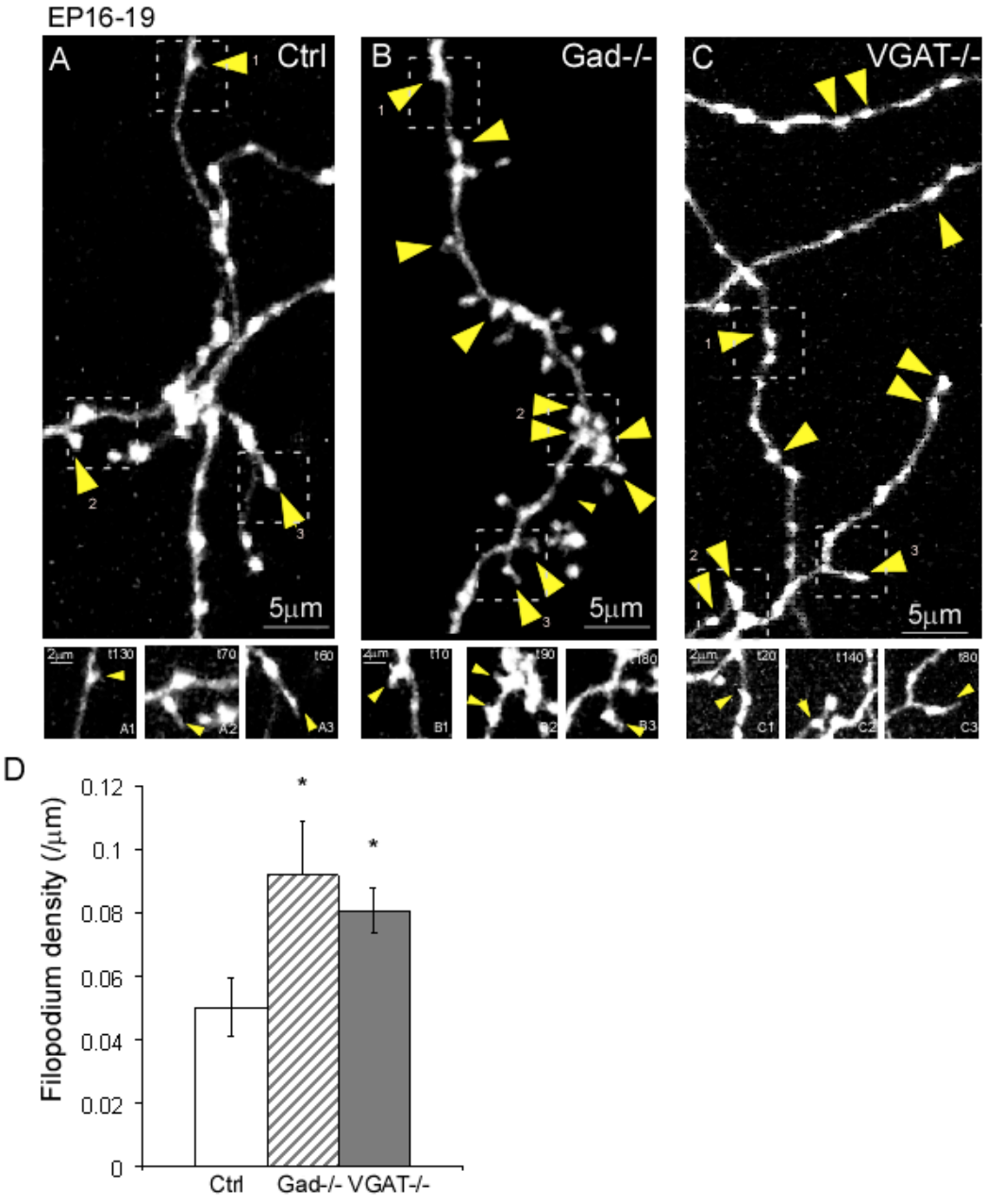

Figure 2.11 Blockade of GABA transmission results in increased filopodia in developing basket cell axons

(A) Filopodia are observed in control basket cell at EP19 over 3 hours. Yellow arrowheads points to the sites of filopodium extension over a 3-hour imaging period. (A1-A3) Examples of filopodia extension.
(B) More filopodia are observed in Gad-/- basket cell over 3 hours. Yellow arrowheads points to the sites of filopodium extension over a 3-hourperiod. (B1-B3) Examples of filopodia extension.
(C) More filopodia are observed in VGAT-/- basket cell over 3 hours. Yellow arrowheads points to the sites of filopodium growth.(C1-C3) Examples of filopodia extension.

(D) Comparison of filopodium density in Ctrl, Gad-/- and VGAT-/- basket cells (n=5 cells for each group). Note that the filopodium density over a 3-hourperiod is significantly increased in both Gad-/- and VGAT-/- when compare to controls (t test, $p<0.05$). Error bar represents standard deviation (SD).

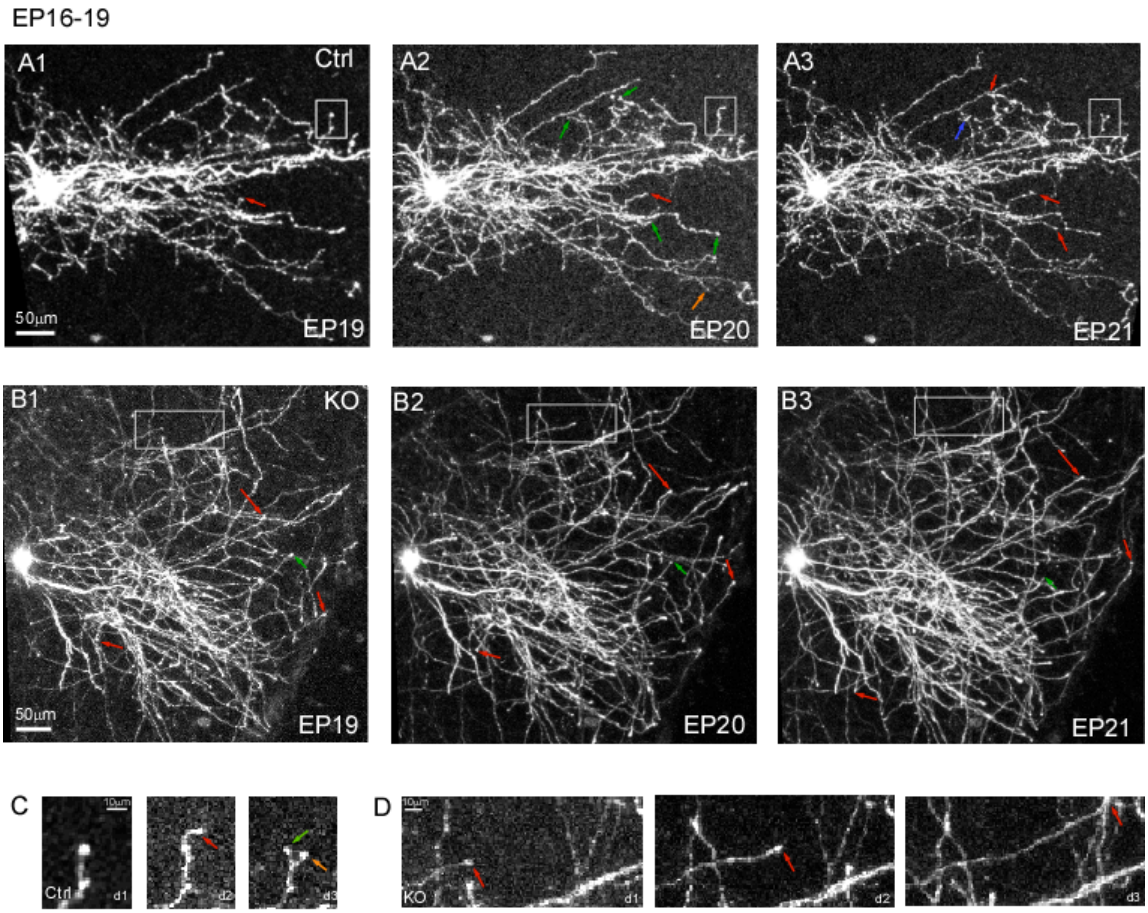

Figure 2.12 Basket cell axon grow recurrently over days and axon extension dominates basket cell axon arbor growth dynamics in the absence of transmission

(A1-A3) A control basket cell axon shows branch addition (orange arrows), extension (red arrows), loss (green arrows), and retraction (blue arrows) during the development axon arbor from EP19 to EP21. Note that the overall axon arbor size was largely maintained over the 3-day period.
(B1-B3) A mutant basket cell shows a massive increase in branch extension (red arrows) and substantial decrease in branch loss and retraction (green arrows), yet the overall axon arbor size is largely constant over the 3 day period. Mutant basket cell at EP19, at EP20 and at EP21.
(C) A close look of the boxed region in the control cell (A1). Note that the axon tip extended (red arrow) in day 2; it then retracted in day 3 (green arrow) and extended another branch (orange arrow) in day3.
(D) A close look of the boxed region in the mutant cell (B1). Note that axon extended (red arrow) in day 2 and then further extend with large distance in day 3 (red arrow).

A

Branch Behavior Category	Extended	Added	Retracted	Lost
Branch Behavior Example	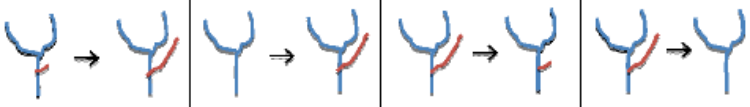			
Criteria for Branch Behavior	Day 1<Day 2 Day 1> 0μm	Day 1<Day2 Day 1= 0μm	Day 1>Day 2 Day 1> 0μm Day 2> 0μm	Day 1>Day2 Day 1> 0μm Day 2= 0μm

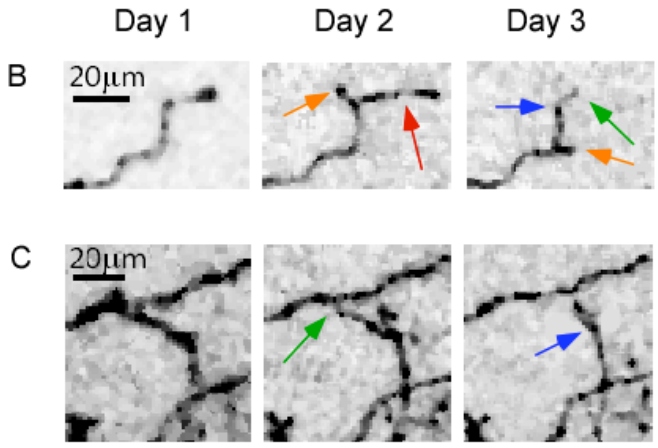

Figure 2.13 Classification of basket cell axon growth behaviors.

(A) Four categories of dynamic branch behaviors. Dynamic branches are classified as extended, added, retracted and lost according to their change compared to the previous day.
(B) An example of extension (red arrow) and addition (orange arrow) from day1 to day2, followed by loss (blue arrow) and retraction (green arrow) and a separate addition event (orange arrow) from day2 to day3.
(C) An example of branch retraction (green arrow) from day1 to day2, followed by the loss of that particular branch (blue arrow) from day2 to day3.

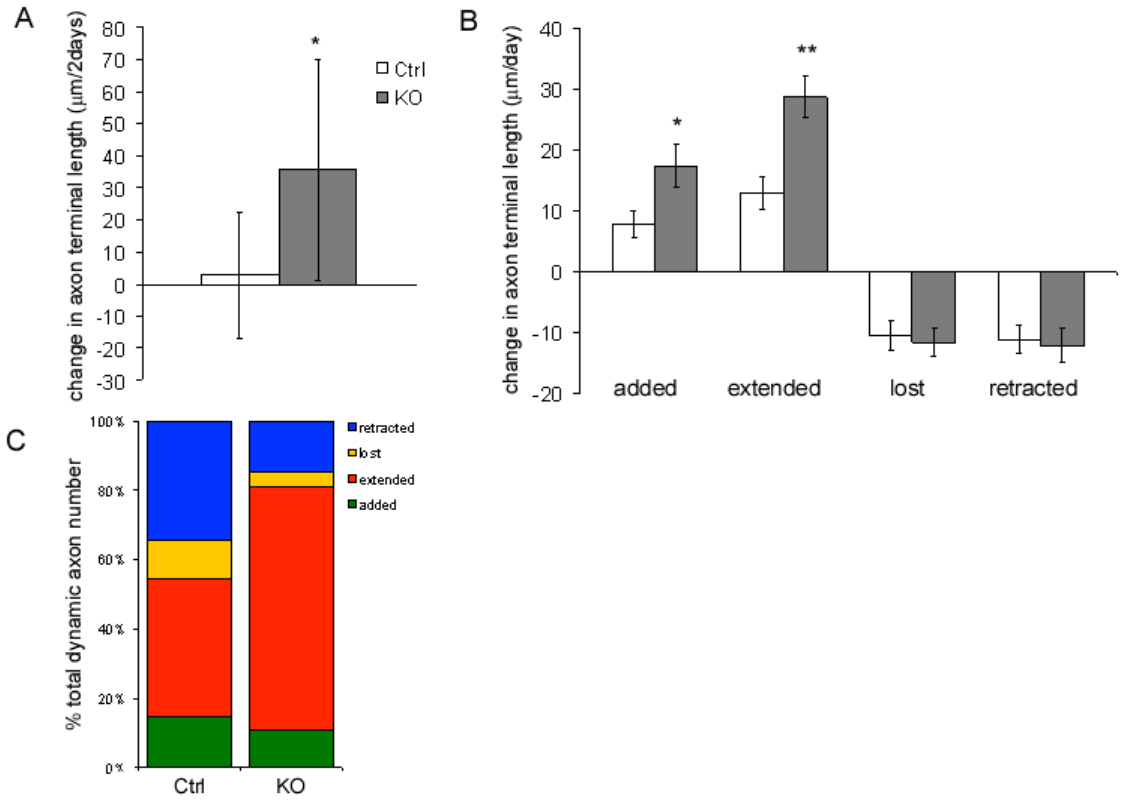

Figure 2.14 Blockade of synaptic transmission results in reduced branch pruning and increased branch extension.

(A) Overall change in axon terminal length (mm/2days) is increased in mutant basket cells (t test, $p<0.05$). Error bars represent standard deviation (SD).
(B) Comparison of changes in average length compared to the previous day for each of four axon dynamic behaviors.
Added and extended groups have significant increase in axon length change (t test, $p<0.05$ for added group and $p<0.001$ for extended group). However there is no significance between control and mutant basket cell axons in the lost and retracted group. Error bars represent standard error mean (SEM).
(C) Comparison of the proportion of each of four axon dynamic behaviors between control and mutant basket cell axons shows a highly significant difference between the two groups (x^2 test, $p<0.001$). There are twice as many extended axons (red) and half as many lost (yellow) and retracted (blue) axons.

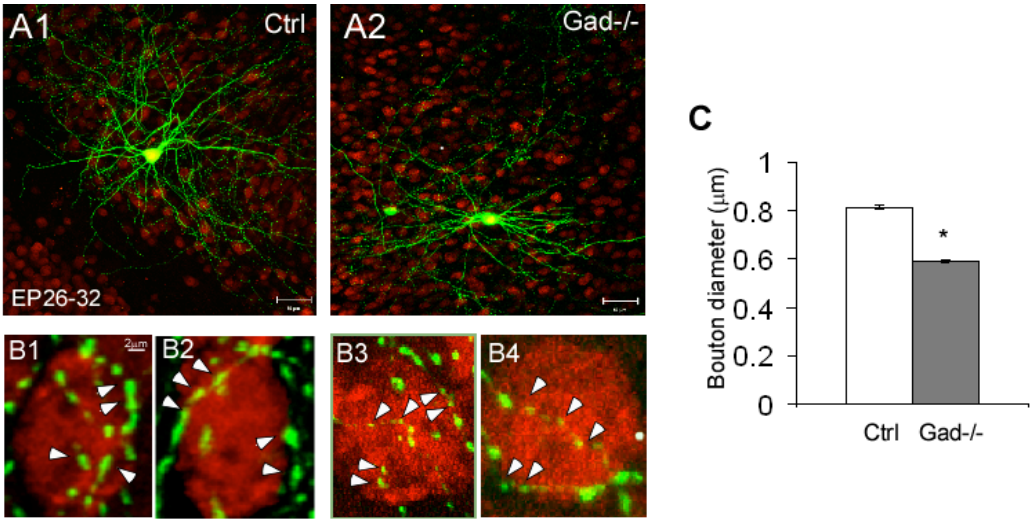

Figure 2.15 GABA transmission is necessary for the maintenance of basket cell perisomatic innervation and axon arbor.

(A1) Example of a control basket cell at EP32.
(A2) Example of a Gad-/- cell at EP32 after 6 days of genetic depletion. Note the reduced axon arbor complexity when compared to control cells (A1).
(B1-B2) Example of control basket cell perisomatic boutons (arrowheads) at EP32.
(B3-B4) Example of Gad-./- basket cell perisomatic boutons (arrowheads) at EP32. Note the reduced size and density of perisomatic boutons.
(C) Comparison of bouton diameter in boutons of control and Gad-/- basket cell (n=5 cells for each group, 100 boutons from each cell. t-test, $p<0.05$. Error bars represent standard error mean (SEM)).

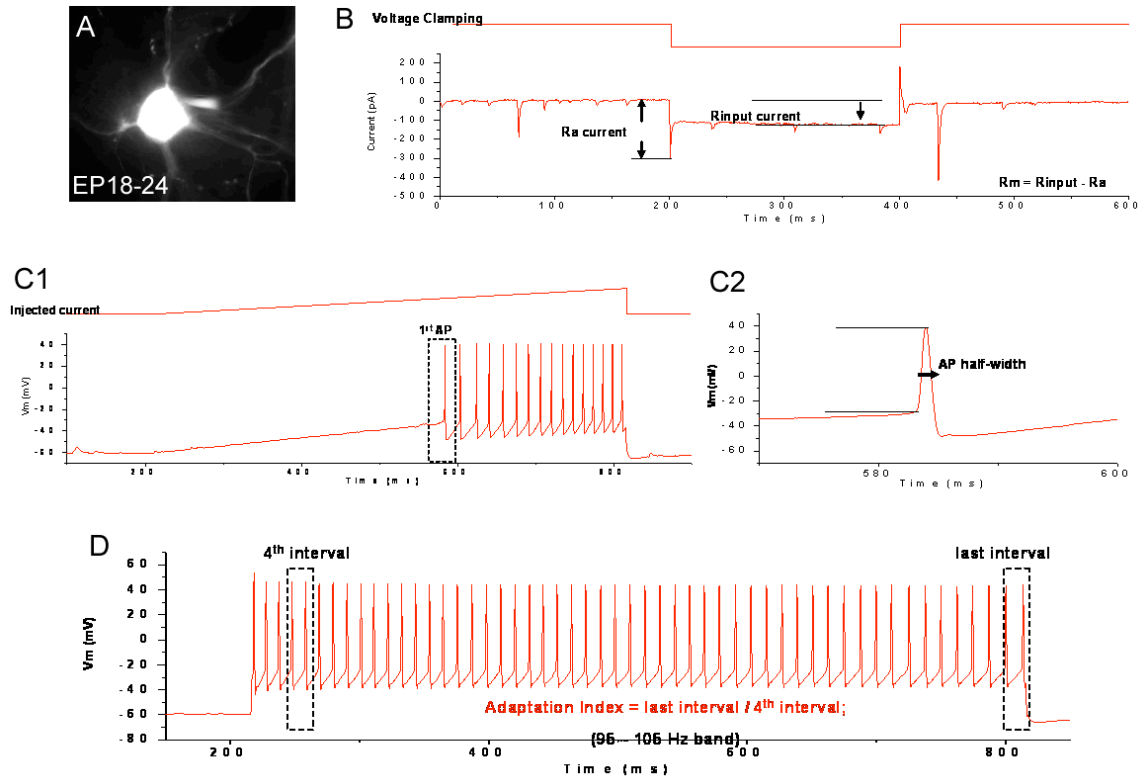

E

Genotype	Rm	AP HW	FS adaptation
Ctrl	30.4 ± 14.4	0.64 ± 0.13	1.07 ± 0.16
Gad-/-	32.2 ± 8.6	0.64 ± 0.10	1.14 ± 0.09

Figure 2.16 Absence of GABA transmission does not alter intrinsic biophysical properties of basket cell.

(A) Basket cell was identified by GFP labeling and targeted for intracellular recording.
(B) Input resistance testing protocol and analysis.
(C1) Action potential (AP) testing protocol and analysis. (C2) explains how AP half width was determined.
(D) Fast Spiking (FS) adaptation index analysis.
(E) Control and Gad-/- basket cells are not significantly different in intrinsic property parameters: Rm, Action Potential Half Width and Fast Spiking Adaptation (n=6 cells for each group, numbers present mean ± standard deviation. For all three parameters, two groups are not significantly different (n=6 for each group, t-test, $p>0.05$).

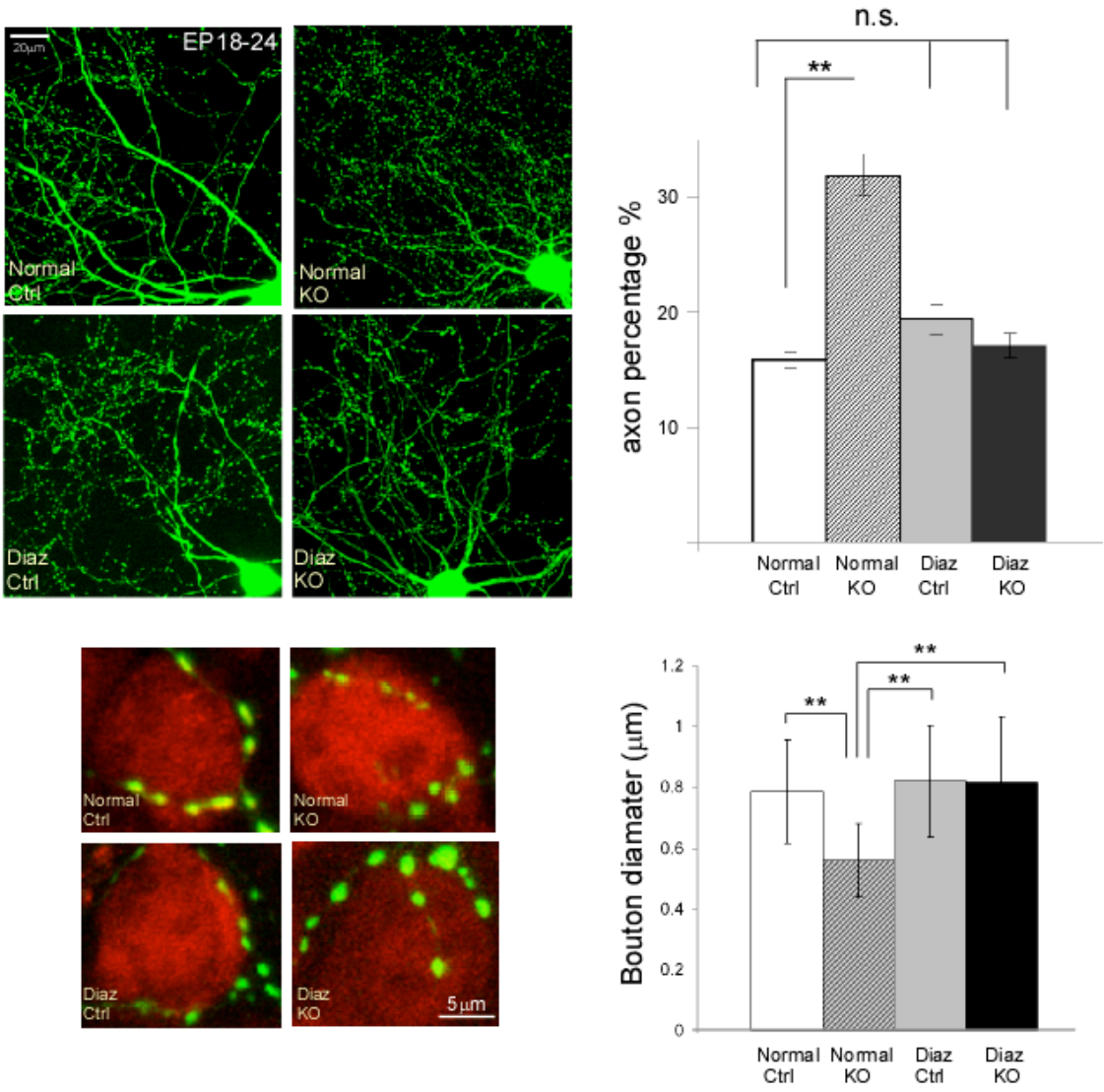

Figure 2.17 GABA signaling regulates basket cell axon and synapse refinement through $GABA_A$ receptors.

(A) Representative examples of axon arbors in control cell treated with normal media (upper left), knock out cell treated with normal media (bottom left), control cell treated with diazepam media (upper right), knock out cell treated with diazepam media (bottom right).

(B) Quantification of axon density percentage in all four groups (n=5 cells for each group, t test).

(C) Representative examples of perisomatic boutons in control cell treated with normal media (upper left), knock out cell treated with normal media (bottom left), control cell treated with diazepam media (upper right), knock out cell treated with diazepam media (bottom right). Pyramidal cell bodies are labeled by NeuN (red).

(D) Quantification of bouton diameter in all four groups (200 boutons from n=5 cells for each group).

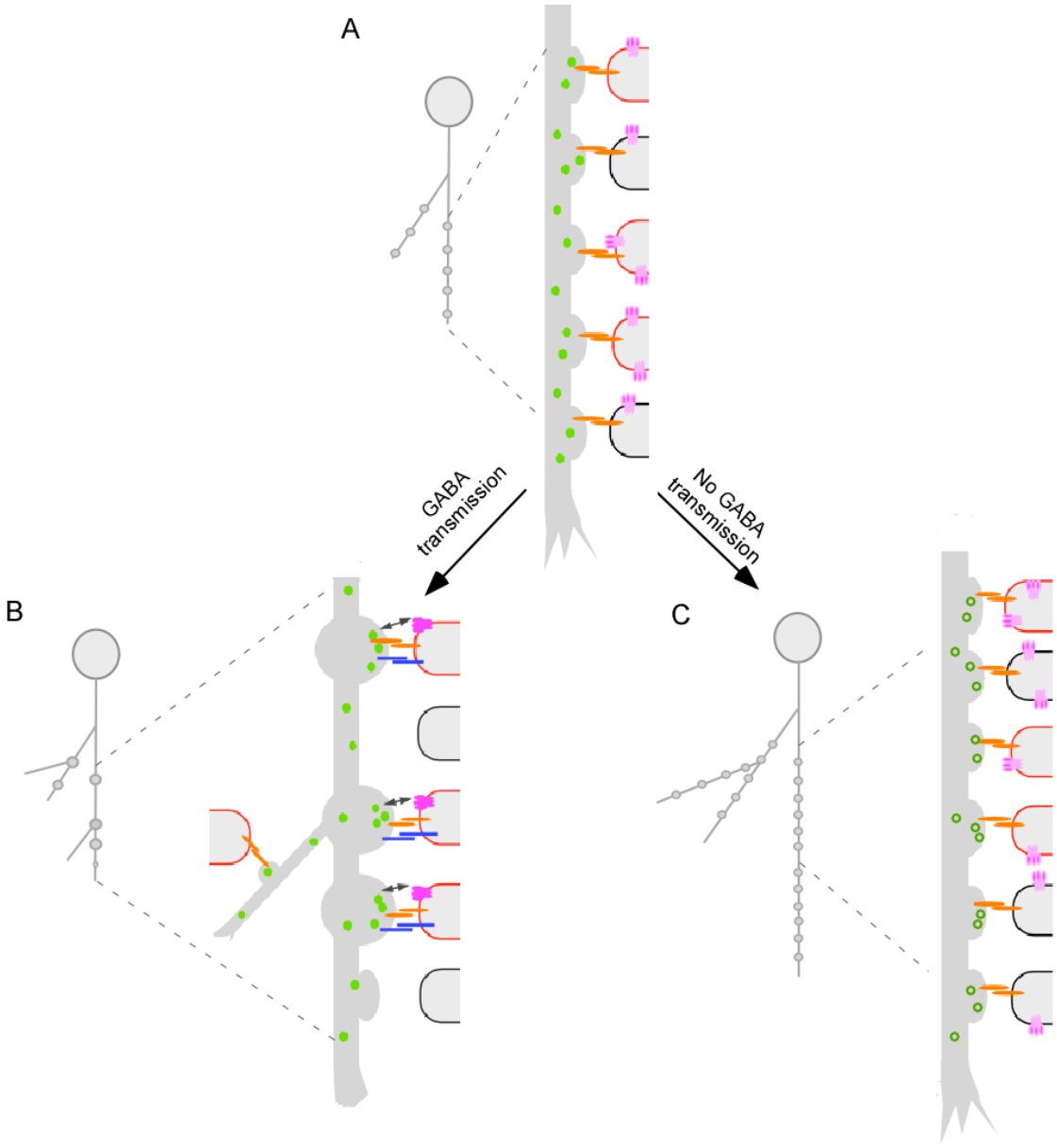

Figure 2.18 A model on the role of GABA transmission in inhibitory synapse and axon development

(A) A developing GABAergic axon (gray lines) explores potential synaptic targets (gray rounded rectangles) by making transient synaptic contacts. Shapes with red outline represent appropriate targets; those with black outline represent inappropriate cellular or subcellular targets. Synaptic vesicles (green filled circles) shuttle in the axon and aggregate at transient synapses, and may be anchored by synaptic adhesion molecules (orange). (B) Through GABA transmission, transient synapses at the appropriate targets are validated. GABA transmission further stimulates the maturation of these synapses, which extend new branches and explore new targets. At the inappropriate contacts,

GABA transmission promotes the elimination of these transient synapses and pruning of branches bearing inappropriate contacts.

(C) Without GABA transmission, developing GABAergic axons cannot discriminate between appropriate and inappropriate targets. Thus appropriate contacts cannot be validated and stimulated to mature, and inappropriate contacts cannot be eliminated; this results in increased bouton density with more homogenous bouton size. At the level of axon arbor, transmission deficient axons are unable to prune branches bearing inappropriate contacts, resulting in increased branch extension and massive increase in axon density.

Chapter 3. Development of Gad67 transcriptional reporter mice to study the plasticity of inhibitory circuits

3.1 Introduction

Interneurons, though heterogeneous, have one thing in common - they all use GABA as the only neurotransmitter. GAD67 is the rate-limiting enzyme for GABA synthesis. Alterations in GAD67 levels readily influence the cellular and vesicular GABA contents (Engel et al 2001). GAD67 activity is mainly controlled at the level of transcription, which is dynamically regulated during development and by neural activity and experience (Kiser et al 1998; Liang et al 1996; Patz et al 2003). Importantly, Gad67 is differentially regulated in different GABAergic cell types in response to various stimuli and is misregulated in several pathological states (e.g. transcription is reduced in a few subtypes of interneurons in the prefrontal cortex of schizophrenic patients (Lewis et al 2005)). It is thus critical to understand how GAD67 transcription is precisely regulated in defined classes of interneurons, with cellular resolution and ideally in live brain.

Visualization of Gad67 transcriptional level provides a unique opportunity to understand how cellular changes in GABAergic cells are integrated at the brain circuit level. Efforts starting in early 1990s demonstrated that transgenic reporters of Immediate Early Gene (IEG) expression could provide high-throughput functional analysis of the CNS (Barth et al 2004; Grinevich et al 2009; Impey et al 1996; Smeyne et al 1992; Wang et al 2006). However, IEGs such as c-FOS and Arc are not induced in the cortical interneurons at a detectable level, precluding the application of these animals to study GABAergic circuits. In contrast, Gad67 transcription is highly regulated in an activity dependent manner in all GABAergic cells and is therefore well suited to be visualized.

The goal of this project is to identify the specific cell ensemble and time course of Gad67 regulation in response to sensory experiences and emotional state. Because different classes of interneurons have different physiological functions, I expect that GAD67 expression will be regulated in one direction in certain classes of interneurons but not regulated or regulated in an opposite direction in other classes of interneurons. My questions are: Where and when in the cortical network is GAD67 regulated by sensory experience? Is the activation pattern stereotyped? Does stress only affect pyramidal cell or interneurons as well? Does stress prefertially affect certain class of interneurons?

In order to accurately measure changes in Gad67 transcription in the live brain I developed two versions of knock-in reporter mice; Gad67-d2EGFP and Gad67-t2a-nls-d4EGFP. Both constructs express a short half-life EGFP under the control of the endogenous Gad67 promoter in order to visualize changes in GAD67 transcription with cellular and accurate temporal resolution. For the first reporter design, a fluorescent protein d2EGFP is produced under the direct control of GAD67 gene locus. This is achieved by inserting a DNA sequence coding for d2EGFP directly under the endogenous gene coding for GAD67, through DNA recombination in mouse embryonic stem cells. D2EGFP is a derivative of EGFP, which has a short half-life of 2 hours because of its C-terminal PEST domain (Li et al 1998). Because d2EGFP is rapidly degraded, its fluorescence reflects the ongoing levels of GAD67 mRNA production. For the second design, a nuclear localized fluorescent protein nls-d4EGFP is produced together with GAD67.

Nucleus Localization Signal was used to concentrate the fluorescence signal and yield a better cellular resolution. NLS-d4EGFP has a 2-hour half-life, similar to d2EGFP (data not shown). A t2a sequence is used to achieve bicistronic translattion so both Gad67 alleles are intact. For the second design, the overall genetic modification is Gad67-t2a-nls-d4EGFP. I validated that GFP fluorescence in both reporter strains reliably reports Gad67 transcription bi-directionally in response to pathological, pharmacological, physiological stimulus. Furthermore, in a chronic restraint stress paradigm, the reporter revealed cell-type specific change of interneurons in the hippocampus. Therefore, these reporters allow visualization of the transcriptional state of the GAD67 gene with cellular and cell type resolution and will facilitate our understanding of plasticity in GABAergic circuits.

3.2 Generation of two Gad67 transcriptional reporter mouse strains

The recombineering approach used to generate Gad67-d2EGFP mice

A destabilized GFP at the translational initiation site should be an accurate reporter for Gad67 transcriptional level, as the GFP transcript is located at the same position as the endogenous gene and therefore all transcriptional regulation of the Gad67 gene is pre-served. Below I describe the generation of the reporter mouse using recombineering method.

A BAC clone RPCI22-56I19 containing the Gad67 gene spanning 70kb genomic region and 60kb flanking genomic regions on each side was obtained from the C57B6 mouse BAC library (Research Genetics) and transformed into the electrocompetent,

recombination inducible EL250 bacteria cells. All the plasmids and protocols were based on reagents provided by Copeland lab (Liu et al 2003). Briefly, a BAC targeting vector was constructed by cloning d2EGFP cDNA and PGK-PolyA into the PL450 plasmid, with homologous arms of ~500bp targeting the ATG site located in the Exon 2 of the Gad67 gene. After the first round of recombination in bacteria the targeted BAC was obtained. A retrieval vector was constructed based on PL253 plasmid, with homologous arms of ~500 bp targeting a region 4kb upstream of ATG on the 5' side and a region 2kb downstream of ATG on the 3' side. Another round of recombination was induced in bacteria, generating the final ES cell knockin vector, containing a 4kb homologous arm on the 5' side and a 2kb homologous arm on the 3'side (Figure 3.1 A). The long homologous arms are crucial for targeting success in the mouse ES cells.

Hybrid ES cell clones (B6/129) were transformed with linerized knock-in construct and selected for homologous recombination using Neo resistance marker to exclude any clones without genomic integration. A PCR screen was conducted using a primer pair, which one of them was located inside the knockin construct and one of them was located outside of the homologous arm. 81 of the 96 ES cell clones were positive in the PCR screen. Five ES cell clones were further expanded to obtain enough DNA for southern blotting. All ES cell clones have both a modified and an unmodified Gad67 allele. One clone (F2) (Figure 3.1A) was chosen for blastocyst injection and used to generate chimeric founders. The neo resistance gene cassette was removed by breeding the founders with Flpase line expressing Flpase recombinase in their germ line (Susan Dymecki, Harvard University, Cambridge, MA). The offspring were then bred into C57B6 background for three generations prior to analysis.

Direct Cloning Approach to generate Gad67-t2a-NLS-D4EGFP mice

The Gad67-d2EGFP mouse has one disrupted allele of Gad67. While being hetereozygous in Gad67 is not lethal to the animal, it does have some effect on inhibitory circuit (Chattopadhyaya et al 2007). Ideally, both Gad67 alleles should be present and functional. Therefore a second reporter strain was designed that uses the t2a bicistronic transcriptional system to coexpress a destablized GFP together with Gad67 at the native locus.

To increase cellular resolution of imaging GFP labeled neurons, I tagged a NLS (peptide sequence PKKKRKV from SV40 Large T-antigen) to the N terminal of the D4EGFP to concentrate GFP signal in the cell body. NLS-d4EGFP has a half-life of ~2 hours in U2O2 cells (result not shown), comparable to D2EGFP. The t2a sequence from Foot and Mouth Disease Virus (Ryan & Drew 1994), when translated, mediates self-cleavage in cis. Compared to the IRES strategy, the t2a strategy is advantageous because of a smaller size and much higher co-translation efficiency (Chinnasamy et al 2006). T2a was inserted in-frame N terminal to the NLS. 5' homologous arm of 2kb and 3' homologous arm of 5kb were PCR amplified from the Gad67 BAC clone RPCI22-56I19 using high-fidelity DNA polymerase (Phusion, Finnzymes) and subsequently cloned into the PL450 plasmid to generate Gad67-t2a-nls-D4EGFP knock-in vector (Figure 3.1 B). Restriction enzyme digestions were conducted to make sure the integrity of the plasmid, and thorough DNA sequencing was done to make sure there was no mutation in the cloned fragments.

Six of the 96 ES cell clones were positive in the PCR screen. Two ES cell clones were further expanded to obtain enough DNA for southern blotting. On the 5' side, the selected ES cell clones have both modified and unmodified Gad67 allele (Figure 3.1B). Unfortunately, 3' side southern blotting did not yield either the unmodified band or modified band and even on wildtype ES cells (results not shown). The ES cell clone was then injected into tetrapore-staged embryos and constitutes germline cells in the founder animals. Similarly to Gad67-D2EGFP, the neo cassette was removed and offspring backcrossed to C57B6 background prior to analysis.

3.3 EGFP is specifically expressed in the GABAergic neurons brain wide

Both Gad67-d2EGFP and Gad67-t2a-nls-d4EGFP lines express GFP specifically in interneurons in the neocortex. Because both Gad67-d2EGFP and Gad67-t2a-nls-d4EGFP lines are knock in transgenic lines with definite genetic modification, the expression pattern of GFP is stable and does not vary from one animal to another. In the neocortex, the basal GFP level in Gad67-d2EGFP is low but adequate to observe using confocol and two-photon microscopy with image averaging (Figure 3.2A). Unfortunately the basal GFP level in Gad67-t2a-nls-d4EGFP was too low for our current imaging setup but GFP antibody amplification of Gad67-t2a-nls-d4EGFP brain tissue demonstrates a comparable expression pattern to Gad67-d2EGFP. Almost all the Gad67 antibody staining positive cell bodies are also GFP+ (103 of the 106 cells). Because Gad67 antibody staining does not give definitive signal in all GABAergic cells, GFP + cells greatly outnumber Gad67+ cells (225 cells versus 106 cells). GFP+ cells also colocalize with various interneuron class markers. All PV+, SOM+ and CR+ cells are GFP+ (89/89, 26/26 and 18/18 respec-

tively). Interestingly, the average GFP fluorescent intensity in PV+ cells is the highest (78.6 $\pm$ 6.4, n = 89), and SOM+ is lower (71.0 $\pm$ 5.2, n = 26), and CR+ is the lowest (64.7 $\pm$ 5.8, n = 18). These intensity differences most likely reflect the difference in Gad67 transcriptional level in interneuron classes. Furthermore, both Gad67-D2EGFP and Gad67-t2a-nls-D4EGFP lines express GFP in the GABAergic cells brain wide (Figure 3.2 B). GFP expression is typical of GABAergic cells in the hippocampus, cerebellum and olfactory bulb. Particularly, GFP level are the highest in olfactory bulb, providing a possibility for *in vivo* 2-photon imaging in the future.

3.4 Validation of Gad67 transcription reporting ability using a kainic acid induced limbic seizure model

To validate Gad67 transcriptional reporting ability in these reporter mouse strains, I employed a kainic Acid limbic system seizure model, which was known to massively regulate Gad67 mRNA level in dentate gyrus granule cells (Sperk et al 1983). A single dose of kainic acid (20 mg/kg) was injected intraperitoneally to the Gad67-D2EGFP mice. Analysis of EGFP expression was done at three time points post injection: 6 hours, 12 hours and 48 hours. Control animals were Gad67-D2EGFP mice injected intraperitoneally with saline.

At 6 hours, mice injected with kainic acid revealed robust induction of EGFP labeling in hippocampal dentate gyrus regions relative to saline-injected controls (Figure 3.3 A2, red arrow). At 12 hours, EGFP labeling had returned almost to baseline in dentate gyrus (Figure 3.3 A3, red arrow). At 48 hours, EGFP labeling was significantly elevated in the CA1/CA3 interneuron region (Figure 3.3 A4, yellow arrow). Quantification demon-

strates that the GFP intensity in the dentate gyrus is increased 4 fold relative to saline injected controls at 6 hours and decreases to 119% at 12 hours and further to 108% at 48 hours. On the contrary, the GFP intensity in the CA1 interneurons remained a stable 99% at 6 hours, decreased to 85% at 12 hours and increased to 157% at 48 hours. The percentages are calculated of the saline injected control animals and each time point group has 3 Gad67-D2EGFP animals. These data demonstrate not only that GFP expression is activated by a stimulus that activates Gad67, but also that the GFP level faithfully reports both the onset and decay of Gad67 expression. More over, the quantification based on GFP fluorescence intensity is similar in induction magnitude as the reported quantification of in situ data (Schwarzer & Sperk 1995).

3.5 Gad67 expression is increased in the specific stimulated barrel with single whisker stimulation

To validate Gad67 transcriptional reporting ability under physiological stimulus, I stimulate a single whisker and monitor GFP level change in the corresponding barrel. Whiskers provide crucial sensory input for rodents and their inputs form a stereotyped structure, from one facial whisker to one primary cortical column in somatosensory cortex (Woolsey & Van der Loos 1970). Trimming of all but one whisker and stimulation of the single whisker with an electromagnetic device at a physiological frequency of 8Hz induces EGFP expression in the C2 cortical column (Figure 3.4 B). Following 24 hours of simulation the cells in C2 column have 25.3% higher fluorescence intensity than the cells in the nearby D1 column (Figure 3.4 D). This demonstrates that my reporter mouse strains can be used to map Gad67 induction in response to sensory-evoked neural circuit

plasticity in the mouse cortex. The same sensory stimulation was shown to induce structural plasticity in inhibitory synapses (Knott et al 2002). This suggests that neural activity may act through GAD67 to regulate the innervation pattern of inhibitory neurons.

3.6 Use of Gad67 transcriptional reporters strains to map changes in inhibitory circuit after restrain stress

Stress can be deleterious to the physiological and psychological integrity of an individual and may result in psychic and behavioral changes (McEwen & Stellar 1993; Sapolsky 1996). The stress response is mediated by activity in many brain areas and there is experimental evidence that stress induces structural changes in neuronal networks, particularily in the hippocampus and prefrontal cortex. In addition, stress inhibits adult neurogenesis in the dentate gyrus (Pham et al 2003). I show that GABAergic cells in the dentate gyrus area reduce their GFP level after chronic stress in the Gad67-nls-t2a-d4EGFP mice. Within the hippocampus, stress exposure results in remodeling of dendrites of the CA3 pyramidal neurons and in reduced numbers of synapses on these neurons (Kole et al 2004; Watanabe et al 1992). I show that interneurons in CA1 and CA3 have reduced GFP level after chronic stress, but a cell population in the molecular layer has increased GFP level. In the prefrontal cortex, repeated exposure to stress causes dendritic retraction and loss of spines in pyramidal neurons (Radley et al 2006). I show that particularly in layer V, PV+ cells have increased GFP level while the PV marker expression is decreased. These new data on Gad67 regulation, taken together support the hypothesis that inhibitory circuit is involved both in the response and the adaption to stress.

As generally accepted stress increases extracellular glutamate levels and thus enhances excitatory activity (McEwen 2000). The change in GABA level is more controversial. Chronic stress and glucocorticoid treatment increase GAD expression in the hippocampus, presumably leading to enhanced GABA synthesis (Bowers et al 1998; Stone et al 2001), most probably to facilitate inhibitory neurotransmission. However, counter evidence that chronic psychosocial stress reduces the number of PV+ interneurons in the CA3 region (Czeh et al 2005). A model of posttraumatic stress disorder reduced GABA level in the hippocampus and evoked a sustained increase in NOS activity (Harvey et al 2004). The discrepancy from the different studies is likely to stem from the heterogeneity of the GABAergic neurons. One class of interneuron is likely to act differently than the other class thus it is necessary to examine the change of GABA level systematically in several different interneuron subtypes.

Numerous IEGs, including c-fos, c-jun, and zif268 (egr1), have been used extensively for identification of brain circuits affected by stress (Cullinan et al 1995; Martinez et al 1998; Stamp & Herbert 1999; Umemoto et al 1997). However, these IEGs does not express in the majority of interneurons and therefore preclude the identification of inhibitory circuits affected by stress. Gad67 transcriptional reporter mouse strains provide a systematic tool for mapping GABAergic circuit response to stress.

I first used Gad67-D2EGFP mice to examine the effect of acute stress on GABAergic circuits. Mice were immobilized in a tight, metal mesh pocket individually for 5 hours before they were perfused with paraformaldehyde. Control animals are littermates

without stress manipulation. As reported, cFOS was induced in the primary stress circuit comprising brain areas of hypothalamic paraventricular nucleus, ventrolateral septum, amygdala, locus coeruleus and nucleus of the solitary tract. The two places where contain cells of induction of both cFOS immunoreactivity and GFP is the hypothalamic paraventricular nucleus and ventrolateral septum (Figure 3.5). These neurons are GABAergic, spiny projection neurons that are known to be involved in stress response (Herman et al 2002; Kubo et al 2002). This result shows that Gad67-D2EGFP reporter mouse can reliably report stress related change in the GABAergic neurons.

Then I used Gad67 transcriptional reporter mouse strains to investigate the effect of repeated stress on GABAergic circuits. Mice were immobilized in a tight, metal mesh pocket for 6 hours everyday from 10am – 4pm, for 10 consecutive days. Control animals are littermates without stress manipulation but otherwise handled similarly. In medial prefrontal cortex, chronic stress induces GFP expression in the layer V. Interestingly, most layer V cells are PV+ interneurons and stress also decrease PV marker expression in the layer V (Figure 3.6). This result identified PV+ class of interneuron as a cell population in the medial prefrontal cortex that is particularly vulnerable to repeated stress. In the hippocampus, chronic stress decrease GFP expression in the majority of cell populations including PV+, SOM+ and CR+ cells (Figure 3.7). However, in the stratum lacunosum-moleculare (slm), GFP expression was induced, with a higher density of GFP+ cells (Figure 3.8). Stereology is being conducted to have a quantitative assessment of GFP+ cell numbers in specific hippocampal regions. About 30% of the GFP+ cells are NOS+ (Figure 3.9), the rest of GFP+ cell did not colocalize with any subtype markers examined so far and remain to be identified. Previously, there was one report of GABA reduction in

PV+ and SOM+ cells (Czeh et al 2005), and another report of stress inducing NOS activity (Harvey et al 2004). I see my results as reconciling the disparate evidences on stress response in the hippocampus. Chronic repeated stress may aversely affect certain class of interneurons and elicit adaptive, homeostatic response in another class of interneurons.

The dentate gyrus area is the primary area where adult neurogenesis is known to occur (Eriksson et al 1998) and it is known that stress has a rapid effect in halting neurogenesis (Gould et al 1997). In addition to the interneurons in the granule cell layer, there is another population of immature granule cells that transiently express GABA (Gutierrez 2005). Both cells could be the source of GABA, which is important for the integration of newly born neurons in the adult brain (Ge et al 2006). To determine how chronic stress affects GABAergic neurons in the dentate gyrus area and may in turn affect neurogenesis, I measured GFP expression in the Gad67-t2a-nls-D4EGFP mouse after chronic stress. I observed that in the control animal, GFP+ cells show clear, long, vertical leading processes, as previously identified in new born neurons (Alvarez-Buylla & Garcia-Verdugo 2002); while in chronically stressed animals the GFP level is reduced and GFP+ cell number is decreased; a leading process is also no longer visible in GFP+ cells. Stereology is currently being conducted in order to have a quantitative assessment of GFP+ cell numbers in the dentate gyrus. PSA-NCAM marker will be used to distinguish newly born cells versus existing interneurons. In summary, the Gad67 transcriptional reporters could be used to examine how stress impact neurogenesis at the cellular level.

3.7 Discussion

I have developed two mouse strains that reliably report Gad67 transcriptional regulation at a cellular resolution and with accurate temporal dynamics. Because Gad67 is regulated by activity, this allows near real time monitoring of the physiological state of GABAergic neurons by visualizing activity dependent transcription of the GAD67 gene.

The reliable activation of EGFP expression in Gad67-d2EGFP and Gad67-t2a-nls-d4EGFP mice has been confirmed by experimental paradigms previously applied by others. First, a kainic acid induced limbic seizure result in massive increase of EGFP expression in the dentate gyrus after 6 hours, and decline almost back to baseline after 12 hours. The same stimulus did not induce any EGFP expression in interneurons until 48 hours later. These results demonstrate that the destabilized form of EGFP allows monitoring the time-course of neural activity. Second, single whisker stimulation induce EGFP in the stimulated barrel after 24h physiological stimulation. The endogenous EGFP rose by about 25%. Third, acute stress induces EGFP in GABAergic neurons in hypothalamic paraventricular nucleus and ventrolateral septum. In addition to confirming previous results, I provided new results on the impact of a repeated restraint stress on inhibitory neurons in prefrontal cortex and hippocampus. I observed an induction of EGFP expression in the layer V of medial prefrontal cortex, accompanying a decrease in Parvalbumin expression, possibly reflecting excitoxicity in the PV cells upon exposure to chronic stress. In the hippocampus, most cell types showed decrease in GFP level while a cell population in the stratum lacunosum-moleculare (slm) showed an increase in GFP level. Some of the cells in slm are NOS+, agreeing with the previous literature on stress inducing NOS expression (Harvey et al 2004). This slm cell population possibly reflects

adaption of the inhibitory circuit to chronic stress.

The expression of Gad67 has so far been preferentially evaluated by classical histological methods, such as immunohistochemistry and as in situ hybridization. The immunohistochemistry of GAD67, because of antibody staining quality, does not capture all GABAergic cells. Furthermore, because GAD67 is also present in the axon terminals, antibody stains the prominent layer 5 perisomatic boutons on the pyramidal cells and thus yielding false positive signal. Antibody staining is inherently variable as well. The variation is also big on Gad67 antibody staining. In situ method has similar caveats and is more expensive and labor intensive. In comparision, visualizing Gad67 transcription with GFP means first, all interneurons are labeled and second, the level of GFP reflects the activity level of the interneuron.

The real advantage of reporter mouse strains lies in the enablement of long term, repetitive investigation of the same neuronal circuit over time. I have tested *in vivo* imaging the olfactory bulb of Gad67-D2EGFP mouse and the result appears encouraging. I was able to image the baseline level of GFP in paraglomeruli interneurons and also observed an elevation of GFP level after activation of the specific glomeruli. In the cortex, the baseline level of GFP is too low to be reliably detected by our current imaging setting and therefore preclude further analysis. New reporter mouse strains, which have better, brighter fluorophores, should be developed for this purpose.

Compare with fast indicators such as voltage, Ca2+, or vesicle release, Gad67 based GFP reporter mice indicate longer-term plasticity in GABAergic cells. Gad67's mRNA

half-life is 4 hours, in comparision with millisecond events such as action potential. The Gad67 transcriptional reporters examine plasticity at the cellular level, the result of cellular integration of firing properties, excitability, short-term plasticity and etc. The cosolidation of synaptic activity at the cellular level leave traces of prior activity history and the long lasting fluorescence provides a broad window for analysis of the cellular eletrcophysiological properites.

In conclusion, I developed knock-in reporter mouse strains that express quick degradable EGFP under the control of the Gad67 gene. EGFP faithfully express in GABAergic neurons brain wide and the short EGFP half-life reports Gad67 transcriptional level. These mouse strains provide a convenient model for in vitro, in vivo and ex vivo studies of GAD67 functions and for the mapping of activated inhibitory circuits under different physiological and pathological conditions.

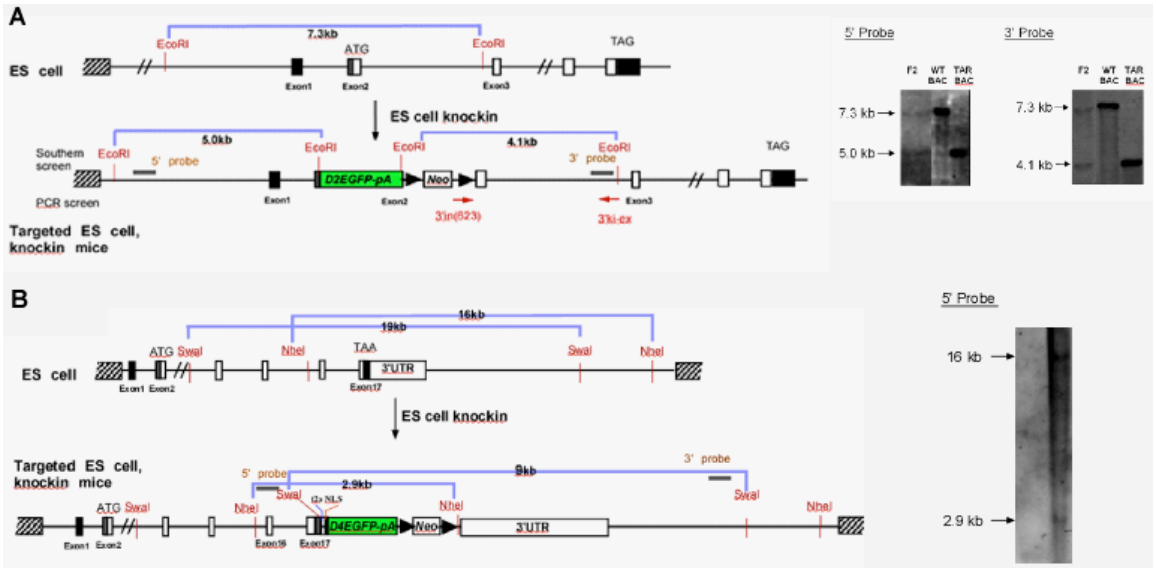

Figure 3.1 Generation of two Gad67 transcriptional reporter mouse strains

(A) Design of the Gad67-D2EGFP mice. D2EGFP was inserted in the translation start site (ATG) of the endogenous Gad67 gene locus by homologous recombination. The targeted Gad67 locus has a EcoRI digested fragment of 5.0kb at the 5' side and a EcoRI digested fragment of 4.1 kb at the 3' side, in comparison to the fragment of 7.0kb in the unmodified Gad67 locus. Southern blotting results show the targeted ES cell clone F2 has both the bands expected from modified locus and the unmodified locus for 5' and 3' side.

(B) Design of the Gad67-t2a-NLS-D4EGFP mice. A nuclear localized D4EGFP was inserted to and replace the stop codon(TAA) of the endogenous Gad67 gene locus by homologous recombination. The targeted Gad67 locus has a NheI digested fragment of 2.9kb at the 5‘ side, in comparison to the fragment of 16.0kb in the unmodified Gad67 locus. Southern blotting result shows the targeted ES cell clone has both the bands expected from modified locus and the unmodified locus for 5' side.

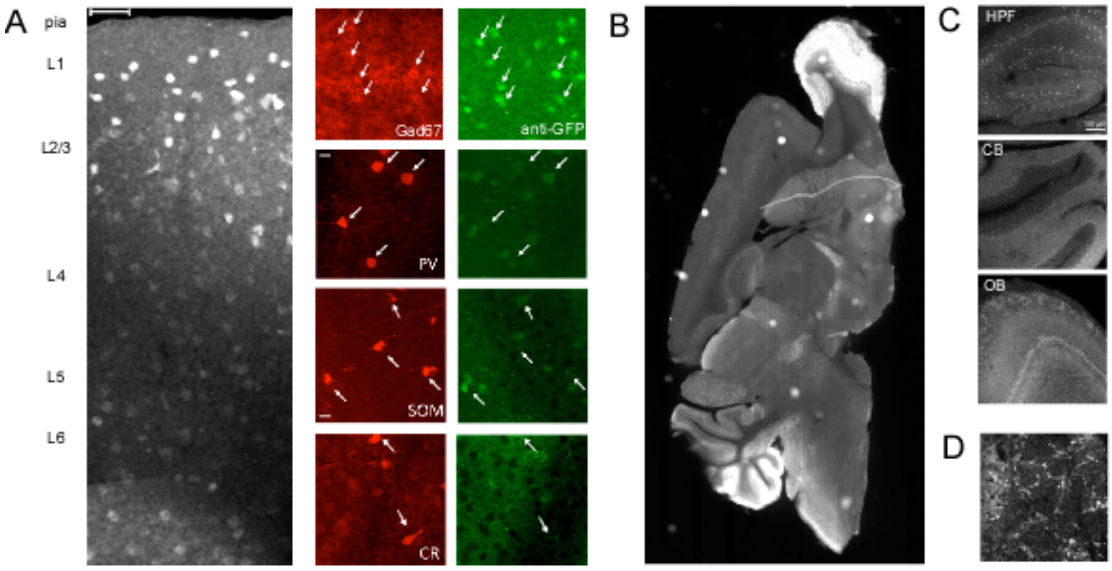

Figure 3.2 Gad67 reporter mouse strains express GFP specifically in GABAergic neurons brain wide

(A) GFP expression pattern in the visual cortex of Gad67-D2EGFP mouse. All Gad67 staining positive cells are GFP positive (n=106). Major interneuron markers PV+, SOM+ and CR+ also colocalize with GFP, respectively. Note that the GFP levels are the highest in PV+ populations, lower in SOM+ population and the lowest in CR+ populations.

(B) GFP expresses in all brain areas containing GABAergic neurons in Gad67-t2a-nls-D4EGFP mouse.

(C) Representative images of GFP expression pattern in hippocampus, cerebellum and olfactory bulb of Gad67-t2a-nls-D4EGFP mouse.

(D) A two-photon *in vivo* image of GFP in the olfactory bulb of Gad67-D2EGFP mouse.

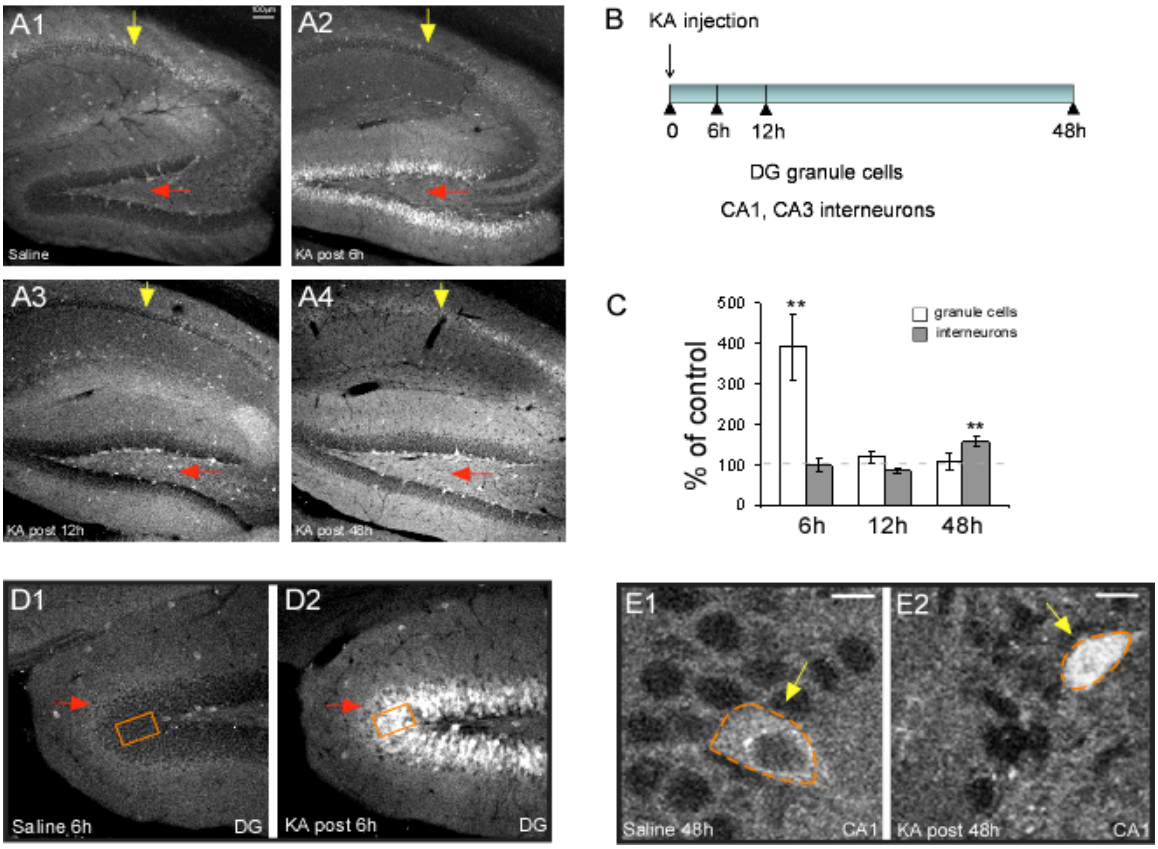

Figure 3.3 Validation of Gad67 transcriptional reporter ability using a kainic acid induced limbic seizure model

(A1) Representative image of the hippocampus from saline injected Gad67-D2EGFP mouse. Note that GFP labels many interneurons throughout hippocampus. In the dentate gyrus, there is almost no GFP signal.
(A2) Representative image of the hippocampus from KA injected Gad67-D2EGFP mouse after 6 hours. Note the robust induction of GFP signal in the dentate gyrus area (red arrow).
(A3) Representative image of the hippocampus from KA injected Gad67-D2EGFP mouse after 12 hours. Note the GFP signal in the dentate gyrus area goes down to almost base-line level (red arrow).
(A4) Representative image of the hippocampus from KA injected Gad67-D2EGFP mouse after 48 hours. Note the GFP signal in the dentate gyrus area remain at baseline level while interneurons in CA1 and CA3 regions show significant induction of GFP (yellow arrow).

(B) The schema of KA injection and analysis protocol
.
(C) Quantification of the GFP intensity change in hippocampus cell populations.

KA post 6 hours, granule cell GFP level are of 391% of the control granule cell GFP level (n=3 animals, t-test,$p<0.001$). KA post 12hours, granule cell GFP level is 118% of control (n=3 animals, t-test,$p>0.05$). KA post 48 hours, granule cell GFP level is 108% of control (n=3 animals, t-test,$p>0.05$).
KA post 6 hours, interneuron GFP level is of 98% of the control group interneuron GFP level (n=3 animals, t-test,$p>0.05$). KA post 12hours, interneuron GFP level is 85% of the control (n=3 animals, t-test,$p>0.05$). KA post 48 hours, interneuron GFP level increase significantly higher, is 157% of the control(n=3 animals, t-test,$p<0.001$).

(D1) and (D2) Representative images of the dentate gyrus in saline control and KA post 6 hours animals. Intensity is calculated by measuring the mean intensity of a boxed region (orange box) inside dentate gyrus.

(E1) and (E2) Representative images of CA1 interneurons in saline control and KA post 48 hours animals. Intensity is calculated by outlining the cell body and measuring the mean intensity of the outline (orange shape).

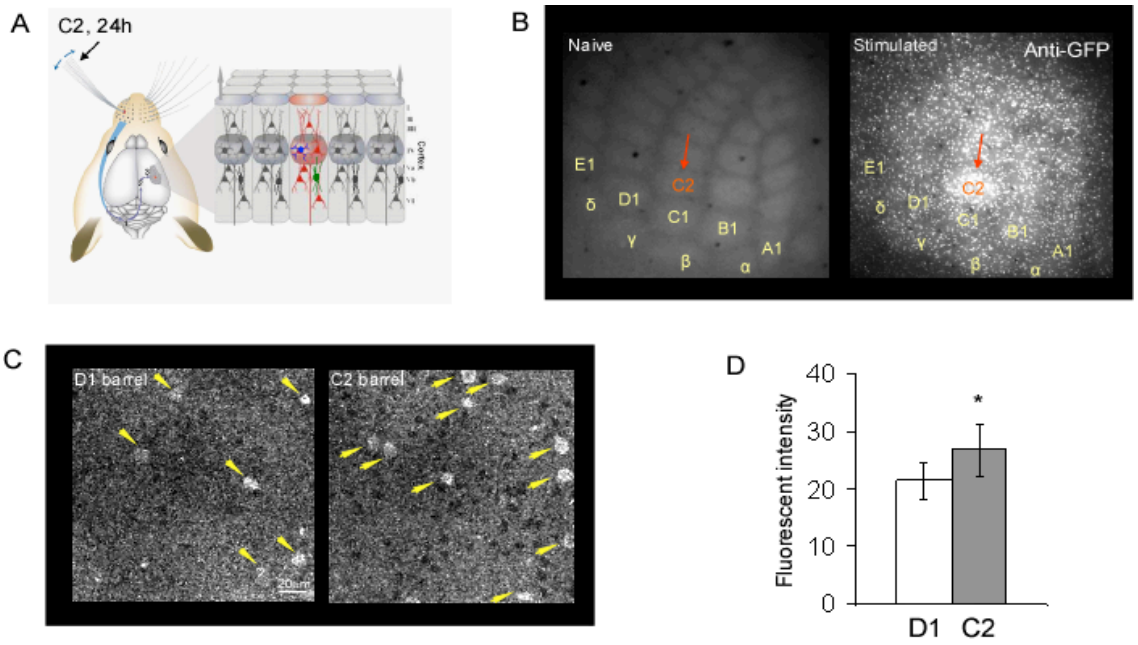

Figure 3.4 GFP is increased in the specific stimulated barrel with single whisker stimulation

(A) Schema of the single whisker stimulation. All whiskers on the left side are removed except for the C2 whisker. A small piece of magnetic wire is attached to the end of the C2 whisker so the whisker reflects at a frequency of 8Hz in the magnetic device.
(B) Comparision of naive animal barrel field and stimulated animal barrel field. Barrel C2 can be easily located by these flattened cortex preparations. Note the C2 barrel (red arrow) has elevated level of GFP compared to other barrels.
(C) At the cellular level, cells in the nearby unstimulated D1 barrel have lower fluorescent level than the cells in stimulated C2 barrel.
(D) Comparison of the average fluorescent intensity in cells of D1, C2 barrels. Cells in the C2 barrel have significantly higher intensity (n=31 cells from 3 animals in each barrel, t-test, $p<0.05$, error bars represent standard deviation (SD)).

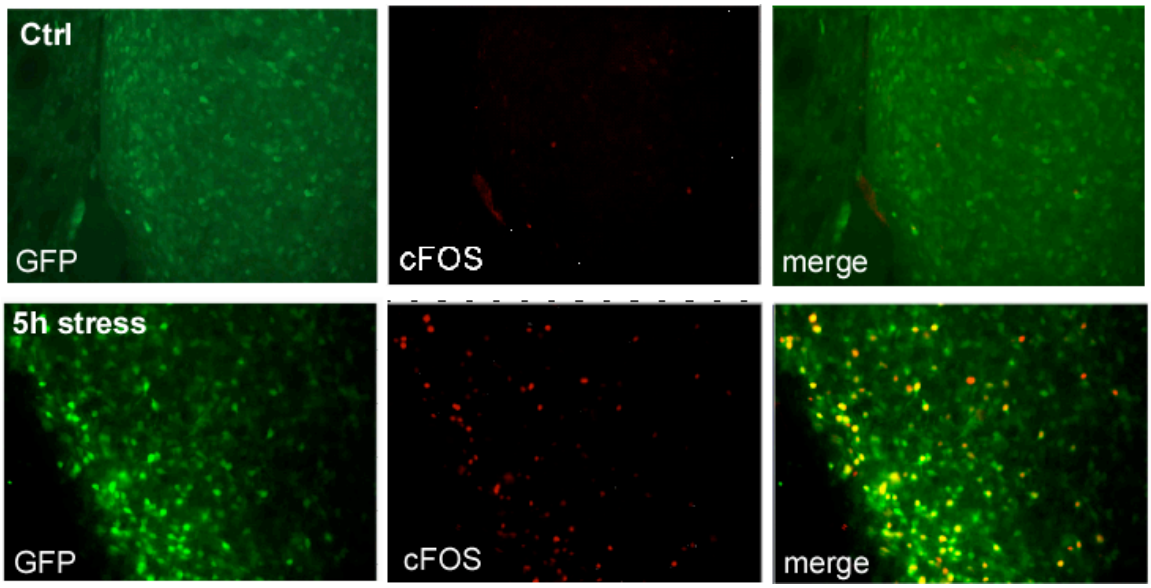

Figure 3.5 GFP expression in the lateral septum after acute stress

Acute 5 hour stress induces specific expression of c-fos (Red) and higher level of GFP in lateral septum. More than 90% of c-fos positive neurons are stained with GFP, and c-fos +GFP double labeled neurons exhibits highest brightness of green.

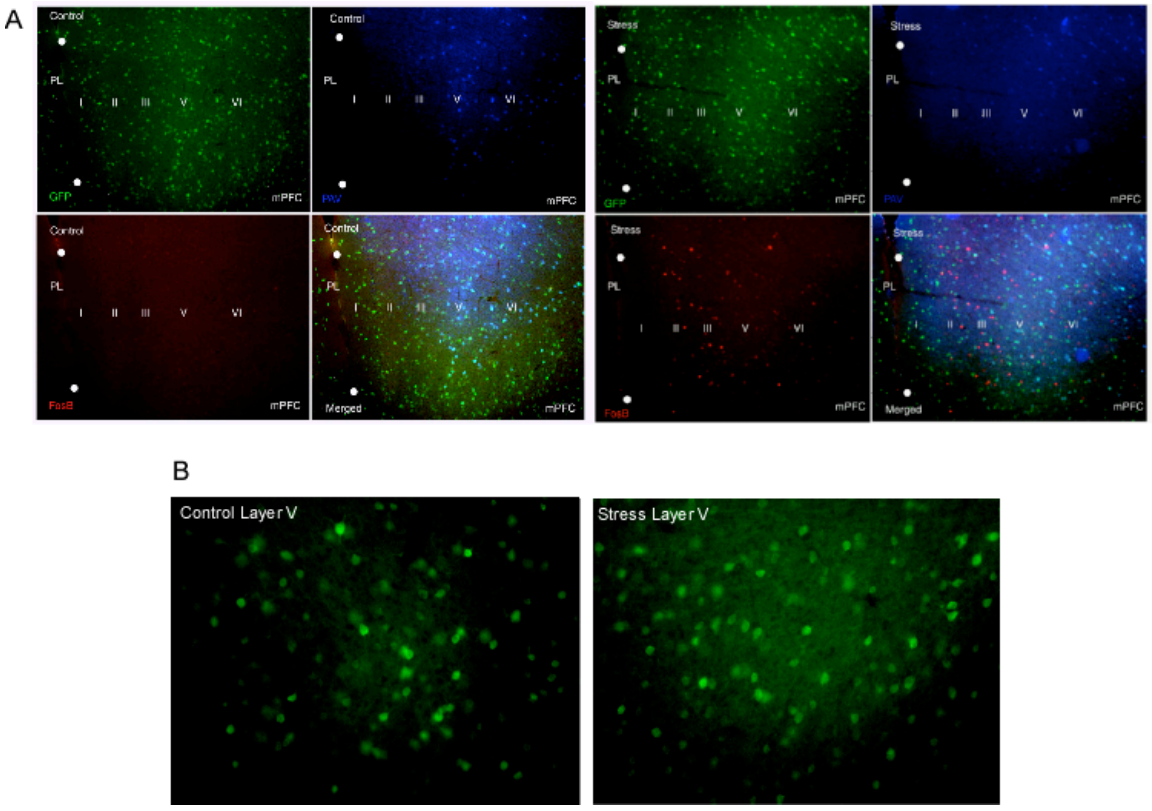

Figure 3.6 Chronic stress induces cell-type specific change in GFP expression pattern in the hippocampus CA1 region.

Chronic stress reduces PV marker(red), PNN marker (blue) and GFP level (green) in PV+ cells which are primarily located at the pyramidal cell layer (sp)
However, in the slm area, GFP+ cell numbers are increased after chronic stress.

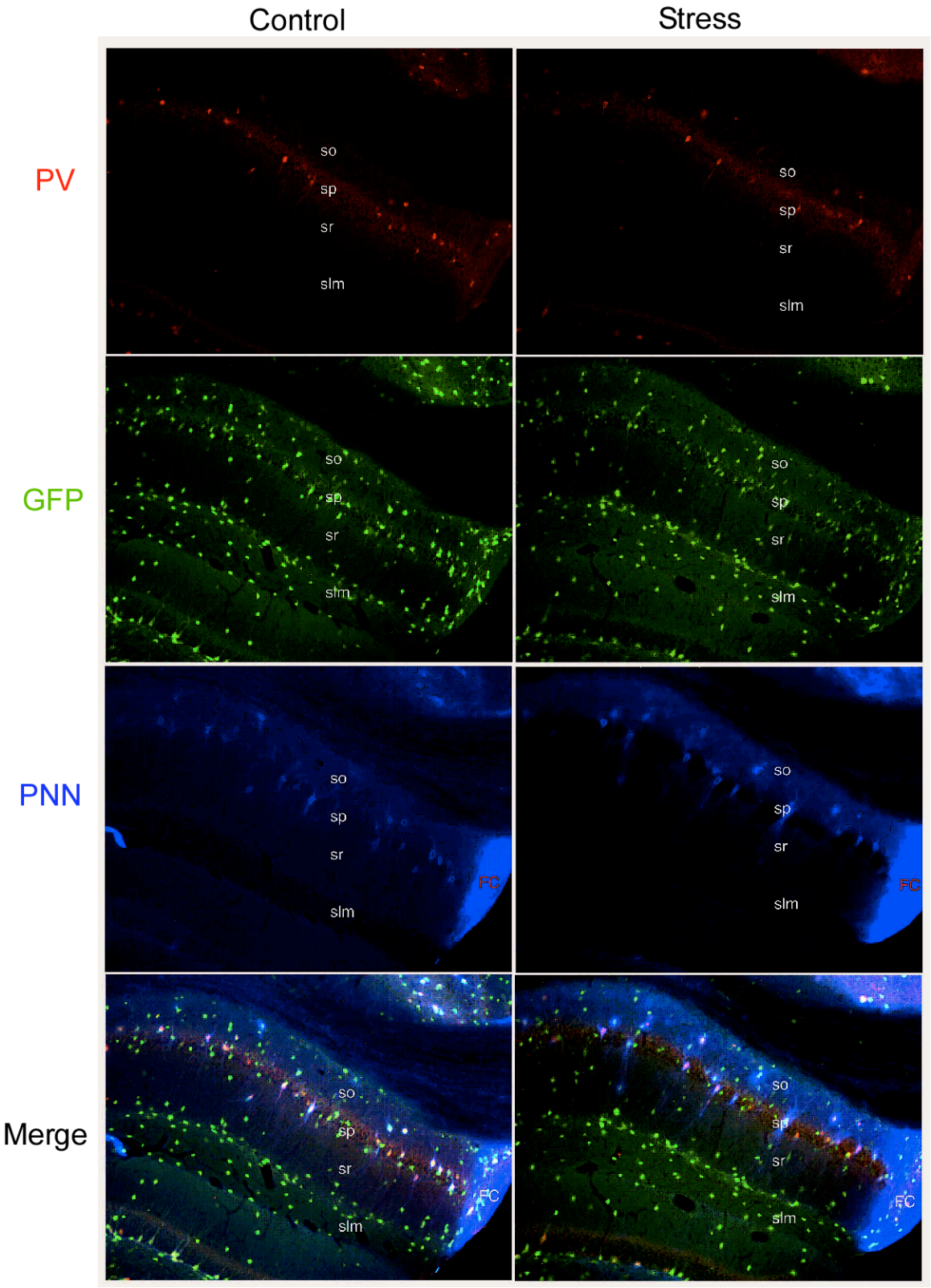

Figure 3.7 Chronic stress induces cell-type specific change in GFP expression pattern in the hippocampus CA1 region.

Chronic stress reduces PV marker (red), PNN marker (blue) and GFP level (green) in PV+ cells which are primarily located at the pyramidal cell layer (sp)
However, in the slm area, GFP+ cell numbers are increased after chronic stress.

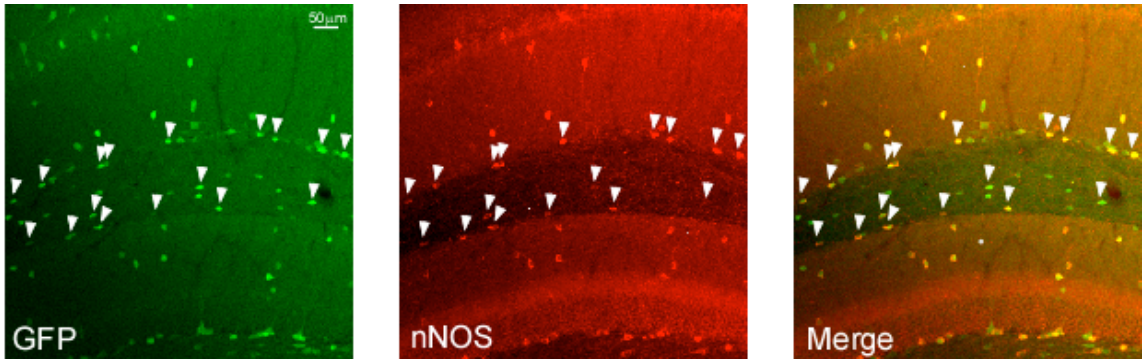

Figure 3.8 Some GFP+ cells in the slm region are nNOS+ interneurons

Arrows point to cells positive for both GFP and nNOS staining, which comprise of at least 30% of the total slm cells.

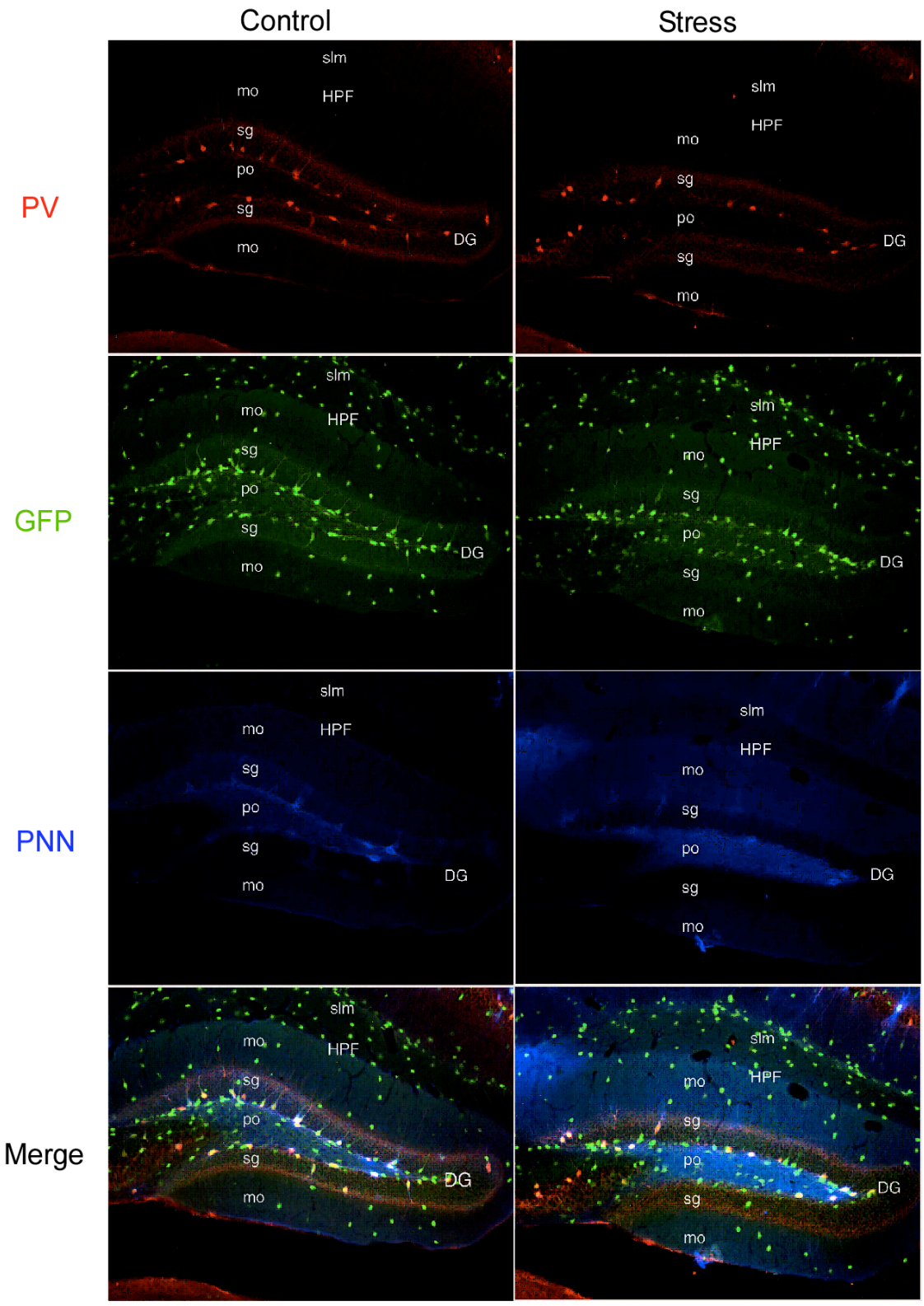

Figure 3.9 Chronic stress reduces GFP expression in the hippocampus dentate gyrus region

Similar to the results in the CA1 region, chronic stress also reduce PV (red) and PNN (blue) expression in the dentate gyrus. GFP levels (green) in the PV+ cells are also reduced.
Note the reduction of GFP in the granule cell layer. Particularly in the control animal, GFP+ cells in the granule cell layer have long processes. While in the stressed animal, GFP level is reduced in the granule cell layer and there is a lack of labeled neuronal process.

Chapter 4. Materials and Methods

Constructs

P_{G67}- GFP, Cre, Amp, Syn-GFP, tdTomato were described previously in (Chattopadhyaya et al 2007). For P_{G67}- Nrx1 b , the Neurexin 1 b construct does not contain the splice site 4. Super-Ecliptic-GFP (SEP) was cloned into an EcoRI site created in the extracellular domain but immediately before transmembrane domain. SEP fragment was PCR amplified by Pfu Ultra II Fusion HS DNA Polymerase (Stratagene) with EcoRI sites on both ends but without the stop codon.

Injection, Tissue Processing and Analysis of Perisomatic Boutons in Visual Cortex of $Gad67^{lox/lox}$: $Gad65^{-/-}$ Mice Injected with AAV- GFP-ires-Cre

For controls, I used a strain of adeno-associated virus expressing GFP in $Gad67^{flx/flx}$: $Gad65^{+/+}$ mice or $VGAT^{flx/flx}$ mice at P18. For knockouts, I used a strain of adeno-associated virus expressing Cre and GFP (AAV- GFP-ires-Cre) to inactivate Gad or VGAT in $Gad67^{flx/flx}$: $Gad65^{-/-}$ mice at P18. Mice were anesthetized with an intraperitoneal injection of ketamine/xylazine mixture (0.13 mg/g, 0.01 mg/g body weight). A small hole in the skull was made using a dental drill (Henry Schein), 1 mm anterior from Lambda, and 4 mm from the midline. The dura was slightly punctured and virus was delivered by pressure injection using a glass micropipette (tip size of roughly 10 μm) attached to a Picospritzer (General Valve). The glass micropipette was lowered to 0.5 mm below the pia surface. To inject virus into the brain, air puffs were delivered (25 psi, 10 ms duration) at a frequency of 0.2–0.4 Hz to inject a virus volume of 0.5-1ml.The

pipette was then held in place for approximately 5 minutes before completely retracting out of the brain.

At P26, AAV-injected mice were anesthetized (sodium pentobarbitone, 6 mg/100 g body weight) and perfused transcardially with 4% paraformaldehyde in phosphate buffer (pH 7.4). Coronal sections (80 μm) were cut from visual cortex using a vibratome (Leica VT100). Brain sections were blocked in 10% NGS (Normal Goat Serum) and 1% Triton X-100. Slices were then immunostained with anti-NeuN (monoclonal, 1:400, Chemicon), and anti-parvalbumin (Pv) antibody (rabbit 1:1000, Sigma) for analysis of bouton size, or anti-GABA (rabbit 1:1000, Sigma) and Pv (mouse 1:1000, Sigma) for analysis of GABA level followed by Alexa594-conjugated anti-rabbit IgG and Alexa633-conjugated anti-mouse IgG (Molecular Probes, 1: 400) and mounted in Vectashield mounting medium (Vector).

Slice culture and biolistic transfection

Slice culture was prepared as described (Stoppini et al 1991). Postnatal day 2–5 mouse pups were decapitated, and brains rapidly removed and immersed in ice-cold artificial low sodium cerebrospinal fluid (ACSF, containing 4 mM KCl, 5 mM MgCl2, 1 mM CaCl2, 26 mM NaHCO3, 10 mM glucose and 8% sucrose, saturated with 95%:5% O2:CO2). Coronal brain slices of occipital cortex, 400 μm thick, were cut with a Chopper (Stoelting) into ice-cold ACSF. Slices were then placed on transparent Millicell membrane inserts (Millipore, Bedford, MA), usually two slices/insert, in 30 mm Petri dishes containing 1 ml of culture medium (containing DMEM, 20% Horse serum, 1 mM Glutamine, 13 mM Glucose, 1 mM$CaCl_2$, 2 mM $MgSO_4$, 0.5 μm/ml Insulin, 30 mM Hepes, 5

mM $NaHCO_3$ and 0.001% Ascorbic acid). Finally, they were incubated in a humidified incubator at 34°C with a 5% CO_2 enriched atmosphere, and the medium changed twice a week. All procedures were performed under sterile conditions.

Constructs to be transfected were incorporated into "bullets" which are made using 1.6-micron gold particles coated with 50ug of the DNA of interest. These bullets were used to biolistically transfect slices by gene gun (BioRad) at high pressure (helium gas, 180 psi) and the transfected slices incubated for 72 hours under the same conditions as described above, before imaging.

GAD67 floxed: Gad65-/- mice and single cell recombination

GAD67 floxed mice were made in the lab of Dr.Richard Palmiter at the University of Washington, Seattle. Exon 2 of the GAD67 gene was floxed, and complete knockouts died at birth. Gad65 $^{+/-}$ mice were obtained from Dr. Shera Kash (Kash et al 1997). Gad65 -/- mice live although with increase chance of seizure and they have difficulty with breeding. To create a conditional GABA knock-out, Gad67 floxed and $Gad65^{+/-}$ mice were bred together to generate mice of genotypes $Gad67^{flx/flx}$: $Gad65^{+/-}$. Such genotyped animals were then used as breeders to generate $Gad67^{flx/flx}$: $Gad65^{+/+}$ and $Gad67^{flx/flx}$: $Gad65^{-/-}$ animals in the same litter. Single cell deletion of both GADs was done in organotypic cultures made from $Gad67^{flx/flx}$: $Gad65^{-/-}$ mice. They were biolistically co-transfected with 10kbGFP and 10kbCre to knockout both GADs by Cre mediated recombination and label the cell with GFP at the same time.

Immunohistochemistry

Mice were anesthetized (sodium pentobarbitone, 6 mg/100 g body weight) and transcardially perfused with 4% paraformaldehyde in phosphate buffer (pH 7.4). 60 μm thick coronal sections were cut from visual cortex using a vibratome (Leica VT100). Brain sections were blocked in 10% NGS and 1% triton. Slices were then incubated overnight at 4°C in 10% NGS, 0.1% triton and the following primary antibody: GAD65 (monoclonal antibody, 1:1000, Chemicon), NeuN, a monoclonal antibody that specifically label neuronal nuclei (1:400, Chemicon), Parvalbumin (Pv, monoclonal antibody, 1:1000, Sigma), Somatostatin (SOM, rabbit polyclonal antibody, 1:1000, Chemicon), Calretinin (CR, goat polyclonal antibody, 1: 1000, Chemicon), CKK (monoclonal antibody #9303, 1:1000, CURE/Digestive Disease Research Center, Vaglahs, CA), GABA (rabbit polyclonal antibody, 1:1000, Sigma). Sections were then incubated with appropriate Alexa594-conjugated goat IgG (Molecular Probes, 1: 400) and mounted.

Organotypic cultures were fixed overnight at 4C in 4% paraformaldehyde in phosphate buffer (pH 7.4), frozen and thawed in 30% sucrose in PBS, and subjected to immunofluorescence as described above for brain sections. Freeze-thaw is known to increase exposure of antigen and sensitivity of immunostaining in brain tissue.

Confocal Image Acquisition and Analysis

Non-overlapping images from a single confocal plane were acquired with a 63X oil immersion objective (Zeiss, NA 1.4) using confocal microscopes (Zeiss LSM 510 &710). Scans from each channel were collected in multiple track mode and subsequently merged. Care was taken to use the lowest laser power and no bleed through was visible between

Alexa594 and Alexa488 channels. Images were acquired using the same acquisition parameters for all the samples. Images were saved as TIFF files and analyzed with NeuroLucida (MicroBrightField, VT). Pyramidal cell somata were identified by NeuN immunofluorescence.

Bouton density was determined by measuring the total length of axon and counting the total number of varicosity. Axon was traced in 3D using NeuroLucida software (Micro-BrightField, VT). Bouton size was measured by the diameter of a bouton perpendicular to the basket axon around pyramidal cell soma using Zeiss LSM software. All quantifications were done blind to the genotype.

Two-Photon Laser Scanning Microscopy

Live slice cultures were imaged using a custom-built 2-photon laser scanning microscope based on an Olympus laser scanning microscope (Olympus America Inc., Melville, NY). I used a 60X objective (NA 0.9, Olympus) and the Ti-Sapphire laser (Chameleon Ultra, Coherent) as light source. All imaging experiments were performed under 910nm unless noted otherwise. Fluorescence was detected in whole field detection mode with a photomultiplier tube (Hamamatsu, Bridgewater, NJ). Laser power was adjusted so that additional power failed to reveal previously undetected boutons. Optical sections were collected at 0.5mm spacing. Slices were kept in a transparent chamber with ACSF (2.5 mM KCl, 1 mM $MgSO_4$, 2 mM $CaCl_2$, 25 mM $NaHCO_3$, 1.25 mM NaH_2PO4, 126 mM NaCl, and 14 mM glucose) saturated with 95% O_2/5% CO_2 and maintained at 35 degree Celsius (Inline heater, Warner Instrument).

Two-photon Microscopy Data acquisition and analysis

Image acquisition was by Fluoview (Olympus, NY). Several time-lapse protocols were used. For observating Syn-GFP puncta refinement at EP24, a two-photon Z-stack was taken every 15 minutes for 2 hours. For observing Syn-GFP formation at EP18, a two-photon Z-stack was taken every 1 minute for 60 minutes. For observating axonal filopodia, a two-photon Z-stack was taken every 10 minutes for 3 hours.

Puncta were analyzed by custom-made Matlab applications. Briefly, a projection of 20-30mm Z-stack of puncta was made for subsequent analysis individually. A look up table was set by taking into account of the 10% brightest pixels and 10% dimmest pixels. Puncta were thesholded and binerated. The fate of each punctum was tracked in all the time series. Puncta intensity was measured by masking the binerated punctum area back to the grayscale image.

Filopodia were analyzed by tracing the axon arbor and calculate the number of filopodium site. Filopodia were defined as 0.3-2mm protusions coming out perpendicular from the axonal bouton.

Long Term Time-Lapse Confocol Microscopy and Analysis

Images were acquired with a 20X long working distance objective (Zeiss, NA 0.7) on a confocal microscope (Zeiss LSM 710). Slices were kept in a heated chamber (35 degree Celsius) with 5% CO_2, the same condition as in the incubator. Right before the 3-day experiment, slices were transferred into the glass bottom petri dishes (No 1.5 glass,

MatTek Corporation, MA). Scans were collected at a Z interval of 3mms from the tdTomato channel (Zen Software, Zeiss). Care was taken to use as little laser power as possible to minimize the phototoxicity effect. On each cell, every imaging session is less than 2 minutes. Images were acquired every day on each slice for three consecutive days. Images were saved as TIFF files.

Images were analyzed with ImageJ. Projections were made and the StackReg Plug-in (EPFL, Switzerland) was used to align the images so as to identify the dynamics of axon terminals over days. The change in length (mm) was measured by the Manual Tracing Plug-in. An Excel spreadsheet was generated to record each dynamic axon terminal's status over 3 days. Axon terminal dynamics was categorized in four classes: Addition, Extension, Lost and Reduction.

Statistical analysis

Differences between groups were assessed with Kruskal-Wallis one-way ANOVA on ranks with Dunn's post hoc test for not normally distributed data. Differences in bouton density and bouton size between KO cultures and littermate Ctrls were assessed with Mann-Whitney test for not normally distributed data.

Immuno Electron Microscopy (Collaboration with Dr. Graham Knott)

P26 mice were anaesthetized with sodium pentobarbitone (6mg/100g body weight, intraperitoneal) and perfused immediately with 100ml of 0.2% glutaraldehyde and 2% PFA in 0.1M phosphate buffer, pH7.4. One hour after perfusion, the brains were removed

and 50mm vibratome (Leica VT100) sections cut coronally from the visual cortex. Sections were cryoprotected in 2% glycerol and 20% DMSO in 0.1M PBS, for 15 minutes, and freeze thawed twice in liquid nitrogen. These were then incubated overnight in the primary antibody (GFP 1:600, Chemicon) in PBS at 4C, then for 2 hours at room temperature in biotinylated secondary antibody (1:500 goat anti-rabbit (F)ab fragment, Jackson Laboratories, USA). To reveal the labeling, avidin biotin peroxidase complex (ABC Elite, Vector Laboratories, USA) was used for 2 hours, and incubated in 3, 3'-diaminobenzidine tetrachloride (Fluka, Switzerland) and 0.015% hydrogen peroxide. Following enhancement, the sections were then washed, postfixed in osmium tetroxide and embedded in Epon resin (Fluka). Once cured the regions of interest were localized with the light microscope and this area cut away from the section. This was then attached to a blank resin block and serially thin sectioned at a thickness of between 50-60nm. Images were acquired with a Philips CM12 electron microscope with a filament voltage of 80kV using a digital camera (Megaview 3, SIS, Germany).

Electrophysiology recording

Single whole-cell recordings of fluorescent labeled cells (Basket cells) were made with Axopatch 200B or 700B amplifiers (Molecular Devices, Union City, CA), using an upright microscope (Olympus, BX51) equipped with infrared-differential interference contrast (IR-DIC) optics and fluorescence excitation source. Both IR-DIC image and fluorescence image were captured with a digital camera (Microfire, Optronics, CA). The organotypic slice culture was rapidly moved into the recording chamber, perfused with the oxygenated ACSF (composition in mM: 124 NaCl, 2.5 KCl, 2 $MgSO_4$, 2 $CaCl_2$, 1.25 NaH_2PO_4, 26 $NaHCO_3$, 11 D-glucose, pH 7.35, ~300 mOsm) at 32-34 °C. The internal

solution of the recording pipette contained (in mM): 130 K-gluconate, 15 KCl, 10 Na-phosphocreatine, 10 HEPES, 4 ATP-Mg, 0.3 GTP and 0.3 EGTA, adjusted to pH 7.3 with KOH and to ~300 mOsmol. The pipette resistance was 3 - 5 MΩ. Signals were recorded and filtered at 2 kHz, digitalized at 10 or 20 kHz (DIGIDATA 1322A, Molecular Devices) and further analyzed using the pClamp 9.0 software (Molecular Devices) for intrinsic properties.

Recombineering

BAC clone containing the mouse GAD67 gene was identified from the RPCI-22 library (Research Genetics). The mouse GAD67 gene contains 16 exons, spanning a 70Kb genomic region. A BAC clone RPCI22-56I9 containing the entire gene and 60kb of upstream and downstream regions were used for BAC modifications. The identity and entirety of the BAC was confirmed by southern blotting.

A BAC targeting vector was constructed in which the d2EGFP and the PGK poly adenylation signal and the Neo cassette were flanked by 5' targeting arm and 3' targeting arm in the vector PL450 (Liu et al 2003). 5' targeting arm and 3' targeting arm are each of ~500 bp homologous regions and they are designed in such that d2EGFP expression cassette were inserted in the first coding exon at translation initiation site of the *Gad67* gene. After the induced recombination in the bacteria, PCR was performed to screen for the correct targeted clones that contain the whole cassette at the targeted site. Then a retrieval vector was built to have 5' retrieval arm and 3' retrieval arm of ~500bp homologous regions in the vector PL253(Liu et al 2003). A second round of recombination was induced in the bacteria containing the targeted BAC with the retrieval vector to generate

an ES targeting vector which has the d2EGFP expressing cassette flanked by a 4 kb 5' Knock-In arm and 2 kb 3' Knock-In arm.

The Knock-In vector was confirmed by PCR and restriction enzyme digestions. Afterwards a maxi-prep product of the Knock-In vector was linearized by SwaI digestion and send to Woodbury facility for targeting in the ES cells (Hybrid ES cells, 129/B6 Background). The targeted ES cells were selected by positive marker of Neomycin resistance. Subsequently, the targeted ES cell clones are confirmed by the PCR. Two clones are selected and southern Blotting was done to confirm the clones for further ES cell expansion. One expanded clone was used to inject into blastcyst of the surrogate mother to generate chimera founders. All chimeras have 100% recombination rate judged by fur color and have germline transmission of the targeted region.

Southern blotting

On the first day, 10mg of genomic DNA prepared from the ES cell is digested over-night with the enzyme of choice. On the second day, the DNA digests are run on a 1% gel at 30V for ~18 hours. On the third day, the gel is soaked in the denaturing solution (1.5M NaCl/ 0.5M NaOH) before it is placed in the transfer system. Due to capilliary effect, DNA from the gel is transferred to the negatively charged membrane. On the fourth day, the membrane is taken out, air-dryed and UV crosslinked. Digoxigenin (DIG) based Southern probes are synthesized by PCR reactions using DIG labeled dUTP (DIG DNA labeling Kit, Roche). Membrane is submerged in EasyHyb (Roche) for 1 hour at 42c to block nonspecific epitopes. Then the membrane is hybridized at 42c for overnight with

new EasyHyb containing the specific Southern probe. On the fifth day, the membrane is taken out of the hybridization bag and subject to several stringency washes with SSC and SDS solutions. Afterwards, the membrane is submerged in blocking solution (Roche) and then incubated with blocking solution containing Alkaline Phosphatase (AP) conjugated anti-DIG antibody for 30 minutes. Two quick washes ensue with detection buffer (Roche). Then the substrate CDP-Star (Roche) for Alkaline Phosphatase was added to the detection buffer covering the member for five minutes. Excessive liquid is taken away from on top of the membrane. The membrane is then exposed to film (Kodak) and the film is developed.

Whisker Stimulation

Mouse was passively stimulated for 24 hr by attaching a small piece of ferrous metal (Alloy 28, California Wire Company, CA) to the C2 whisker and placing the animal in a magnetic field based stimulation device (Melzer et al 1985). The device is consisted of a cylindrical cage inside an electromagnetic coil which delivered a field intensity of approximately 7 $X10^3$ A/m rms in bursts with a duration of 40 ms and interburst interval of 85 ms. This delivers a stimulation frequency of 8 Hz which mimics the normal whisking frequency.

Kainic Acid Treatment

GAD67-d2EGFP or Gad67-t2a-NLS-d4EGFP positive mice were backcrossed to C57BL/6J background for at least 3 generations. Young adult (6 – 8 weeks of age) male mice (20 –27 g) were used. Mice were injected with KA (20 mg/kg, i.p, in buffered saline) or with saline. KA initiated an acute behavioral syndrome, which included early

staring, “wet dog shakes,” and seizures from mild forehead nodding to severe limbic convulsions with rearing and foaming at the mouth as described previously in the literature (Sperk et al 1983). Periods of generalized seizures were observed 30–90 min after KA injection. Thereafter, seizure activity declined.

After KA treatment, mice were fixed with 4% paraformaldehyde at time points of 6 hours, 12 hours and 48 hours. Vibratome sections of 80mm were made and imaged under Confocal Microscope (Zeiss 510 and 710). GFP signaling was quantified by drawing a box, which lies completely in the dentate gyrus area and the average fluoresent intensity in the boxed area was calculated. For CA1 and CA3 interneurons, care was taken to draw an outline of each individual cell and the average fluoresent intensity in the boxed area was calculated.

Chronic restraint stress

9 young adult (6 – 8 weeks of age) male Gad67-T2A-NLS-D4EGFP positive mice weighing 20-27g at the start of the experiment were used. Littermates were used to pair the control/stressed animals. Control (n=4) and stressed (n=5) animals are housed in separate cages. The stressed animals were restrained in wire-mesh container for 6 hours daily (10:00am to 4:00pm) for 10 days. All the animals have free access to food and water except when in restraint sessions.

Chapter 5. Future directions

Role of GABA transmission in inhibitory axon and synapse development

One aspect that would strengthen my study is to correlate presynaptic puncta stability with axonal growth. My data suggests that synaptic transmission control axon growth by destabilizing inappropriate presynaptic puncta. My hypothesis is that branches with destabilize puncta tend to retract or lost and new branches emerge from stable boutons. Synpatic transmission regulates the iterative growth of axon and sculpts axon arbor development. I would like to image a RFP tagged synaptophysin together with cytosolic GFP in the control and mutant basket cell axons. I can observe filopodia/branches growth simultaneously with monitoring puncta intensity change. Most likely, I need to observe for an extended period of time to obtain enough axon growth as interneurons at the stage I examined grow 1-2% over an hour. The analysis will be similar to (Ruthazer et al 2006).

One important question that my study has not answered is whether synaptic transmission determines subcellular innervation of the basket cell. In the transmission depleted basket cells, I observe plenty of perisomatic boutons surrounding pyramidal cells but since I do not know the location of pyramidal cell dendrites, I could not say whether the mutant basket cell still prefentially target somata and proximal dendrite. In order to answer this question, I will need to do a study similar to one done by Di Cristo and colleague (Di Cristo et al 2004) where I will label entire pyramidal cells, record the location of GABAergic boutons relative to the pyramidal cell and analysis the bouton distribution pattern.

The mechanisms linking GABA transmission to synapse maturation remain to be determined. My finding suggests that signal from the postsynaptic side may trigger a retrograde signal mediating such process. One possibility is that released GABA could signal through $GABA_A$ receptors and trigger local release of trophic factors, such as BDNF to promote the maturation of inhibitory synapses. I propose to locally infuse BDNF on part of the mutant cell axon arbor and observe if axon will start to eliminate some of the excessive boutons.

The downstream signaling for GABA transmission mediated refinement could be a mechanism similar to the scenario in NMJ where acetylcholine was shown to negatively regulate neuromuscular synapse formation through a cyclin-dependent kinase 5 (Cdk5) dependent mechanism (Lin et al 2005). It will be of interest to delete Cdk5 in the postsynaptic pyramidal cells and observe whether this will cause the innervating presynaptic GABAergic axons to have a bouton overgrowth phenotype. Conditional knockout animal of Cdk5 has been generated (Agarwal et al 2004). I can use gene gun transfection to knock out Cdk5 in sparsely labeled pyramidal cells and examine the presynaptic innervation by VGAT staining. Or I can use AAV-GFPiresCre to infect a small area of pyramidal cells and label the presynaptic basket cell to examine the axon arbor dynamics inside the infected area. Alternatively, I can use Cdk5 antagonist to inhibit Cdk5 action and examine if it results in a similar phenotype to GABA transmission null cells.

I am also interested in characterizing further on the basic properties of mutant boutons. First, I would like to know if GABA is restored, for example via the introduction of an intracellular electrode into the GAD-/- cell body, whether GABA could diffuse or transported to these excessive mutant synaptic sites and whether mutant synapses are still capable of releasing GABA. Second, I would like to identify cell adhesion molecules that are present in the mutant synaptic sites in comparison with those present in mature periosmatic synapse. Since synaptic transmission may recruit many more adhesion molecule in order to aid synapse maturation, it is important to find out what are the early stage cell adhesion molecules that might involve in nascent synapse formation and what are the later stage cell adhesion molecules that might play a role in strengthening synaptic structure.

Gad67 transcriptional reporters

I would like to use Gad67 transcriptional reporter mice to ask several questions. For example, how long do GFP induced cells remain more excitable after stimulus cessation? Is the response to sensory experience stereotyped? Are cells activated by fear conditioning, memory retrieval and fear extinction overlapping or distinct?

I have done some preliminary in vivo time-lapse imaging in the olfactory bulb and it looks promising. I would like to apply the reporter to map the input/output and the plasticity of the circuit. For example, it is not clear whether integration or divergence happen at the level of paraglomeruli cells. Whether continuation of exposure to a certain odor evokes more defined or enlarged response in paraglomeruli cells.

Live imaging of the brain tissues preparing from Gad67 transcriptional reporter mice could be instrumental in the development of better pharmaceutics, particularly those aiming at increasing Gad67 level. A decreased Gad67 mRNA level is one of the most reliable biomarkers in postmortem schizophrenia brains (Guidotti et al 2000). Treatment that increases Gad67 transcription improves behavior in a schizophrenia mouse model (Tremolizzo et al 2005). The Gad67 transcriptional reporter mice can serve as a convenient tool for high throughput screening of drugs targeting the Gad67 gene.

Recently, a human study using magnetic resonance spectroscopy found that GABA concentration in the frontal cortex, but not in the visual cortex, predicts saccade distractibility (Sumner et al 2010). This further supports the activity dependent, brain region specific regulation of GABA and it is likely to be mediated by activity dependent regulation of Gad67. In physiological terms, increase in GABA may reflect increase in the number of GABA interneurons in certain regions, or the number of synapses per neuron, or the GABA concentration per synapse. Being able to monitor GABA level at a cellular resolution could help narrow down some of these possibilities.

Bibliography

Addington AM, Gornick M, Duckworth J, Sporn A, Gogtay N, et al. 2005. GAD1 (2q31.1), which encodes glutamic acid decarboxylase (GAD67), is associated with childhood-onset schizophrenia and cortical gray matter volume loss. *Mol Psychiatry* 10:581-8

Agarwal N, Offermanns S, Kuner R. 2004. Conditional gene deletion in primary nociceptive neurons of trigeminal ganglia and dorsal root ganglia. *Genesis* 38:122-9

Ahmari SE, Smith SJ. 2002. Knowing a nascent synapse when you see it. *Neuron* 34:333-6

Akaaboune M, Culican SM, Turney SG, Lichtman JW. 1999. Rapid and reversible effects of activity on acetylcholine receptor density at the neuromuscular junction in vivo. *Science* 286:503-7

Alonso-Nanclares L, Minelli A, Melone M, Edwards RH, Defelipe J, Conti F. 2004. Perisomatic glutamatergic axon terminals: a novel feature of cortical synaptology revealed by vesicular glutamate transporter 1 immunostaining. *Neuroscience* 123:547-56

Alsina B, Vu T, Cohen-Cory S. 2001. Visualizing synapse formation in arborizing optic axons in vivo: dynamics and modulation by BDNF. *Nat Neurosci* 4:1093-101

Alvarez-Buylla A, Garcia-Verdugo JM. 2002. Neurogenesis in adult subventricular zone. *J Neurosci* 22:629-34

Asada H, Kawamura Y, Maruyama K, Kume H, Ding R, et al. 1996. Mice lacking the 65 kDa isoform of glutamic acid decarboxylase (GAD65) maintain normal levels of GAD67 and GABA in their brains but are susceptible to seizures. *Biochem Biophys Res Commun* 229:891-5

Asada H, Kawamura Y, Maruyama K, Kume H, Ding RG, et al. 1997. Cleft palate and decreased brain gamma-aminobutyric acid in mice lacking the 67-kDa isoform of glutamic acid decarboxylase. *Proc Natl Acad Sci U S A* 94:6496-9

Bacci A, Huguenard JR, Prince DA. 2005. Modulation of neocortical interneurons: extrinsic influences and exercises in self-control. *Trends Neurosci* 28:602-10

Bagri A, Cheng HJ, Yaron A, Pleasure SJ, Tessier-Lavigne M. 2003. Stereotyped pruning of long hippocampal axon branches triggered by retraction inducers of the semaphorin family. *Cell* 113:285-99

Barth AL, Gerkin RC, Dean KL. 2004. Alteration of neuronal firing properties after in vivo experience in a FosGFP transgenic mouse. *J Neurosci* 24:6466-75

Bartoletti A, Medini P, Berardi N, Maffei L. 2004. Environmental enrichment prevents effects of dark-rearing in the rat visual cortex. *Nat Neurosci* 7:215-6

Battaglioli G, Liu H, Martin DL. 2003. Kinetic differences between the isoforms of glutamate decarboxylase: implications for the regulation of GABA synthesis. *J Neurochem* 86:879-87

Bazemore A, Elliott KA, Florey E. 1956. Factor I and gamma-aminobutyric acid. *Nature* 178:1052-3

Ben-Ari Y. 2002. Excitatory actions of gaba during development: the nature of the nurture. *Nat Rev Neurosci* 3:728-39

Bettler B, Tiao JY. 2006. Molecular diversity, trafficking and subcellular localization of GABAB receptors. *Pharmacol Ther* 110:533-43

Bowers G, Cullinan WE, Herman JP. 1998. Region-specific regulation of glutamic acid decarboxylase (GAD) mRNA expression in central stress circuits. *J Neurosci* 18:5938-47

Brandon EP, Lin W, D'Amour KA, Pizzo DP, Dominguez B, et al. 2003. Aberrant patterning of neuromuscular synapses in choline acetyltransferase-deficient mice. *J Neurosci* 23:539-49

Broeke JH, Roelandse M, Luteijn MJ, Boiko T, Matus A, et al. 2010. Munc18 and Munc13 Regulate Early Neurite Outgrowth. *Biol Cell*

Buddhala C, Hsu CC, Wu JY. 2009. A novel mechanism for GABA synthesis and packaging into synaptic vesicles. *Neurochem Int* 55:9-12

Buzsáki G. 2006. *Rhythms of the brain*. Oxford ; New York: Oxford University Press. xiv, 448 p. pp.

Chao DL, Ma L, Shen K. 2009. Transient cell-cell interactions in neural circuit formation. *Nat Rev Neurosci* 10:262-71

Chattopadhyaya B, Di Cristo G, Higashiyama H, Knott GW, Kuhlman SJ, et al. 2004. Experience and activity-dependent maturation of perisomatic GABAergic innervation in primary visual cortex during a postnatal critical period. *J Neurosci* 24:9598-611

Chattopadhyaya B, Di Cristo G, Wu CZ, Knott G, Kuhlman S, et al. 2007. GAD67-mediated GABA synthesis and signaling regulate inhibitory synaptic innervation in the visual cortex. *Neuron* 54:889-903

Chinnasamy D, Milsom MD, Shaffer J, Neuenfeldt J, Shaaban AF, et al. 2006. Multicistronic lentiviral vectors containing the FMDV 2A cleavage factor demonstrate robust expression of encoded genes at limiting MOI. *Virol J* 3:14

Chiu CS, Brickley S, Jensen K, Southwell A, McKinney S, et al. 2005. GABA transporter deficiency causes tremor, ataxia, nervousness, and increased GABA-induced tonic conductance in cerebellum. *J Neurosci* 25:3234-45

Clancy B, Defelipe J, Espinosa A, Fairen A, Jinno S, et al. 2010. Cortical GABAergic Neurons: Stretching it Remarks, Main Conclusions and Discussion. *Front Neuroanat* 4:7

Cline HT. 2001. Dendritic arbor development and synaptogenesis. *Curr Opin Neurobiol* 11:118-26

Cobb SR, Buhl EH, Halasy K, Paulsen O, Somogyi P. 1995. Synchronization of neuronal activity in hippocampus by individual GABAergic interneurons. *Nature* 378:75-8

Cochilla AJ, Angleson JK, Betz WJ. 1999. Monitoring secretory membrane with FM1-43 fluorescence. *Annu Rev Neurosci* 22:1-10

Cohen-Cory S. 2002. The developing synapse: construction and modulation of synaptic structures and circuits. *Science* 298:770-6

Craig AM, Graf ER, Linhoff MW. 2006. How to build a central synapse: clues from cell culture. *Trends Neurosci* 29:8-20

Cullinan WE, Herman JP, Battaglia DF, Akil H, Watson SJ. 1995. Pattern and time course of immediate early gene expression in rat brain following acute stress. *Neuroscience* 64:477-505

Czeh B, Simon M, van der Hart MG, Schmelting B, Hesselink MB, Fuchs E. 2005. Chronic stress decreases the number of parvalbumin-immunoreactive interneurons in the hippocampus: prevention by treatment with a substance P receptor (NK1) antagonist. *Neuropsychopharmacology* 30:67-79

de Lanerolle NC, Kim JH, Robbins RJ, Spencer DD. 1989. Hippocampal interneuron loss and plasticity in human temporal lobe epilepsy. *Brain Res* 495:387-95

De Paola V, Holtmaat A, Knott G, Song S, Wilbrecht L, et al. 2006. Cell type-specific structural plasticity of axonal branches and boutons in the adult neocortex. *Neuron* 49:861-75

DeChiara TM, Bowen DC, Valenzuela DM, Simmons MV, Poueymirou WT, et al. 1996. The receptor tyrosine kinase MuSK is required for neuromuscular junction formation in vivo. *Cell* 85:501-12

DeFelipe J. 2002. Cortical interneurons: from Cajal to 2001. *Prog Brain Res* 136:215-38

Deitcher DL, Ueda A, Stewart BA, Burgess RW, Kidokoro Y, Schwarz TL. 1998. Distinct requirements for evoked and spontaneous release of neurotransmitter are revealed by mutations in the Drosophila gene neuronal-synaptobrevin. *J Neurosci* 18:2028-39

Di Cristo G, Wu C, Chattopadhyaya B, Ango F, Knott G, et al. 2004. Subcellular domain-restricted GABAergic innervation in primary visual cortex in the absence of sensory and thalamic inputs. *Nat Neurosci* 7:1184-6

Dong E, Agis-Balboa RC, Simonini MV, Grayson DR, Costa E, Guidotti A. 2005. Reelin and glutamic acid decarboxylase67 promoter remodeling in an epigenetic methionine-induced mouse model of schizophrenia. *Proc Natl Acad Sci U S A* 102:12578-83

Edwards JA, Cline HT. 1999. Light-induced calcium influx into retinal axons is regulated by presynaptic nicotinic acetylcholine receptor activity in vivo. *J Neurophysiol* 81:895-907

Engel D, Pahner I, Schulze K, Frahm C, Jarry H, et al. 2001. Plasticity of rat central inhibitory synapses through GABA metabolism. *J Physiol* 535:473-82

Eriksson PS, Perfilieva E, Bjork-Eriksson T, Alborn AM, Nordborg C, et al. 1998. Neurogenesis in the adult human hippocampus. *Nat Med* 4:1313-7

Erlander MG, Tillakaratne NJ, Feldblum S, Patel N, Tobin AJ. 1991. Two genes encode distinct glutamate decarboxylases. *Neuron* 7:91-100

Etherton MR, Blaiss CA, Powell CM, Sudhof TC. 2009. Mouse neurexin-1alpha deletion causes correlated electrophysiological and behavioral changes consistent with cognitive impairments. *Proc Natl Acad Sci U S A* 106:17998-8003

Fagiolini M, Hensch TK. 2000. Inhibitory threshold for critical-period activation in primary visual cortex. *Nature* 404:183-6

Fang C, Deng L, Keller CA, Fukata M, Fukata Y, et al. 2006. GODZ-mediated palmitoylation of GABA(A) receptors is required for normal assembly and function of GABAergic inhibitory synapses. *J Neurosci* 26:12758-68

Fletcher TL, Cameron P, De Camilli P, Banker G. 1991. The distribution of synapsin I and synaptophysin in hippocampal neurons developing in culture. *J Neurosci* 11:1617-26

Foldy C, Dyhrfjeld-Johnsen J, Soltesz I. 2005. Structure of cortical microcircuit theory. *J Physiol* 562:47-54

Fonnum F. 1984. Glutamate: a neurotransmitter in mammalian brain. *J Neurochem* 42:1-11

Foster AC, Kemp JA. 2006. Glutamate- and GABA-based CNS therapeutics. *Curr Opin Pharmacol* 6:7-17

Freund TF. 2003. Interneuron Diversity series: Rhythm and mood in perisomatic inhibition. *Trends Neurosci* 26:489-95

Freund TF, Buzsaki G. 1996. Interneurons of the hippocampus. *Hippocampus* 6:347-470

Freund TF, Katona I. 2007. Perisomatic inhibition. *Neuron* 56:33-42

Friedman HV, Bresler T, Garner CC, Ziv NE. 2000. Assembly of new individual excitatory synapses: time course and temporal order of synaptic molecule recruitment. *Neuron* 27:57-69

Fritschy JM, Brunig I. 2003. Formation and plasticity of GABAergic synapses: physiological mechanisms and pathophysiological implications. *Pharmacol Ther* 98:299-323

Galarreta M, Hestrin S. 1999. A network of fast-spiking cells in the neocortex connected by electrical synapses. *Nature* 402:72-5

Galea LA, McEwen BS, Tanapat P, Deak T, Spencer RL, Dhabhar FS. 1997. Sex differences in dendritic atrophy of CA3 pyramidal neurons in response to chronic restraint stress. *Neuroscience* 81:689-97

Gautam M, Noakes PG, Moscoso L, Rupp F, Scheller RH, et al. 1996. Defective neuromuscular synaptogenesis in agrin-deficient mutant mice. *Cell* 85:525-35

Gautam M, Noakes PG, Mudd J, Nichol M, Chu GC, et al. 1995. Failure of postsynaptic specialization to develop at neuromuscular junctions of rapsyn-deficient mice. *Nature* 377:232-6

Ge S, Goh EL, Sailor KA, Kitabatake Y, Ming GL, Song H. 2006. GABA regulates synaptic integration of newly generated neurons in the adult brain. *Nature* 439:589-93

Gonchar Y, Wang Q, Burkhalter A. 2007. Multiple distinct subtypes of GABAergic neurons in mouse visual cortex identified by triple immunostaining. *Front Neuroanat* 1:3

Goodman CS, Shatz CJ. 1993. Developmental mechanisms that generate precise patterns of neuronal connectivity. *Cell* 72 Suppl:77-98

Gould E, McEwen BS, Tanapat P, Galea LA, Fuchs E. 1997. Neurogenesis in the dentate gyrus of the adult tree shrew is regulated by psychosocial stress and NMDA receptor activation. *J Neurosci* 17:2492-8

Graf ER, Zhang X, Jin SX, Linhoff MW, Craig AM. 2004. Neurexins induce differentiation of GABA and glutamate postsynaptic specializations via neuroligins. *Cell* 119:1013-26

Grinevich V, Kolleker A, Eliava M, Takada N, Takuma H, et al. 2009. Fluorescent Arc/Arg3.1 indicator mice: a versatile tool to study brain activity changes in vitro and in vivo. *J Neurosci Methods* 184:25-36

Guidotti A, Auta J, Davis JM, Di-Giorgi-Gerevini V, Dwivedi Y, et al. 2000. Decrease in reelin and glutamic acid decarboxylase67 (GAD67) expression in schizophrenia and bipolar disorder: a postmortem brain study. *Arch Gen Psychiatry* 57:1061-9

Gutierrez R. 2005. The dual glutamatergic-GABAergic phenotype of hippocampal granule cells. *Trends Neurosci* 28:297-303

Harvey BH, Oosthuizen F, Brand L, Wegener G, Stein DJ. 2004. Stress-restress evokes sustained iNOS activity and altered GABA levels and NMDA receptors in rat hippocampus. *Psychopharmacology (Berl)* 175:494-502

Hendry SH, Jones EG, Guo Y, Kaplan IV, Cooper NG, Mower GD. 1986. Reduction in number of immunostained GABAergic neurones in deprived-eye dominance columns of monkey area 17

Activity-dependent regulation of GABA expression in the visual cortex of adult monkeys. *Nature* 320:750-3.

Herman JP, Cullinan WE, Ziegler DR, Tasker JG. 2002. Role of the paraventricular nucleus microenvironment in stress integration. *Eur J Neurosci* 16:381-5

Holmgren C, Harkany T, Svennenfors B, Zilberter Y. 2003. Pyramidal cell communication within local networks in layer 2/3 of rat neocortex. *J Physiol* 551:139-53

Holtmaat A, Svoboda K. 2009. Experience-dependent structural synaptic plasticity in the mammalian brain. *Nat Rev Neurosci* 10:647-58

Houenou LJ, Pincon-Raymond M, Garcia L, Harris AJ, Rieger F. 1990. Neuromuscular development following tetrodotoxin-induced inactivity in mouse embryos. *J Neurobiol* 21:1249-61

Hua JY, Smear MC, Baier H, Smith SJ. 2005. Regulation of axon growth in vivo by activity-based competition. *Nature* 434:1022-6

Huang ZJ, Kirkwood A, Pizzorusso T, Porciatti V, Morales B, et al. 1999. BDNF regulates the maturation of inhibition and the critical period of plasticity in mouse visual cortex. *Cell* 98:739-55

Huang ZJ, Scheiffele P. 2008. GABA and neuroligin signaling: linking synaptic activity and adhesion in inhibitory synapse development. *Curr Opin Neurobiol* 18:77-83

Impey S, Mark M, Villacres EC, Poser S, Chavkin C, Storm DR. 1996. Induction of CRE-mediated gene expression by stimuli that generate long-lasting LTP in area CA1 of the hippocampus. *Neuron* 16:973-82

Isaacson JS. 2001. Mechanisms governing dendritic gamma-aminobutyric acid (GABA) release in the rat olfactory bulb. *Proc Natl Acad Sci U S A* 98:337-42

Itouji A, Sakai N, Tanaka C, Saito N. 1996. Neuronal and glial localization of two GABA transporters (GAT1 and GAT3) in the rat cerebellum. *Brain Res Mol Brain Res* 37:309-16

Ji F, Kanbara N, Obata K. 1999. GABA and histogenesis in fetal and neonatal mouse brain lacking both the isoforms of glutamic acid decarboxylase. *Neurosci Res* 33:187-94

Jin Y, Jorgensen E, Hartwieg E, Horvitz HR. 1999. The Caenorhabditis elegans gene unc-25 encodes glutamic acid decarboxylase and is required for synaptic transmission but not synaptic development. *J Neurosci* 19:539-48

Jun HS, Khil LY, Yoon JW. 2002. Role of glutamic acid decarboxylase in the pathogenesis of type 1 diabetes. *Cell Mol Life Sci* 59:1892-901

Kanaani J, el-Husseini Ael D, Aguilera-Moreno A, Diacovo JM, Bredt DS, Baekkeskov S. 2002. A combination of three distinct trafficking signals mediates axonal targeting and presynaptic clustering of GAD65. *J Cell Biol* 158:1229-38

Kannenberg K, Sieghart W, Reuter H. 1999. Clusters of GABAA receptors on cultured hippocampal cells correlate only partially with functional synapses. *Eur J Neurosci* 11:1256-64

Kapfer C, Glickfeld LL, Atallah BV, Scanziani M. 2007. Supralinear increase of recurrent inhibition during sparse activity in the somatosensory cortex. *Nat Neurosci* 10:743-53

Kaplitt MG, Feigin A, Tang C, Fitzsimons HL, Mattis P, et al. 2007. Safety and tolerability of gene therapy with an adeno-associated virus (AAV) borne GAD gene for Parkinson's disease: an open label, phase I trial. *Lancet* 369:2097-105

Kash SF, Johnson RS, Tecott LH, Noebels JL, Mayfield RD, et al. 1997. Epilepsy in mice deficient in the 65-kDa isoform of glutamic acid decarboxylase. *Proc Natl Acad Sci U S A* 94:14060-5

Katz LC, Shatz CJ. 1996. Synaptic activity and the construction of cortical circuits. *Science* 274:1133-8

Kawaguchi Y, Kubota Y. 1997. GABAergic cell subtypes and their synaptic connections in rat frontal cortex. *Cereb Cortex* 7:476-86

Kelsch W, Lin CW, Lois C. 2008. Sequential development of synapses in dendritic domains during adult neurogenesis. *Proc Natl Acad Sci U S A* 105:16803-8

Kiser PJ, Cooper NG, Mower GD. 1998. Expression of two forms of glutamic acid decarboxylase (GAD67 and GAD65) during postnatal development of rat somatosensory barrel cortex. *J Comp Neurol* 402:62-74

Klausberger T, Magill PJ, Marton LF, Roberts JD, Cobden PM, et al. 2003. Brain-state- and cell-type-specific firing of hippocampal interneurons in vivo. *Nature* 421:844-8

Klostermann O, Wahle P. 1999. Patterns of spontaneous activity and morphology of interneuron types in organotypic cortex and thalamus-cortex cultures. *Neuroscience* 92:1243-59.

Knott GW, Quairiaux C, Genoud C, Welker E. 2002. Formation of dendritic spines with GABAergic synapses induced by whisker stimulation in adult mice. *Neuron* 34:265-73.

Kole MH, Czeh B, Fuchs E. 2004. Homeostatic maintenance in excitability of tree shrew hippocampal CA3 pyramidal neurons after chronic stress. *Hippocampus* 14:742-51

Kraszewski K, Mundigl O, Daniell L, Verderio C, Matteoli M, De Camilli P. 1995. Synaptic vesicle dynamics in living cultured hippocampal neurons visualized with CY3-conjugated antibodies directed against the lumenal domain of synaptotagmin. *J Neurosci* 15:4328-42

Kravitz EA, Kuffler SW, Potter DD. 1963. Gamma-Aminobutyric Acid and Other Blocking Compounds in Crustacea. Iii. Their Relative Concentrations in Separated Motor and Inhibitory Axons. *J Neurophysiol* 26:739-51

Kubo T, Kanaya T, Numakura H, Okajima H, Hagiwara Y, Fukumori R. 2002. The lateral septal area is involved in mediation of immobilization stress-induced blood pressure increase in rats. *Neurosci Lett* 318:25-8

Kuffler SW, Edwards C. 1958. Mechanism of gamma aminobutyric acid (GABA) action and its relation to synaptic inhibition. *J Neurophysiol* 21:589-610

Kuhlman SJ, Lu J, Lazarus MS, Huang ZJ. 2010. Maturation of GABAergic inhibition promotes strengthening of temporally coherent inputs among convergent pathways. *PLoS Comput Biol* 6:e1000797

Kullmann DM, Ruiz A, Rusakov DM, Scott R, Semyanov A, Walker MC. 2005. Presynaptic, extrasynaptic and axonal GABAA receptors in the CNS: where and why? *Prog Biophys Mol Biol* 87:33-46

Lautermilch NJ, Spitzer NC. 2000. Regulation of calcineurin by growth cone calcium waves controls neurite extension. *J Neurosci* 20:315-25

Levitt P, Eagleson KL, Powell EM. 2004. Regulation of neocortical interneuron development and the implications for neurodevelopmental disorders. *Trends Neurosci* 27:400-6

Lewis DA, Hashimoto T, Volk DW. 2005. Cortical inhibitory neurons and schizophrenia. *Nat Rev Neurosci* 6:312-24

Li G, Bien-Ly N, Andrews-Zwilling Y, Xu Q, Bernardo A, et al. 2009. GABAergic interneuron dysfunction impairs hippocampal neurogenesis in adult apolipoprotein E4 knockin mice. *Cell Stem Cell* 5:634-45

Li X, Zhao X, Fang Y, Jiang X, Duong T, et al. 1998. Generation of destabilized green fluorescent protein as a transcription reporter. *J Biol Chem* 273:34970-5

Li Z, Burrone J, Tyler WJ, Hartman KN, Albeanu DF, Murthy VN. 2005. Synaptic vesicle recycling studied in transgenic mice expressing synaptopHluorin. *Proc Natl Acad Sci U S A* 102:6131-6

Liang F, Isackson PJ, Jones EG. 1996. Stimulus-dependent, reciprocal up- and downregulation of glutamic acid decarboxylase and Ca2+/calmodulin-dependent protein kinase II gene expression in rat cerebral cortex. *Exp Brain Res* 110:163-74

Liang F, Le LD, Jones EG. 1998. Reciprocal up- and down-regulation of BDNF mRNA in tetanus toxin-induced epileptic focus and inhibitory surround in cerebral cortex. *Cereb Cortex* 8:481-91

Lin W, Dominguez B, Yang J, Aryal P, Brandon EP, et al. 2005. Neurotransmitter acetylcholine negatively regulates neuromuscular synapse formation by a Cdk5-dependent mechanism. *Neuron* 46:569-79

Liu P, Jenkins NA, Copeland NG. 2003. A highly efficient recombineering-based method for generating conditional knockout mutations. *Genome Res* 13:476-84

Malenka RC, Nicoll RA. 1997. Silent synapses speak up. *Neuron* 19:473-6

Malinow R, Malenka RC. 2002. AMPA receptor trafficking and synaptic plasticity. *Annu Rev Neurosci* 25:103-26

Markram H, Toledo-Rodriguez M, Wang Y, Gupta A, Silberberg G, Wu C. 2004. Interneurons of the neocortical inhibitory system. *Nat Rev Neurosci* 5:793-807

Martinez M, Phillips PJ, Herbert J. 1998. Adaptation in patterns of c-fos expression in the brain associated with exposure to either single or repeated social stress in male rats. *Eur J Neurosci* 10:20-33

McAllister AK. 2007. Dynamic aspects of CNS synapse formation. *Annu Rev Neurosci* 30:425-50

McEwen BS. 2000. The neurobiology of stress: from serendipity to clinical relevance. *Brain Res* 886:172-89

McEwen BS, Stellar E. 1993. Stress and the individual. Mechanisms leading to disease. *Arch Intern Med* 153:2093-101

Melzer P, Van der Loos H, Dorfl J, Welker E, Robert P, et al. 1985. A magnetic device to stimulate selected whiskers of freely moving or restrained small rodents: its application in a deoxyglucose study. *Brain Res* 348:229-40

Meyer MP, Smith SJ. 2006. Evidence from in vivo imaging that synaptogenesis guides the growth and branching of axonal arbors by two distinct mechanisms. *J Neurosci* 26:3604-14

Miles R, Toth K, Gulyas AI, Hajos N, Freund TF. 1996. Differences between somatic and dendritic inhibition in the hippocampus. *Neuron* 16:815-23

Misgeld T, Burgess RW, Lewis RM, Cunningham JM, Lichtman JW, et al. 2002. Roles of neurotransmitter in synapse formation: development of neuromuscular junctions lacking choline acetyltransferase. *Neuron* 36:635-48.

Missler M, Sudhof TC. 1998. Neurexins: three genes and 1001 products. *Trends Genet* 14:20-6

Morales B, Choi SY, Kirkwood A. 2002. Dark rearing alters the development of GABAergic transmission in visual cortex. *J Neurosci* 22:8084-90.

Moriyama Y, Yamamoto A. 2004. Glutamatergic chemical transmission: look! Here, there, and anywhere. *J Biochem* 135:155-63

Moss SJ, Smart TG. 2001. Constructing inhibitory synapses. *Nat Rev Neurosci* 2:240-50

Nakamura NH, Rosell DR, Akama KT, McEwen BS. 2004. Estrogen and ovariectomy regulate mRNA and protein of glutamic acid decarboxylases and cation-chloride cotransporters in the adult rat hippocampus. *Neuroendocrinology* 80:308-23

Nakata T, Terada S, Hirokawa N. 1998. Visualization of the dynamics of synaptic vesicle and plasma membrane proteins in living axons. *J Cell Biol* 140:659-74

Niell CM, Meyer MP, Smith SJ. 2004. In vivo imaging of synapse formation on a growing dendritic arbor. *Nat Neurosci* 7:254-60

Niell CM, Smith SJ. 2004. Live optical imaging of nervous system development. *Annu Rev Physiol* 66:771-98

O'Rourke NA, Cline HT, Fraser SE. 1994. Rapid remodeling of retinal arbors in the tectum with and without blockade of synaptic transmission. *Neuron* 12:921-34

Obata K. 1972. The inhibitory action of -aminobutyric acid, a probable synaptic transmitter. *Int Rev Neurobiol* 15:167-87

Oh WJ, Westmoreland JJ, Summers R, Condie BG. 2010. Cleft palate is caused by CNS dysfunction in Gad1 and Viaat knockout mice. *PLoS One* 5:e9758

Ong J, Kerr DI. 1990. GABA-receptors in peripheral tissues. *Life Sci* 46:1489-501

Owens DF, Kriegstein AR. 2002. Is there more to GABA than synaptic inhibition? *Nat Rev Neurosci* 3:715-27

Patrizi A, Scelfo B, Viltono L, Briatore F, Fukaya M, et al. 2008. Synapse formation and clustering of neuroligin-2 in the absence of GABAA receptors. *Proc Natl Acad Sci U S A* 105:13151-6

Patz S, Wirth MJ, Gorba T, Klostermann O, Wahle P. 2003. Neuronal activity and neurotrophic factors regulate GAD-65/67 mRNA and protein expression in organotypic cultures of rat visual cortex. *Eur J Neurosci* 18:1-12

Pearce DA, Atkinson M, Tagle DA. 2004. Glutamic acid decarboxylase autoimmunity in Batten disease and other disorders. *Neurology* 63:2001-5

Pham K, Nacher J, Hof PR, McEwen BS. 2003. Repeated restraint stress suppresses neurogenesis and induces biphasic PSA-NCAM expression in the adult rat dentate gyrus. *Eur J Neurosci* 17:879-86

Pinal CS, Tobin AJ. 1998. Uniqueness and redundancy in GABA production. *Perspect Dev Neurobiol* 5:109-18

Pisani A, Bernardi G, Ding J, Surmeier DJ. 2007. Re-emergence of striatal cholinergic interneurons in movement disorders. *Trends Neurosci* 30:545-53

Pouille F, Scanziani M. 2001. Enforcement of temporal fidelity in pyramidal cells by somatic feed-forward inhibition. *Science* 293:1159-63

Purpura DP, Girado M, Grundfest H. 1957. Selective blockade of excitatory synapses in the cat brain by gamma-aminobutyric acid. *Science* 125:1200-2

Radian R, Ottersen OP, Storm-Mathisen J, Castel M, Kanner BI. 1990. Immunocytochemical localization of the GABA transporter in rat brain. *J Neurosci* 10:1319-30

Radley JJ, Rocher AB, Miller M, Janssen WG, Liston C, et al. 2006. Repeated stress induces dendritic spine loss in the rat medial prefrontal cortex. *Cereb Cortex* 16:313-20

Represa A, Ben-Ari Y. 2005. Trophic actions of GABA on neuronal development. *Trends Neurosci* 28:278-83

Ruthazer ES, Akerman CJ, Cline HT. 2003. Control of axon branch dynamics by correlated activity in vivo. *Science* 301:66-70

Ruthazer ES, Li J, Cline HT. 2006. Stabilization of axon branch dynamics by synaptic maturation. *J Neurosci* 26:3594-603

Ryan MD, Drew J. 1994. Foot-and-mouth disease virus 2A oligopeptide mediated cleavage of an artificial polyprotein. *EMBO J* 13:928-33

Sabo SL, Gomes RA, McAllister AK. 2006. Formation of presynaptic terminals at predefined sites along axons. *J Neurosci* 26:10813-25

Saitoe M, Schwarz TL, Umbach JA, Gundersen CB, Kidokoro Y. 2001. Absence of junctional glutamate receptor clusters in Drosophila mutants lacking spontaneous transmitter release. *Science* 293:514-7

Sanes JR, Lichtman JW. 1999. Development of the vertebrate neuromuscular junction. *Annu Rev Neurosci* 22:389-442

Sapolsky RM. 1996. Stress, Glucocorticoids, and Damage to the Nervous System: The Current State of Confusion. *Stress* 1:1-19

Schikorski T, Stevens CF. 1997. Quantitative ultrastructural analysis of hippocampal excitatory synapses. *J Neurosci* 17:5858-67

Schwarzer C, Sperk G. 1995. Hippocampal granule cells express glutamic acid decarboxylase-67 after limbic seizures in the rat. *Neuroscience* 69:705-9

Schwenk F, Baron U, Rajewsky K. 1995. A cre-transgenic mouse strain for the ubiquitous deletion of loxP-flanked gene segments including deletion in germ cells. *Nucleic Acids Res* 23:5080-1

Shaner NC, Campbell RE, Steinbach PA, Giepmans BN, Palmer AE, Tsien RY. 2004. Improved monomeric red, orange and yellow fluorescent proteins derived from Discosoma sp. red fluorescent protein. *Nat Biotechnol* 22:1567-72

Shapiro L, Love J, Colman DR. 2007. Adhesion molecules in the nervous system: structural insights into function and diversity. *Annu Rev Neurosci* 30:451-74

Shigeri Y, Seal RP, Shimamoto K. 2004. Molecular pharmacology of glutamate transporters, EAATs and VGLUTs. *Brain Res Brain Res Rev* 45:250-65

Sin WC, Haas K, Ruthazer ES, Cline HT. 2002. Dendrite growth increased by visual activity requires NMDA receptor and Rho GTPases. *Nature* 419:475-80

Smeyne RJ, Schilling K, Robertson L, Luk D, Oberdick J, et al. 1992. fos-lacZ transgenic mice: mapping sites of gene induction in the central nervous system. *Neuron* 8:13-23

Somogyi P, Kisvarday ZF, Martin KA, Whitteridge D. 1983a. Synaptic connections of morphologically identified and physiologically characterized large basket cells in the striate cortex of cat. *Neuroscience* 10:261-94

Somogyi P, Klausberger T. 2005. Defined types of cortical interneurone structure space and spike timing in the hippocampus. *J Physiol* 562:9-26

Somogyi P, Nunzi MG, Gorio A, Smith AD. 1983b. A new type of specific interneuron in the monkey hippocampus forming synapses exclusively with the axon initial segments of pyramidal cells. *Brain Res* 259:137-42

Somogyi P, Tamas G, Lujan R, Buhl EH. 1998. Salient features of synaptic organisation in the cerebral cortex. *Brain Res Brain Res Rev* 26:113-35

Sperk G, Lassmann H, Baran H, Kish SJ, Seitelberger F, Hornykiewicz O. 1983. Kainic acid induced seizures: neurochemical and histopathological changes. *Neuroscience* 10:1301-15

Stamp JA, Herbert J. 1999. Multiple immediate-early gene expression during physiological and endocrine adaptation to repeated stress. *Neuroscience* 94:1313-22

Stone DJ, Walsh JP, Sebro R, Stevens R, Pantazopolous H, Benes FM. 2001. Effects of pre- and postnatal corticosterone exposure on the rat hippocampal GABA system. *Hippocampus* 11:492-507

Stoppini L, Buchs PA, Muller D. 1991. A simple method for organotypic cultures of nervous tissue. *J Neurosci Methods* 37:173-82

Sumner P, Edden RA, Bompas A, Evans CJ, Singh KD. 2010. More GABA, less distraction: a neurochemical predictor of motor decision speed. *Nat Neurosci*

Sweeney ST, Broadie K, Keane J, Niemann H, O'Kane CJ. 1995. Targeted expression of tetanus toxin light chain in Drosophila specifically eliminates synaptic transmission and causes behavioral defects. *Neuron* 14:341-51

Tamas G, Buhl EH, Somogyi P. 1997. Fast IPSPs elicited via multiple synaptic release sites by different types of GABAergic neurone in the cat visual cortex. *J Physiol* 500:715-38.

Tang F, Dent EW, Kalil K. 2003. Spontaneous calcium transients in developing cortical neurons regulate axon outgrowth. *J Neurosci* 23:927-36

Tillakaratne NJ, Medina-Kauwe L, Gibson KM. 1995. gamma-Aminobutyric acid (GABA) metabolism in mammalian neural and nonneural tissues. *Comp Biochem Physiol A Physiol* 112:247-63

Tong Q, Ye CP, Jones JE, Elmquist JK, Lowell BB. 2008. Synaptic release of GABA by AgRP neurons is required for normal regulation of energy balance. *Nat Neurosci* 11:998-1000

Trachtenberg JT, Chen BE, Knott GW, Feng G, Sanes JR, et al. 2002. Long-term in vivo imaging of experience-dependent synaptic plasticity in adult cortex. *Nature* 420:788-94

Tremolizzo L, Doueiri MS, Dong E, Grayson DR, Davis J, et al. 2005. Valproate corrects the schizophrenia-like epigenetic behavioral modifications induced by methionine in mice. *Biol Psychiatry* 57:500-9

Tsien RY. 1998. The green fluorescent protein. *Annu Rev Biochem* 67:509-44

Turrigiano GG, Nelson SB. 2004. Homeostatic plasticity in the developing nervous system. *Nat Rev Neurosci* 5:97-107

Ullian EM, Christopherson KS, Barres BA. 2004. Role for glia in synaptogenesis. *Glia* 47:209-16

Umemoto S, Kawai Y, Ueyama T, Senba E. 1997. Chronic glucocorticoid administration as well as repeated stress affects the subsequent acute immobilization stress-induced expression of immediate early genes but not that of NGFI-A. *Neuroscience* 80:763-73

Van den Veyver IB, Zoghbi HY. 2000. Methyl-CpG-binding protein 2 mutations in Rett syndrome. *Curr Opin Genet Dev* 10:275-9

Varoqueaux F, Aramuni G, Rawson RL, Mohrmann R, Missler M, et al. 2006. Neuroligins determine synapse maturation and function. *Neuron* 51:741-54

Varoqueaux F, Sigler A, Rhee JS, Brose N, Enk C, et al. 2002. Total arrest of spontaneous and evoked synaptic transmission but normal synaptogenesis in the absence of Munc13-mediated vesicle priming. *Proc Natl Acad Sci U S A* 99:9037-42

Varoqueaux F, Sons MS, Plomp JJ, Brose N. 2005. Aberrant morphology and residual transmitter release at the Munc13-deficient mouse neuromuscular synapse. *Mol Cell Biol* 25:5973-84

Vaughn JE. 1989. Fine structure of synaptogenesis in the vertebrate central nervous system. *Synapse* 3:255-85

Veldic M, Guidotti A, Maloku E, Davis JM, Costa E. 2005. In psychosis, cortical interneurons overexpress DNA-methyltransferase 1. *Proc Natl Acad Sci U S A* 102:2152-7

Verhage M, Maia AS, Plomp JJ, Brussaard AB, Heeroma JH, et al. 2000. Synaptic assembly of the brain in the absence of neurotransmitter secretion. *Science* 287:864-9

Waites CL, Craig AM, Garner CC. 2005. Mechanisms of vertebrate synaptogenesis. *Annu Rev Neurosci* 28:251-74

Wang DD, Kriegstein AR. 2009. Defining the role of GABA in cortical development. *J Physiol* 587:1873-9

Wang KH, Majewska A, Schummers J, Farley B, Hu C, et al. 2006. In vivo two-photon imaging reveals a role of arc in enhancing orientation specificity in visual cortex. *Cell* 126:389-402

Wang Y, Gupta A, Toledo-Rodriguez M, Wu CZ, Markram H. 2002. Anatomical, physiological, molecular and circuit properties of nest basket cells in the developing somatosensory cortex. *Cereb Cortex* 12:395-410

Watanabe Y, Gould E, McEwen BS. 1992. Stress induces atrophy of apical dendrites of hippocampal CA3 pyramidal neurons. *Brain Res* 588:341-5

Watts RJ, Hoopfer ED, Luo L. 2003. Axon pruning during Drosophila metamorphosis: evidence for local degeneration and requirement of the ubiquitin-proteasome system. *Neuron* 38:871-85

Welker E, Soriano E, Dorfl J, Van der Loos H. 1989. Plasticity in the barrel cortex of the adult mouse: transient increase of GAD-immunoreactivity following sensory stimulation. *Exp Brain Res* 78:659-64

Wojcik SM, Katsurabayashi S, Guillemin I, Friauf E, Rosenmund C, et al. 2006. A shared vesicular carrier allows synaptic corelease of GABA and glycine. *Neuron* 50:575-87

Wong CG, Bottiglieri T, Snead OC, 3rd. 2003. GABA, gamma-hydroxybutyric acid, and neurological disease. *Ann Neurol* 54 Suppl 6:S3-12

Woolsey TA, Van der Loos H. 1970. The structural organization of layer IV in the somatosensory region (SI) of mouse cerebral cortex. The description of a cortical field composed of discrete cytoarchitectonic units. *Brain Res* 17:205-42